2001

Optimum hybrid vehicle configurations for heavy duty applications

Jonathan Burke Smith
West Virginia University

Optimum Hybrid Vehicle Configurations for Heavy Duty Applications

Jonathan Burke Smith

Thesis submitted to

The College of Engineering and Mineral Resources

at

West Virginia University

in partial fulfillment of the requirements

for the degree of

Master of Science

in

Mechanical Engineering

Nigel N. Clark, Ph.D., Chair

Christopher M. Atkinson, Sc. D.

Thomas R. Long, Ph. D

Department of Mechanical and Aerospace Engineering

Morgantown, West Virginia

2001

Abstract

Optimum Hybrid Vehicle Configurations for Heavy Duty Applications

Jonathan Burke Smith

Increased concern about the fuel economy of and emissions from automobiles has led to interest in the use of hybrid electric powertrains and the introduction of several production vehicles in both heavy-duty and light-duty applications. Hybrid electric vehicles (HEVs) use a combination of electric motor(s) and another power source such as an internal combustion engine (ICE) or fuel cell. While these vehicles show great potential for use in a wide variety of driving situations, the optimization of components and control strategies is quite complex.

In this thesis, Class 2B, Class 6, and Class 8 vehicles are determined by averaging a variety of actual vehicles from each class and are simulated in Microsoft Excel over a variety of driving cycles to attempt to optimize their design and control. The drive cycles are modified to represent realistic expectations of the dynamic performance of vehicles from each class. Two types of hybrid powertrains are simulated. The series HEV is propelled solely by electric motors with energy coming from batteries and an alternator driven by an ICE. The parallel HEV is propelled by both electric motors and an ICE with charging-while-driving capabilities. The model is based on power requirements for each vehicle class and addresses concerns such as engine, battery, and driveline efficiencies. The control strategy forces the engine to run at a fixed percentage of the power required at the wheels plus or minus a battery state of charge correction factor.

Fuel economy increases of 100 to 150 percent were seen for Class 6 and 8 vehicles on transient cycles while 10 to 20 percent increases were seen on more constant speed cycles. The Yard cycle, a low average demand, highly transient cycle, was shown to be particularly suited to HEVs.

Table of Contents

Table of Figures

Table of Tables

Nomenclature

A	- Frontal Area
C_b	-Battery Energy Capacity
C_D	-Aerodynamic Drag Coefficient
CSHVC	-City-Suburban Heavy Vehicle Cycle
E_b	-Battery Energy
E_{bi}	-Battery Energy at a given time step
F	-Force
F_i	-Inertial Force
F_D	-Aerodynamic Drag Force
F_{rr}	-Rolling Resistance Force
F_w	-Force at the Wheels
$F_{è}$	-Force Due to Road Grade
g	-Gravitational Acceleration
HEV	-Hybrid Electric Vehicle
HDDC	-Heavy Duty Drive Cycle
η_d	-Driveline Efficiency
η_b	-Battery Efficiency
ICE	-Internal Combustion Engine
I_b	-Battery Current
m	- Mass
μ	-Rolling Resistance Constant
N_b	-Number of Batteries

NMHC	-Non-methane hydrocarbons
OTR	-Over-the-Road
P_{bi}	-Battery Power at a given time-step
P_e	-Engine Power
P_w	-Power at the Wheels
P_{aux}	-Auxiliary Load Power
ρ	-Air Density
SoC	-State of Charge
SoC_i	-State of Charge at a given time-step
SoC_t	-Target State of Charge
θ	-Road Grade Angle
V	-Velocity
V_b	-Nominal Battery Voltage

1. Introduction

In recent years, rising fuel costs, declining oil reserves, and increased concern over environmental issues has led to government and public interest in the design of new, more efficient means of motor vehicle transportation. While existing technology has improved the fuel economy and tailpipe emissions of vehicles far beyond standards from only a decade or two ago, further advances are both desired and required. Concern over these issues led the government and the automotive industry to form Partnership for a New Generation of Vehicles (PNGV). PNGV calls for the production of vehicles with three times the fuel economy of current conventional vehicles. [1] The 21st Century Truck Program is a partnership between the heavy-duty truck and bus industry and the federal government for the development of technology that will dramatically reduce their emissions and increase their fuel economy, doubling the fuel economy of Class 8 trucks and tripling the fuel economy of Class 2B and 6 trucks by 2010 as well as decreasing emissions and increasing safety. [2]

One method for increasing the fuel economy of vehicles of all sizes is the use of hybridization. In a hybrid electric vehicle (HEV), two energy sources are used to power the vehicle. One source is an electric motor supported by some type of energy storage device such as batteries, ultra capacitors, or flywheels. The other source has ranged from an internal combustion engine (ICE), to a gas turbine, or fuel cell. While ultra capacitors, flywheels, and fuel cells hold promise for the future, they have not reached a level of availability, reliability, and cost that would allow them to go into mass production in the near future. In this thesis, the HEVs simulated are assumed to be powered by a

conventional diesel ICE , electric motor(s), and batteries. HEVs have several advantages over conventional vehicles. The largest factor in their increased fuel economy is the ability to capture braking energy, often referred to as regenerative braking energy. During braking in a conventional vehicle, the kinetic energy associated with the mass of the vehicle at a given speed is dissipated as heat through friction between the brake pads and rotors or drums to slow the vehicle. This energy is lost and cannot be reused. In an HEV, the electric motor is used to decelerate the vehicle generating power, which is stored in batteries and used to accelerate the vehicle. Some of the energy from the fuel used to accelerate the vehicle can be captured during deceleration and reused for subsequent acceleration. HEVs also allow downsizing of the ICE in most vehicles. The ICE in a conventional vehicle is sized to provide the peak power necessary to provide dynamic performance that is acceptable to the consumer. This peak power is seldom used and the engine often operates at low load and poor efficiency. In an HEV, peak power is provided by supplementing the ICE power with electric power allowing average engine operation to be closer to the optimum range increasing efficiency and often decreasing the weight of the vehicle.

1.1 Literature Review

Hybrid electric vehicles are not a new concept. The first vehicle powerplants were steam engines, internal combustion engines, and electric motors. The first electric vehicle was made by the Dutch Professor Stratingh in 1835. This was followed by several other designs until, in 1899, advances in motor and battery design allowed Baker Electric of the US to manufacture an electric vehicle capable of a maximum speed of 40 km/h and an 80 km range. During this same period, many advances were made in

internal combustion engine technology. The two technologies were combined to provide the increased range of an ICE powered vehicle with the safety and reliability of an electric vehicle. Increasingly powerful and reliable ICEs eventually replaced the widespread use of electric motors. [3]

Recent years have seen a resurgence in the popularity of HEVs both in light and heavy-duty applications. Examples of current production HEVs include light-duty vehicles such as the Toyota Prius and Honda Insight, and heavy-duty vehicles such as Orion/Lockheed transit buses. These vehicles have demonstrated the advantages of HEVs to the public and they can only be expected to become more popular.

The most common current use for heavy-duty HEVs is in the transit bus industry. In-use data from fleets in New York City have demonstrated 30 - 50% gains in fuel economy as well as 50 - 90% lower PM, 30 - 60% lower NO_x and HC, and 20 - 40% lower greenhouse gases. [4]

Using current technology, hybrid electric powertrains are quite expensive, but as consumer interest grows, increased production levels and research and development funding should drive the prices down. The cost of integrating a parallel HEV powertrain into an existing Class 3 vehicle is estimated at $5,800 in 2005 but drops to $3,000 in 2020. Similarly, for Class 6 - 7 vehicles, the 2005 cost is $7,100 dropping to $3,300 in 2020. [5]

1.2 Emissions Regulations

Current and future emissions regulations for heavy-duty vehicles vary between those mandated by the US federal government, the California Air Resources Board (CARB),

and Europe but, they all mandate substantial decreases in the vehicle emissions over the next 5 to 7 years.

Table 1.2.1 European Heavy-Duty Diesel Engine Emissions Regulations [6]

	Year	CO	HC	NOx	PM
		g/kWh	g/kWh	g/kWh	g/kWh
Euro I	1992, <85 kW	4.5	1.1	8.0	0.612
	1992, >85 kW	4.5	1.1	8.0	0.36
Euro II	1996	4.0	1.1	7.0	0.25
	1998	4.0	1.1	7.0	0.15
Euro III	2000	2.1	0.66	5.0	0.10
Euro IV	2005	1.5	0.46	3.5	0.02
Euro V	2008	1.5	0.46	2.0	0.02

Table 1.2.2 US EPA Heavy-Duty Diesel Engine Emissions Regulations [6]

Year	CO	HC	NOx	PM
	g/bhp-hr	g/bhp-hr	g/bhp-hr	g/bhp-hr
Heavy-Duty Diesel Truck Engines				
1990	1.3	15.5	6.0	0.60
1991	1.3	15.5	5.0	0.25
1994	1.3	15.5	5.0	0.10
1998	1.3	15.5	4.0	0.10
2000			4.0	0.05
2002			2.5*	0.01
2004			0.5	0.01
2007			0.2	0.01
Urban Bus Engines				
1991	1.3	15.5	5.0	0.25
1993	1.3	15.5	5.0	0.10
1994	1.3	15.5	5.0	0.07
1996	1.3	15.5	5.0	0.05
1998	1.3	15.5	4.0	0.05
2000			4.0	0.05
2002			2.5*	0.01
2004			0.5	0.01
2007			0.2	0.01

* NOx + NMHC

2. Vehicle Configurations

Three basic vehicle configurations were considered. These included a conventional ICE powered vehicle, a series HEV, and a parallel HEV.

2.1 Conventional Vehicle

In a conventional vehicle, an ICE transmits the power needed to drive the vehicle through a transmission and differential to the wheels. This layout has been used for many years and is fairly inexpensive and easy to control. The main disadvantage is poor efficiency due to the use of an oversized ICE, lack of regenerative braking, and highly transient ICE operation. The transient engine operation also leads to the increased production of emissions and difficulty in controlling them.

2.2 Electric Vehicle

The use of pure electric vehicles is older, in fact, than the use of the ICE. In this type of vehicle, electrical energy is stored in a battery and fed to the motor, which provides power to the wheels.

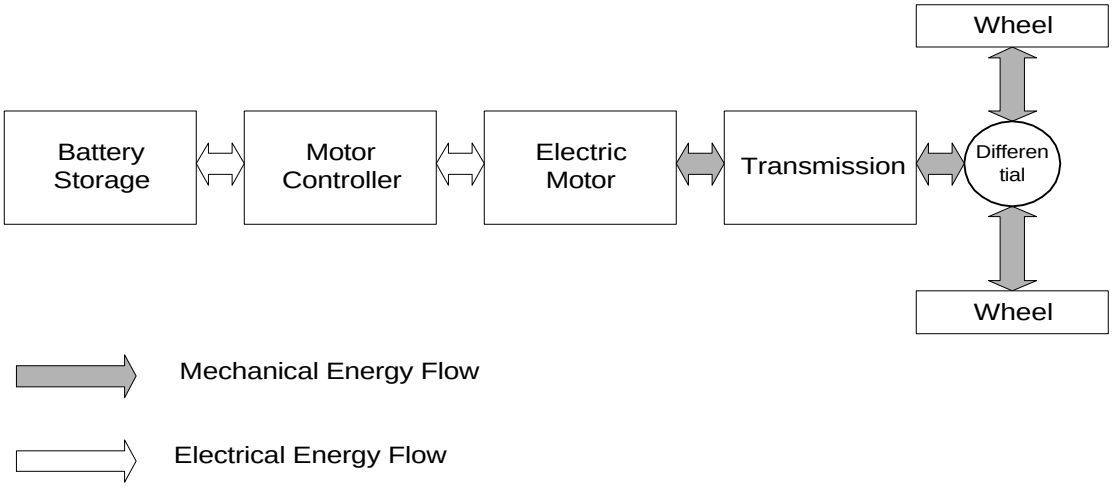

Figure 2.2.1 Electric vehicle layout. [3]

The advantages of electric vehicles include zero tailpipe emissions and nearly silent operation compared to most conventional vehicles.

Disadvantages come in the form of reduced consumer acceptability due to short range and long recharge times. Current production EVs are limited to a maximum of approximately 150 miles on one battery charge. Use of air conditioning or heating increases the demands on the batteries further reducing this range. While this is sufficient for many daily commuters, it is not ideal for long trips. In addition to this short range, the batteries require several hours to recharge once depleted. Deep cycling of batteries causes damage reducing their lifetime and requiring expensive, periodic replacement. The idea of not being able to use a vehicle for several hours out of every day is unacceptable to many consumers.

2.3 Series HEV

In a series HEV, an ICE or fuel cell is used to produce electrical energy that is sent to the battery pack and electric motor. All of the power to drive the vehicle is supplied through the electric motor. Figure 2.3.1 shows a typical series HEV layout.

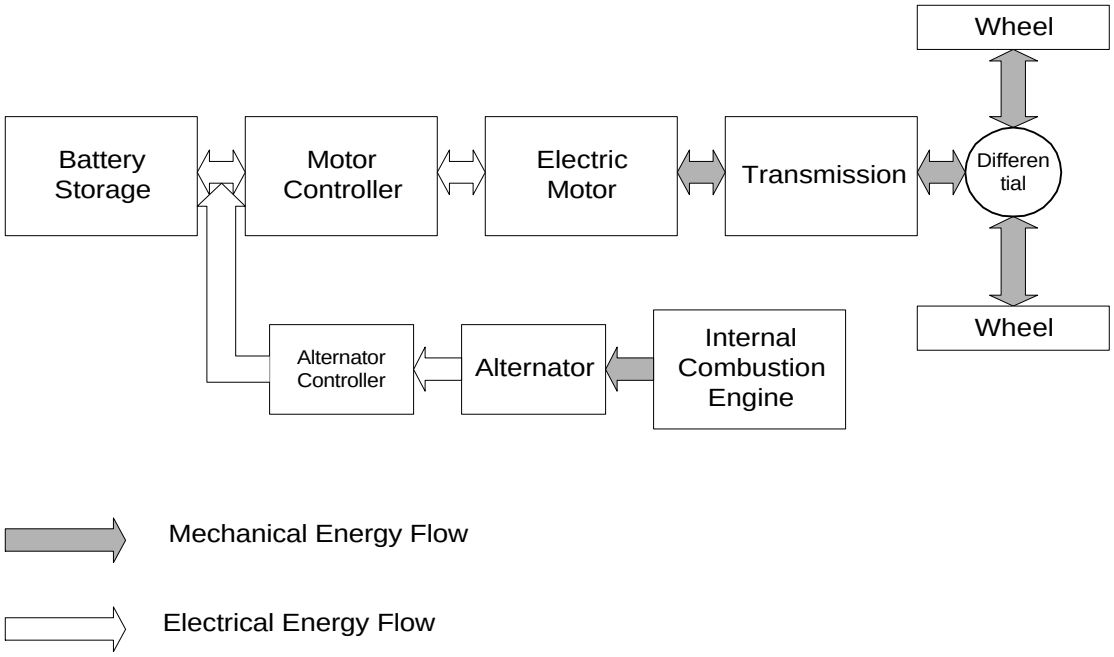

Figure 2.3.1 Series HEV layout. [3]

Some of the advantages of series HEVs include less transient ICE operation, operation of the ICE at optimal, efficient speed and load for improved fuel economy and optimization of emissions control, and the possible omission of the costly, heavy transmission. Disadvantages in current series HEVs include poor dynamic performance, losses during changing energy from chemical to mechanical, mechanical to electrical, and electrical to mechanical forms, and the need for costly, heavy battery packs and electric motors.

Series vehicles typically show substantial fuel economy improvements in highly transient driving in urban situations due to recovery of large amounts of regenerative braking energy. Smaller efficiency gains are realized through less transient operation such as highway driving where there is less available regenerative braking energy.

2.4 Parallel HEV

In a parallel HEV, there is a direct connection between both the ICE and the electric motor and the wheels. This configuration allows a wide variety of control strategies to be employed. When high power is demanded such as for high acceleration, both the ICE and electric motor deliver power to the wheels. In less demanding situations, the ICE can be operated at a higher power that what is required to drive the vehicle and the excess power captured by the electric motor and stored in the batteries for later use, or the electric motor alone can be used to drive the vehicle. This has the advantage of operating the ICE in a more efficient mode or not at all. During long, steady-state cruises, the ICE engine alone can drive the vehicle avoiding the inherent inefficiency of the batteries.

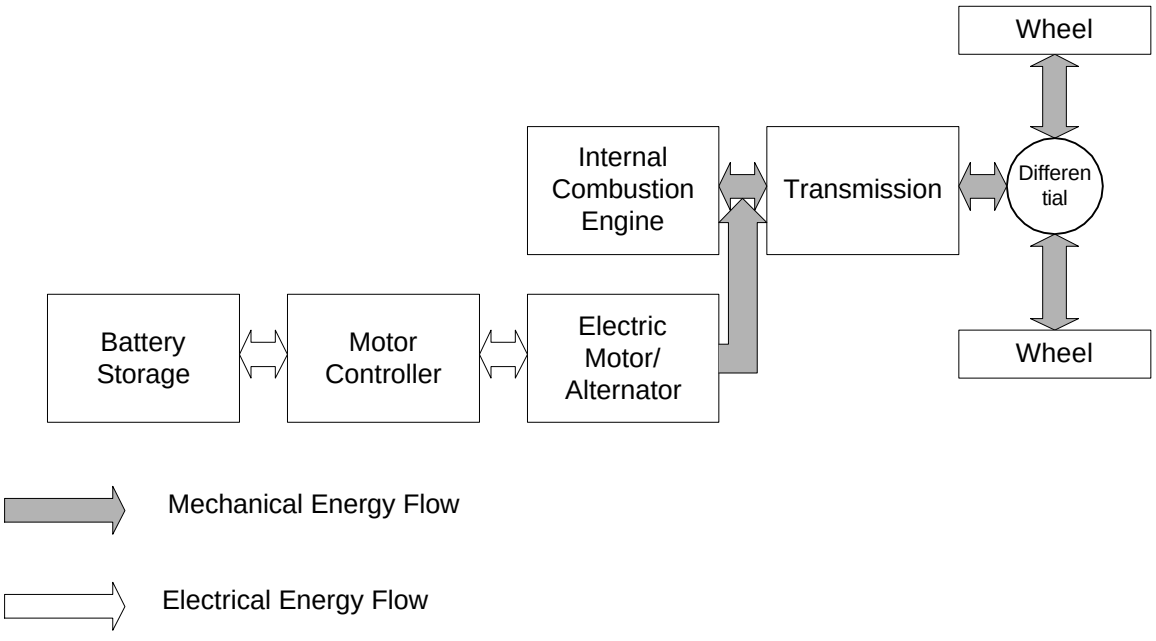

Figure 2.4.1 Parallel HEV layout with electric power delivered between ICE and transmission. [3]

The main advantage of parallel HEVs is improved dynamic performance compared to series HEVs due to the direct coupling between the ICE, electric motor, and the wheels.

This comes with disadvantages. Since the ICE is directly coupled to the wheels, it is forced into more transient operation than the ICE in a series vehicle. This tends to result in poorer efficiency and increased emissions.

3. Simulation

To examine and optimize the various vehicle configurations, they were, first, simulated using a Microsoft Excel based simulation.

3.1 Vehicle Descriptions

Three vehicle weight classes were chosen for simulation. Class 2B vehicles include 1 ton trucks such as GM's 3500 series or Ford's F350. Typical Class 6 vehicles include local delivery box trucks and school buses. There are a wide variety of Class 8 vehicles but those from the WVU database are primarily over-the-road (OTR) tractors and city buses.

Table 3.1.1 Vehicle weight classes. [7]

	Class	Min GVW	Max GVW		Min GVW	Max GVW
		lb	lb		kg	kg
Light Duty	1		<6000		0	<2721
	2A	6001	8500		2722	3856
	2B	8501	10000		3856	4536
	3	10001	14000		4536	6350
Medium Duty	4	14001	16000		6351	7258
	5	16001	19500		7258	8845
	6	19501	26000		8846	11794
Heavy Duty	7	26001	33000		11794	14969
	8	>33001			>14969	

To simulate a vehicle from each of the three weight classes, an average vehicle was calculated using data from vehicle and engine manufacturers and from vehicles tested on the WVU Transportable Heavy-Duty Emissions Testing Laboratory. To avoid requiring a vehicle to meet the high instantaneous power demands encountered in some driving cycles, an average maximum power was calculated for each vehicle class. In any driving situation requiring high power, a vehicle would be expected to operate

somewhere between its maximum rated power and its maximum torque point. Due to this, maximum power given to the averaged vehicle was the average of both the maximum rated power and the power at maximum torque.

The average Class 2B vehicle was calculated from manufacturer data for empty trucks with an added 1500 kg payload. Class 6 data is from both manufacturer data and the WVU database. Class 8 data is taken solely from the WVU database.

Table 3.1.2 Class 2B vehicle data. [8, 9, 10]

Vehicle	Engine	Mass	Max Power	Power @ Max Torque
		kg	kW	kW
GMC 3500HD	6.6L diesel	4024	224	133
Dodge 3500	5.9L diesel	3932	183	115
Ford F350 Super Duty	7.3L diesel	3910	205	119

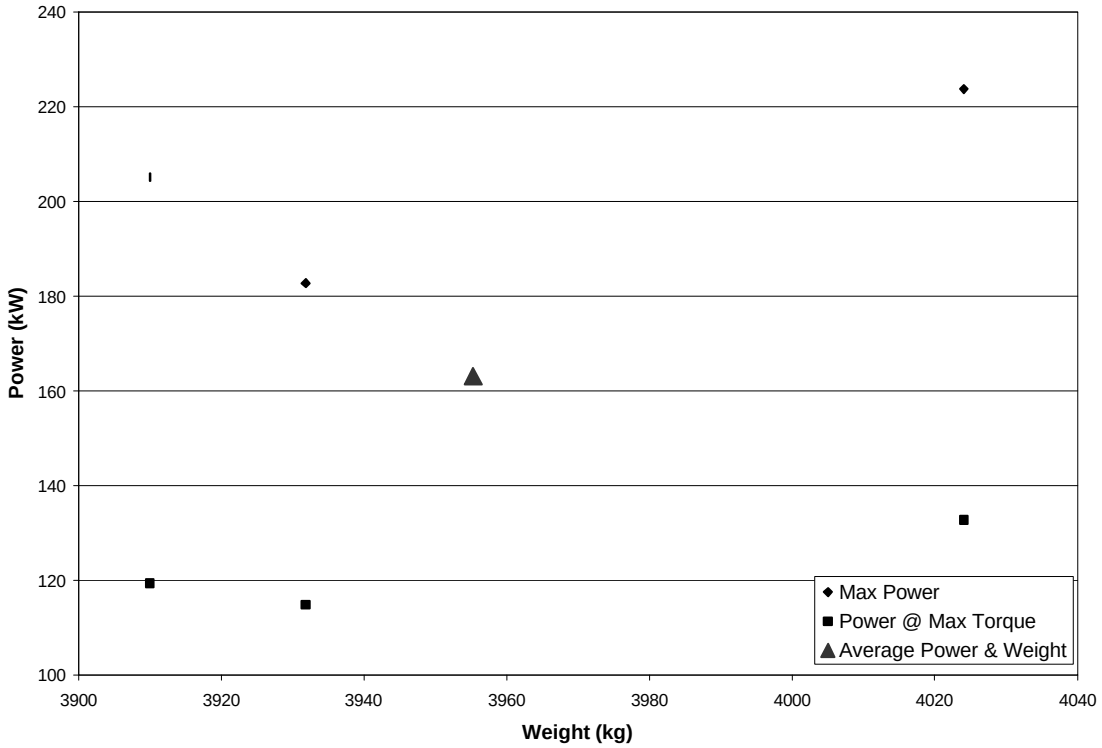

Figure 3.1.1 Class 2B vehicle power and weight.

Table 3.1.3 Class 6 vehicle data. [8, 11]

Vehicle	Engine	Weight	Max Power	Power @ Max Torque
		kg	kW	kW
GMC T6500	7.8L diesel	4545	111	70
GMC T6500	7.8L diesel	5165	128	81
GMC T6500	7.2L diesel	4545	117	80
GMC T6500	7.2L diesel	5165	139	101
Chevrolet	Caterpillar 3116	5362	103	86
International	International DTA3600	4917	100	75
GMC	Caterpillar 3208	4545	95	70
Mack/Renault	Renault MIDR	5269	106	66
Ford	LFM078EPC7	5062	92	61

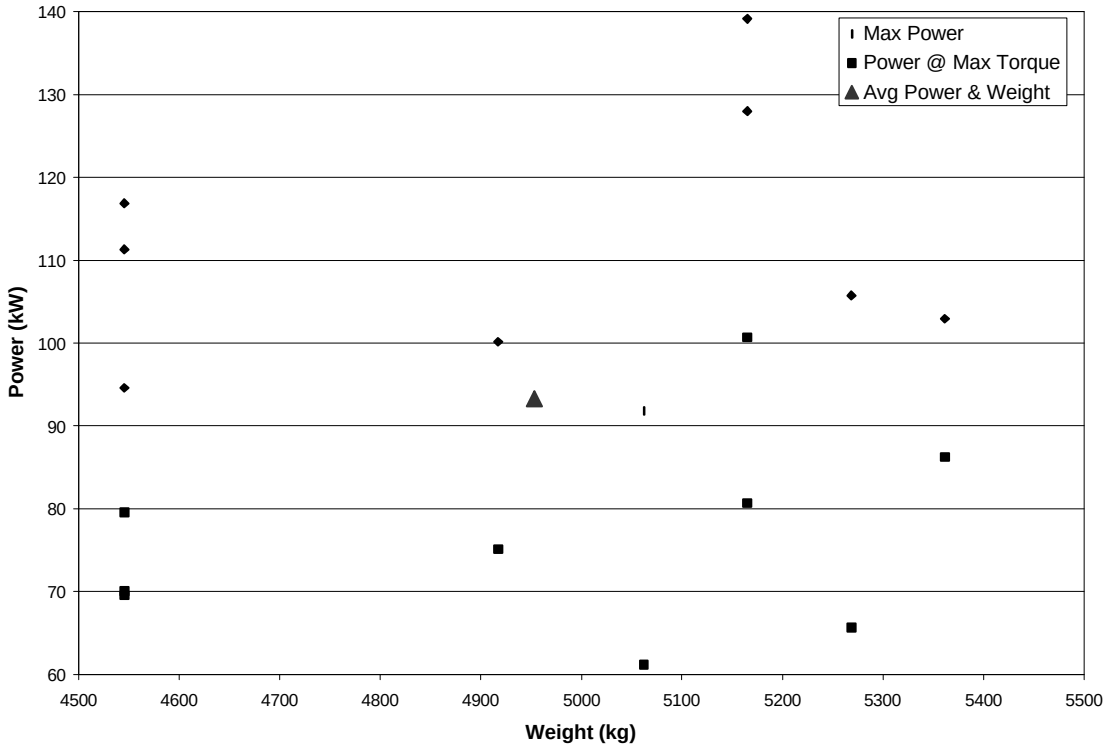

Figure 3.1.2 Class 6 vehicle power and weight.

Table 3.1.4 Class 8 vehicle data. [11]

Vehicle	Engine	Weight	Max Power	Power @ Max Torque
		kg	kW	kW
Neoplan	DDC 6V-92TA	17127	154	120
Orion	Cummins L-10	17688	134	119
General Motors Corp.	DDC 6V-92TA	16773	141	124
Transit Motor Corp.	DDC 6V-92TA	16773	141	124
Navistar	DDC 6V-92TA	25009	154	112
Freightliner	Caterpillar 3406B	36364	195	159
White/General Motor Corp.	DDC 6V-92TA	36364	167	124
Mack	Mack E-6	36364	195	157
International	DDC Series 60	36364	195	172
Ford	Cummins 350	36364	195	172
Grumman	DDC Series 30	14318	117	77
Blue Bird	Cummins L-10	36364	134	119
Kenworth	Cummins M11-330E	36364	184	134
Thomas Built	Cummins C8.3-250G	17000	139	191
Sterling	DDC Series 60	36364	262	197

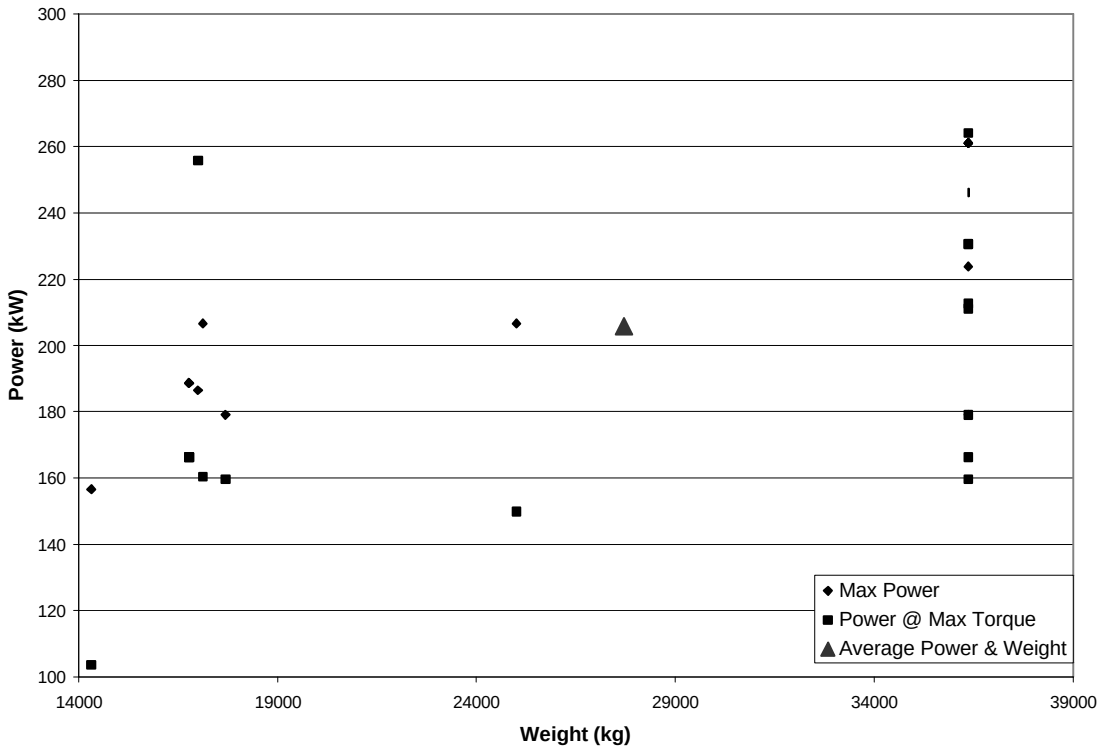

Figure 3.1.3 Class 8 vehicle power and weight.

The vehicle data in Figure 3.1.3 shows two separate groupings of vehicle weights and power ratings. The heavier group is composed of OTR trucks at maximum GVW

while the lighter group is composed primarily of city buses. Although this results in an average vehicle that is an average for neither of these groups, it should be sufficient for this simulation.

Table 3.1.5 Average vehicle characteristics.

Class	Mass	Drag Coefficient	Frontal area	Rolling resistance	Average Power
	kg		m^2		kW
1 Ton	3956	0.44	4.54	0.015	165
Class 6	10907	0.62	8.17	0.01	125
Class 8	27734	0.75	8.31	0.01	206

A driver expects different levels of dynamic performance from different vehicle classes. A Class 2B truck is expected to accelerate at rates similar to light-duty vehicles. 0 – 100 km/h acceleration times on the order of 15 seconds are expected. For a fully loaded Class 8 over-the-road tractor, 0 – 100 km/h times of 4 minutes are not unusual. These expectations are reflected in Figure 3.1.4.

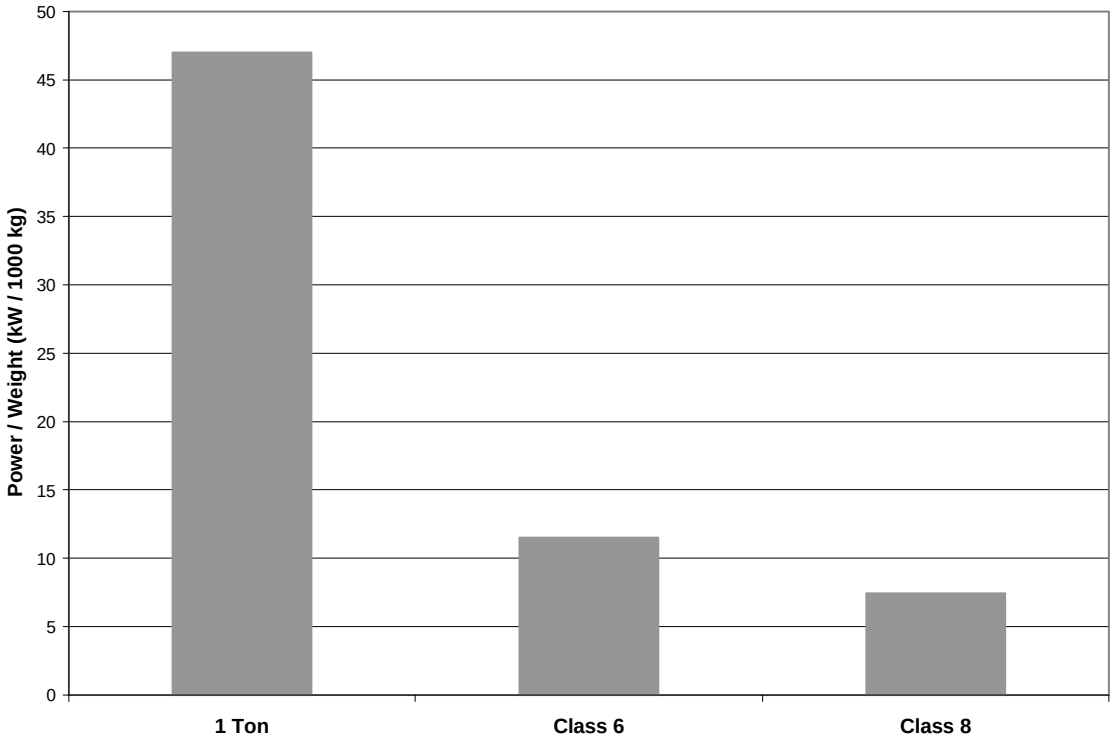

Figure 3.1.4 Typical Power / Weight ratios for various vehicle classes.

3.2 Drive Cycles

The three vehicles were simulated over the following speed - time traces. The traces were chosen to represent a wide variety of driving situations from low speed, highly transient urban routes to high-speed highway scenarios.

The Freeway, City-Suburban Heavy Vehicle Cycle (CSHVC), and Yard Cycles in Figures 3.2.1 to 3.2.3 were developed from examination of actual driving scenarios. The Freeway Cycle includes data from travel on four lane highways including entrance and exit ramps. The CSHVC Cycle is composed of data taken from travel in dense traffic with stoplights as well as delivery routes on the outskirts of cities. The Yard Cycle data involves trips that included changing trailers, changing tires, and driving to fueling sites. [12]

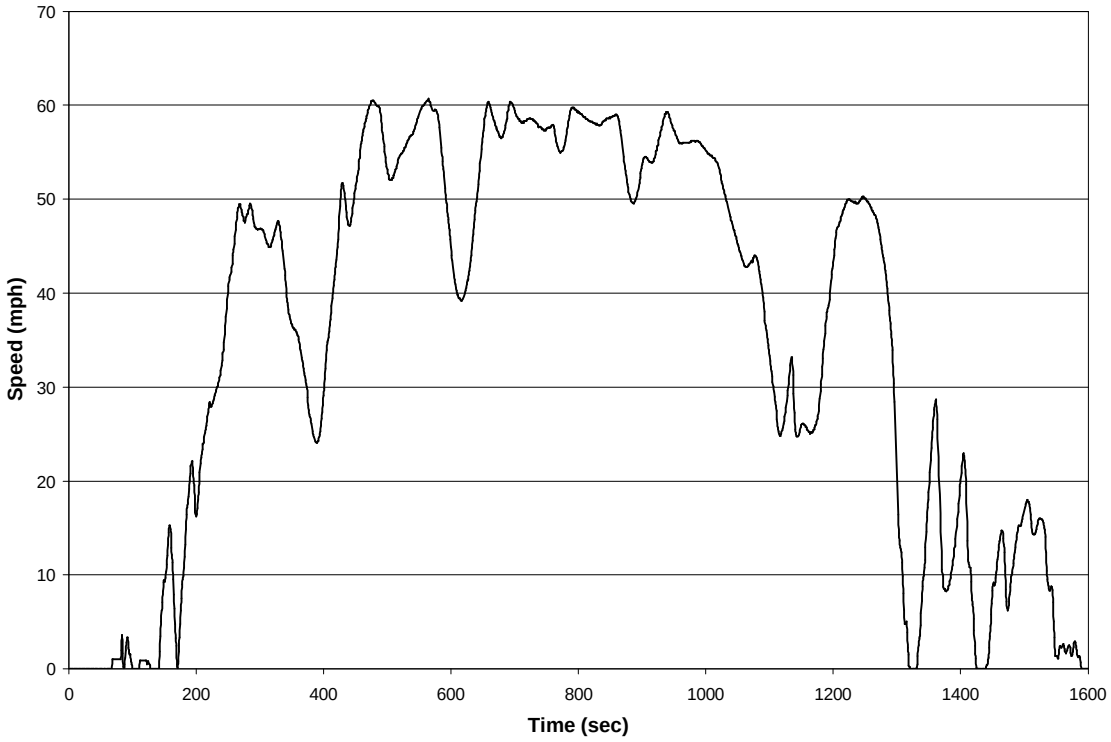

Figure 3.2.1 Speed – Time trace for the Freeway Cycle.

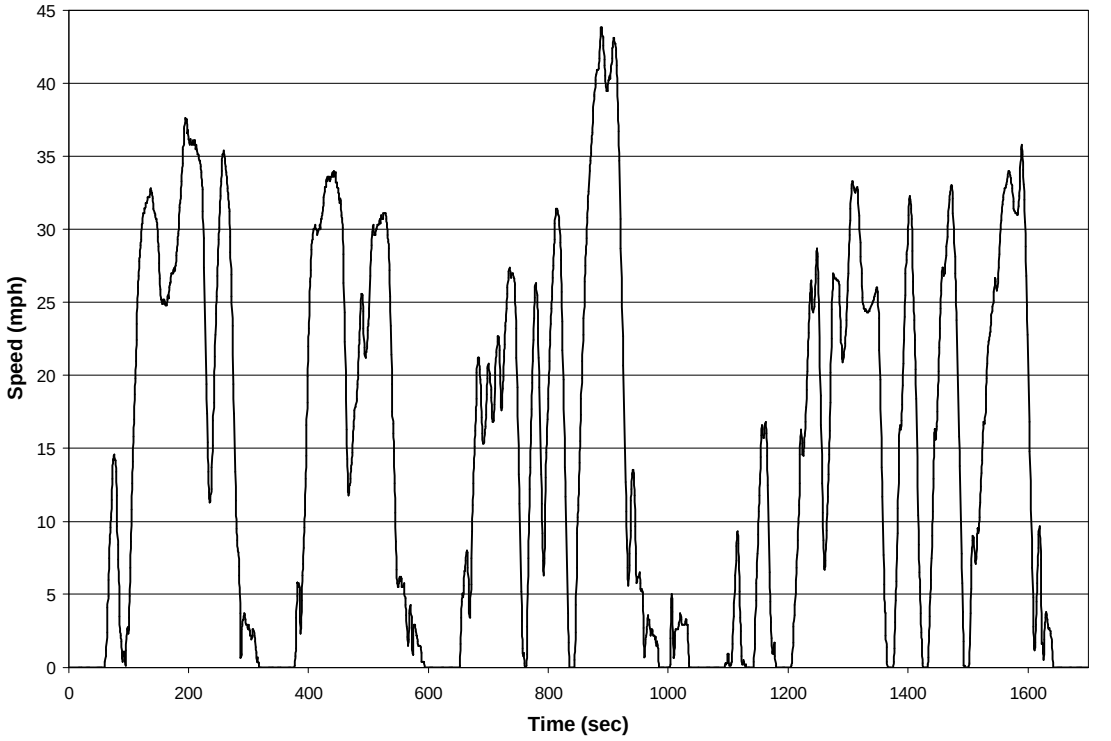

Figure 3.2.2 Speed – Time trace for the CSHVC.

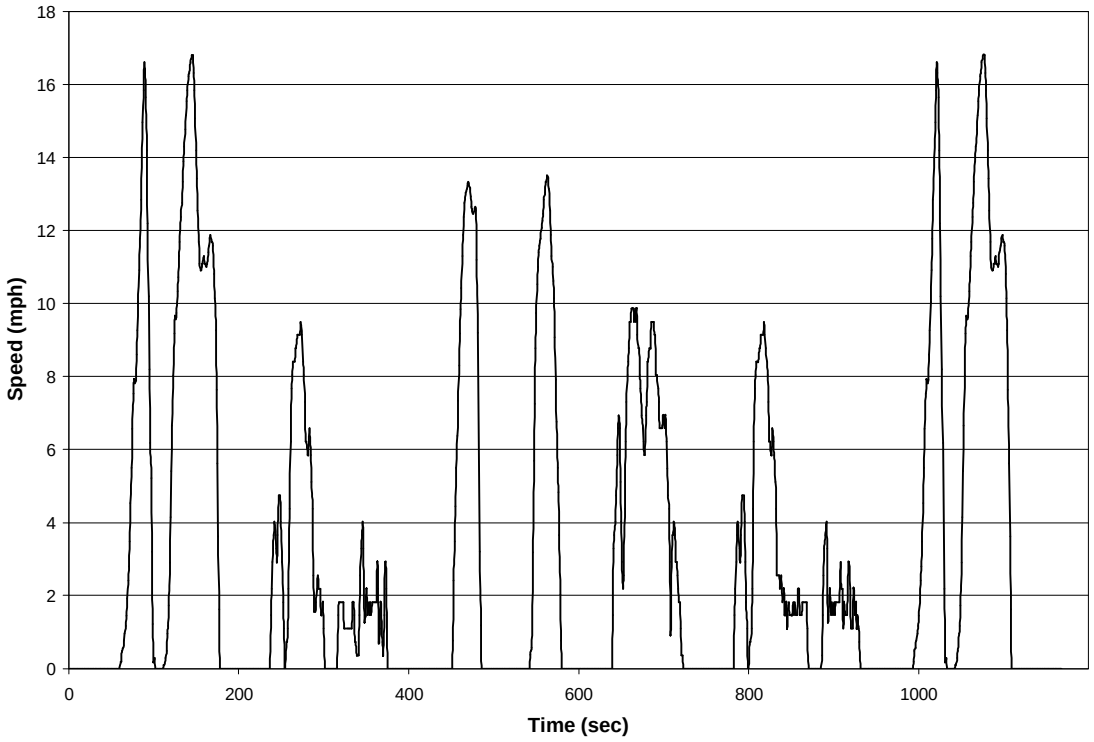

Figure 3.2.3 Speed – Time trace for the Yard Cycle.

The Manhattan Cycle was developed from actual in-use conventional and hybrid-electric transit bus operation in Manhattan. The data was divided into micro-trips consisting of a start from idle, acceleration to speed, and deceleration back to idle. The data set included 399 of these micro-trips. A computer program randomly combined five micro-trips from the hybrid-electric bus data and five micro-trips from the conventional bus data and compared the statistical makeup of the created cycle to the overall data. The combination that most closely matched the overall data was chosen. [13]

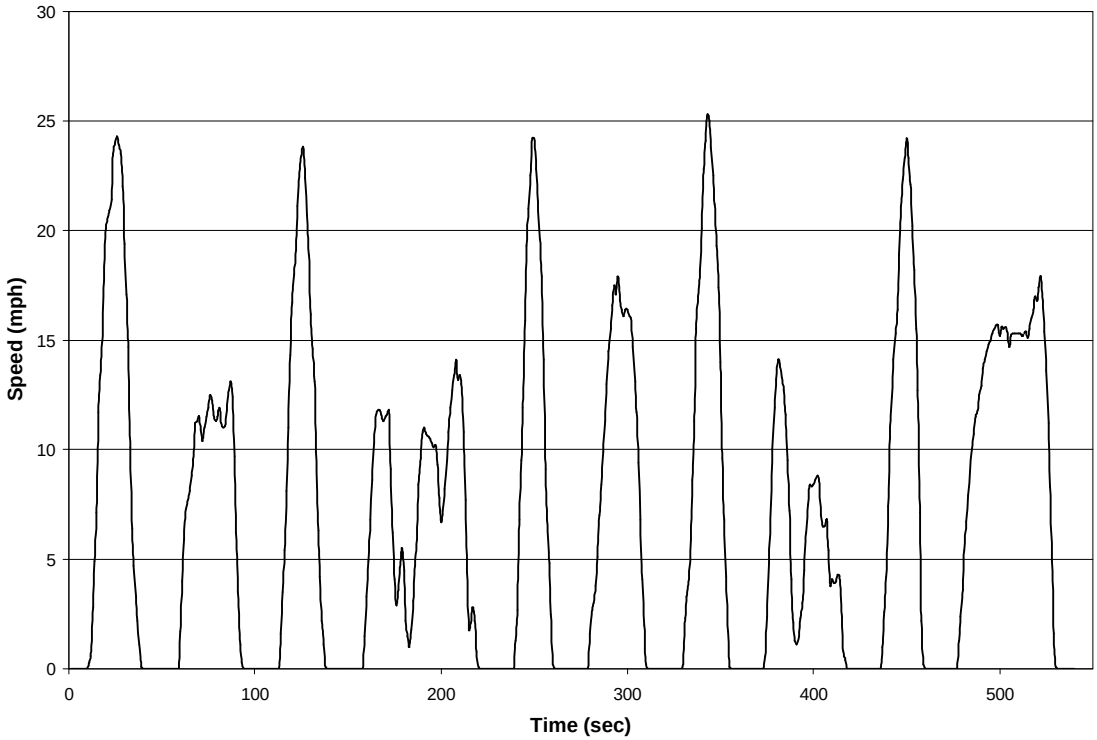

Figure 3.2.4 Speed – Time trace for the Manhattan Cycle.

Test D, also known as the 'EPA urban dynamometer driving cycle for heavy trucks' or UDDC, was developed using data logged from buses, trucks, and tractor-trailers operating in New York and Los Angeles under both freeway and non-freeway conditions. A Monte Carlo simulation was then used to produce the cycle. [14]

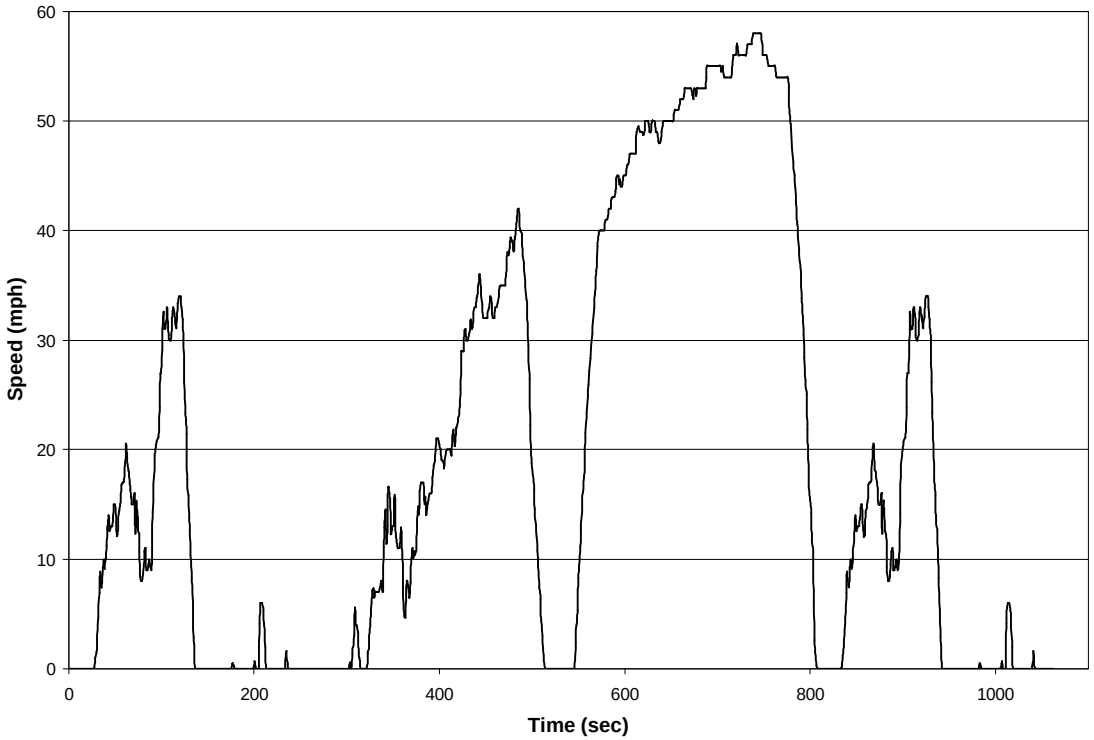

Figure 3.2.5 Speed – Time trace for the Test D Cycle.

To simulate the vehicles over a cycle more representative of a wide variety of driving situations, the five previous cycles were combined to form one, continuous speed-time trace. The ordering was: Yard, Manhattan, CSHVC, Freeway, and Test D. It will be referred to as the Combined Cycle.

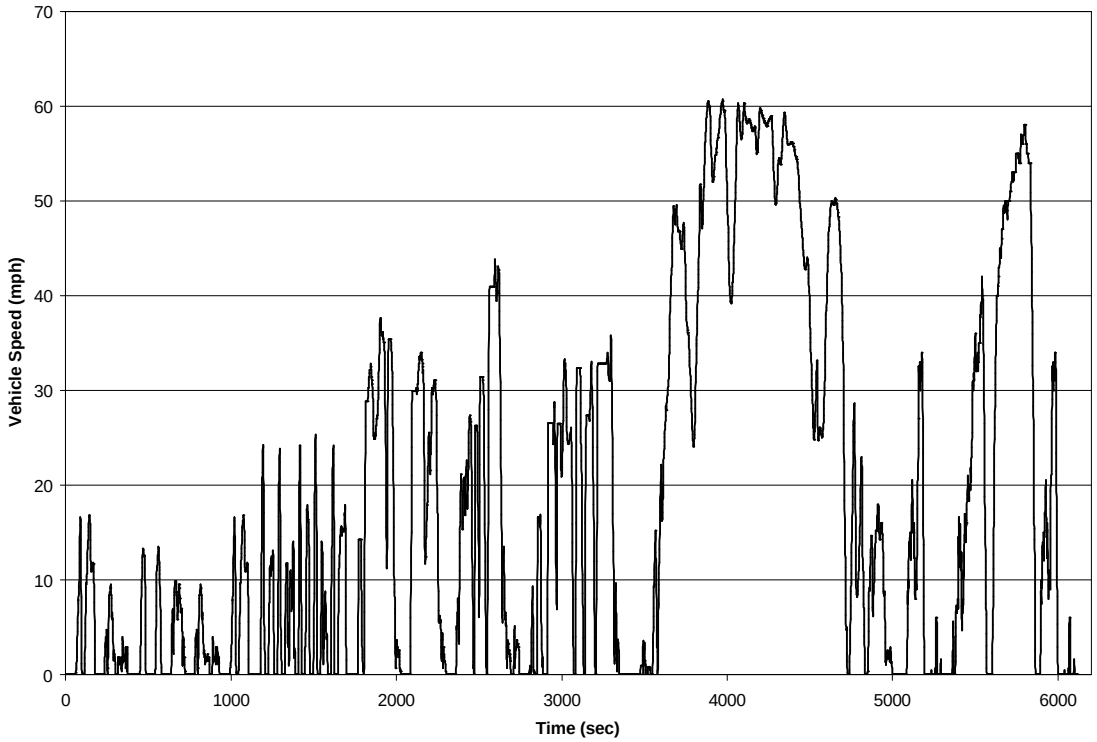

Figure 3.2.6 Speed – Time trace for the Combined Cycle.

Table 3.2.1 Cycle data.

Cycle	max speed	avg speed	% idle	avg spd w/o idle	avg/max spd w/o idle
	mph	mph		mph	
CSHVC	43.84	16.03	23.18	20.87	0.48
Freeway	60.73	33.96	10.86	38.10	0.63
Manhattan	56.58	24.22	21.72	30.98	0.55
Yard	16.80	3.33	47.35	6.32	0.38
Test D	58	18.8	33.4	28.23	0.49
Combined	60.73	18.13	27.39	24.97	0.30

3.3 Drive Cycle Power Requirements

Several factors affect the power required to drive a vehicle. These factors include the vehicle weight, engine efficiency, driveline efficiency, aerodynamic drag, rolling resistance, road grade, and accessory loads.

The forces acting on a moving vehicle include aerodynamic drag, rolling resistance, road grade force, and inertial force.

$$\Sigma F = F_i = F_w - F_D - F_{rr} - F_q \quad (1)$$

The aerodynamic drag on an object is based on the density of the fluid it is traveling in, its velocity, its drag coefficient, and its frontal area. It is the force required to push the vehicle through the air.

$$F_D = \tfrac{1}{2} r V^2 C_D A \quad (2)$$

Rolling resistance comes from a combination of the weight of the vehicle deforming the shape of the tire, the friction between the tire and the roadway, and air friction across the tire surface. [15]

$$F_{rr} = mmg \quad (3)$$

The force on a vehicle due to road grade is due to a portion of the vehicle's weight vector being directed against the direction of travel when θ is positive and with the direction of travel when θ is negative.

$$F_q = mg \sin q \quad (4)$$

From basic statics, any object has an associated inertial force.

$$F_i = m \frac{dV}{dt} \quad (5)$$

Summing the forces on the vehicle yields,

$$\Sigma F = m \frac{dV}{dt} = -\left(\tfrac{1}{2} r V^2 C_D A + mmg + mg \sin q\right) + F_w \quad (6)$$

Since power can be calculated from,

$$Power = Force * Velocity \quad (7)$$

Multiplying Equation 6 by the vehicle velocity yields,

$$mV\frac{dV}{dt} = F_w V - \left(\tfrac{1}{2} r V^3 C_D A + mmgV + mgV\sin q\right) \quad (8)$$

Finally, the power to move an vehicle is based on its aerodynamics, the rolling resistance of its tires, the road grade, and the desired acceleration.

$$P_w = mV\frac{dV}{dt} - \left(\tfrac{1}{2} r V^3 C_D A + mmgV + mgV\sin q\right) \quad (9)$$

In addition to the power requirements for driving the vehicle, auxiliary loads and driveline efficiencies can make a significant difference in the power required from the engine. Here, the driveline is assumed to be 95% efficient although transmissions and differentials tend to become less efficient under low loads. Accessory loads include the power needed to drive air conditioning systems, power steering, and electrical loads. Accessory loads were assumed to be 5kW, 10kW, and 15kW for the Class 2B, Class 6, and Class 8 vehicles, respectively. Accessory loads include air conditioning, power steering, cooling fans, alternator, and air compressors. The Class 8 15kW load represents the load from the air conditioner and other accessories for a city bus with a full load of passengers on a hot day. Auxiliary loads for the other classes were scaled according to vehicle weight. This results in an overall power required from the engine.

$$P_{req\ engine} = \frac{P_{req\ wheels}}{h_{driveline}} + P_{auxilliary\ loads} \quad (10)$$

The significance of each of the power requirements to drive the vehicle changes under different conditions. When high accelerations are demanded, the inertial term dominates the power requirements. At low speeds, rolling resistance is quite significant compared to aerodynamic drag, but at high speeds, the V^3 term causes aerodynamic drag

to dominate. As the road grade becomes increasingly positive or negative, the resulting power demand or available regenerative braking energy can become quite significant.

In Figures 3.3.1 through 3.3.18, the total energy requirements for the vehicle over the cycle can be found by finding the area between the positive sections of the trace and the x-axis and subtracting the area between the negative sections and the x-axis. The negative portion of the power trace represents the opportunity to capture regenerative braking energy. In a conventional vehicle, this energy is lost through conventional braking.

Figures 3.3.1 through 3.3.3 show the power requirements for each vehicle over the Freeway cycle. The power demand for each vehicle is positive over extended periods of time. There is an obvious lack of opportunity for regenerative braking. In a constant speed situation such as an OTR tractor in the mid-west, even less regenerative braking energy is available and any hybrid system that relies heavily on battery power would be at a major disadvantage. This disadvantage would come from the "dead weight" of the batteries and motor. Since there is little opportunity for regenerative braking, any use of the motor would deplete the batteries without a means to recharge them. This limits the use of the hybrid system and any gains that it might bring and only serves to limit the maximum payload of the truck. The 66 kW maximum power requirement for the Class 2B vehicle is well below the 163 kW available power of the average vehicle. While this suggests that the engine is oversized and considerable efficiency improvements might be gained by downsizing the powerplant, consumer demand for high performance from this class limits the extent of change that would still meet consumer acceptability. The power requirements of the Class 6 vehicle exceed the 125 kW ceiling during a few peak

accelerations, but the end effect on performance over the cycle would be minimal and well within acceptable performance bounds. Similarly, the Class 8 power trace exceeds the 205 kW limit over several periods of the cycle, but, again, consumer expectations of dynamic performance are quite low. Also, the power needed to exactly meet the trace would require a very powerful engine or engine-electric motor combination that would tend to be oversized and inefficient under less demanding situations.

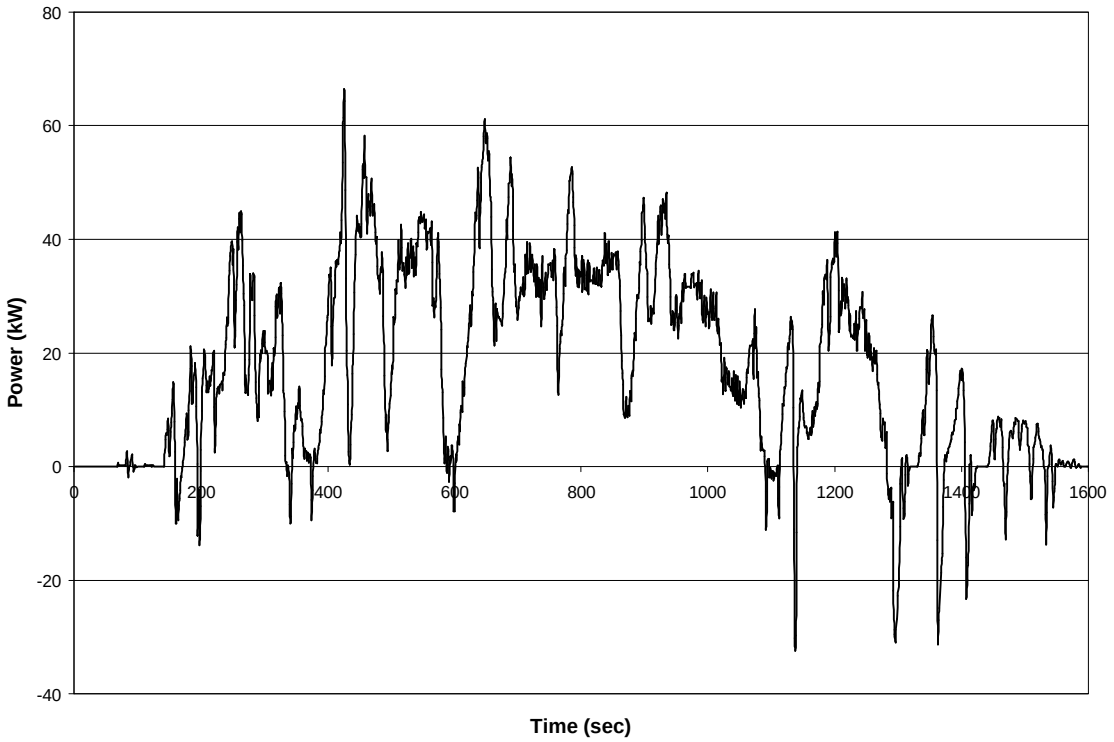

Figure 3.3.1 Power required for Class 2B vehicle over the Freeway Cycle.

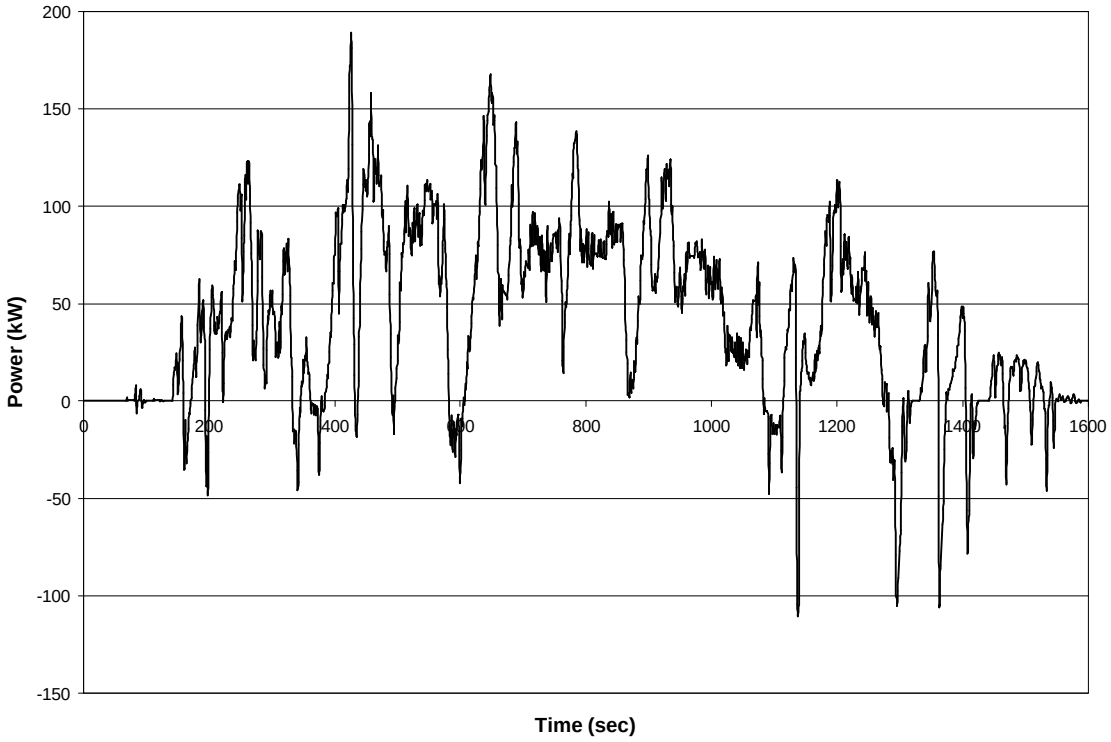

Figure 3.3.2 Power required for Class 6 vehicle over the Freeway Cycle.

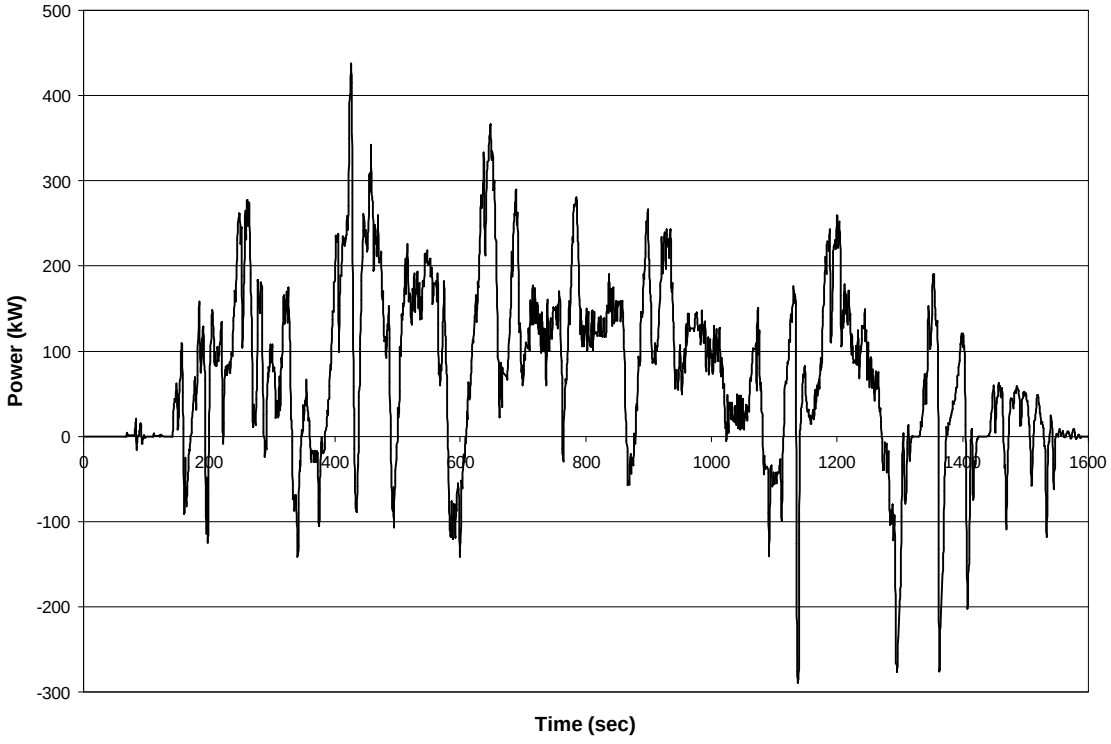

Figure 3.3.3 Power required for Class 8 vehicle over the Freeway Cycle.

Figures 3.3.4 through 3.3.6 show the power requirements for each vehicle over the CSHVC. This cycle is much more transient than the Freeway Cycle. While there are several large power spikes, there is a large amount of regenerative braking energy available. Peak power requirement only exceeds the power available to the vehicle for Class 8.

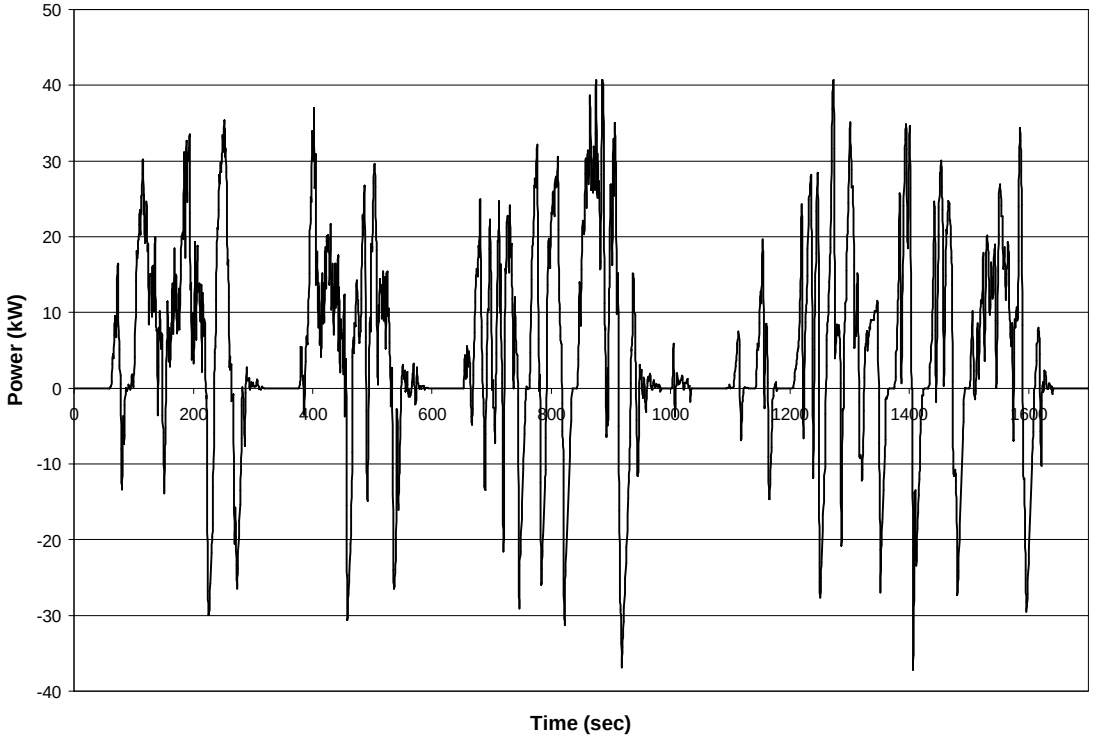

Figure 3.3.4 Power required for Class 2B vehicle over the CSHVC.

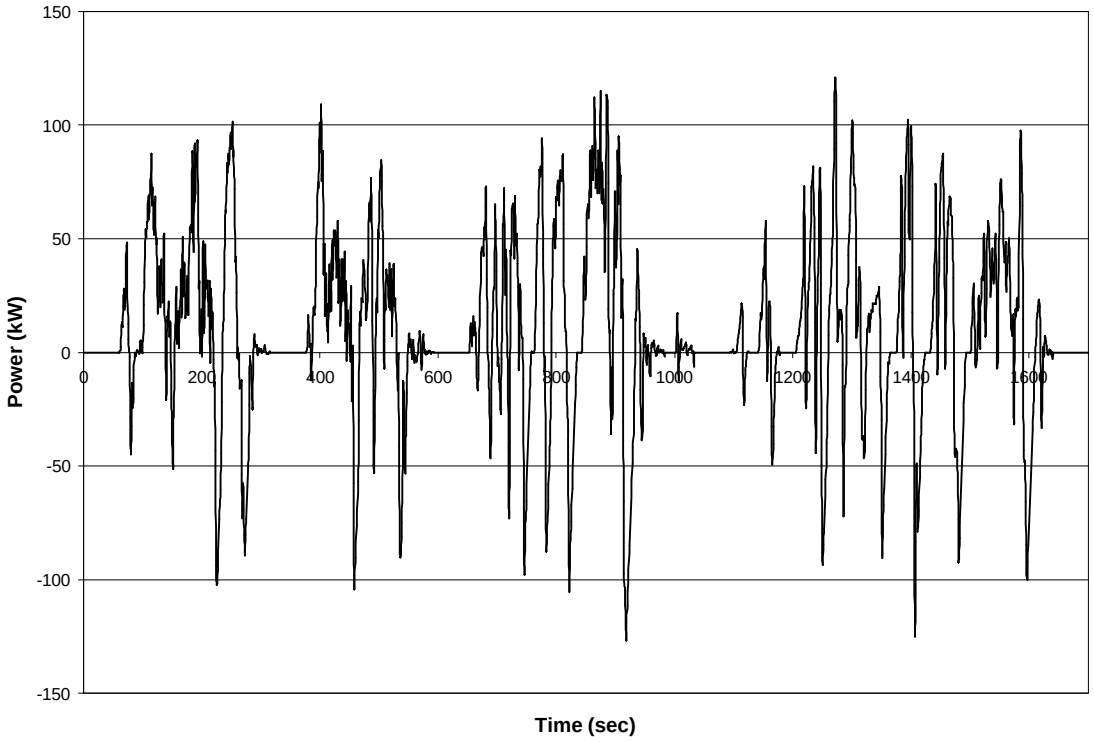

Figure 3.3.5 Power required for Class 6 vehicle over the CSHVC.

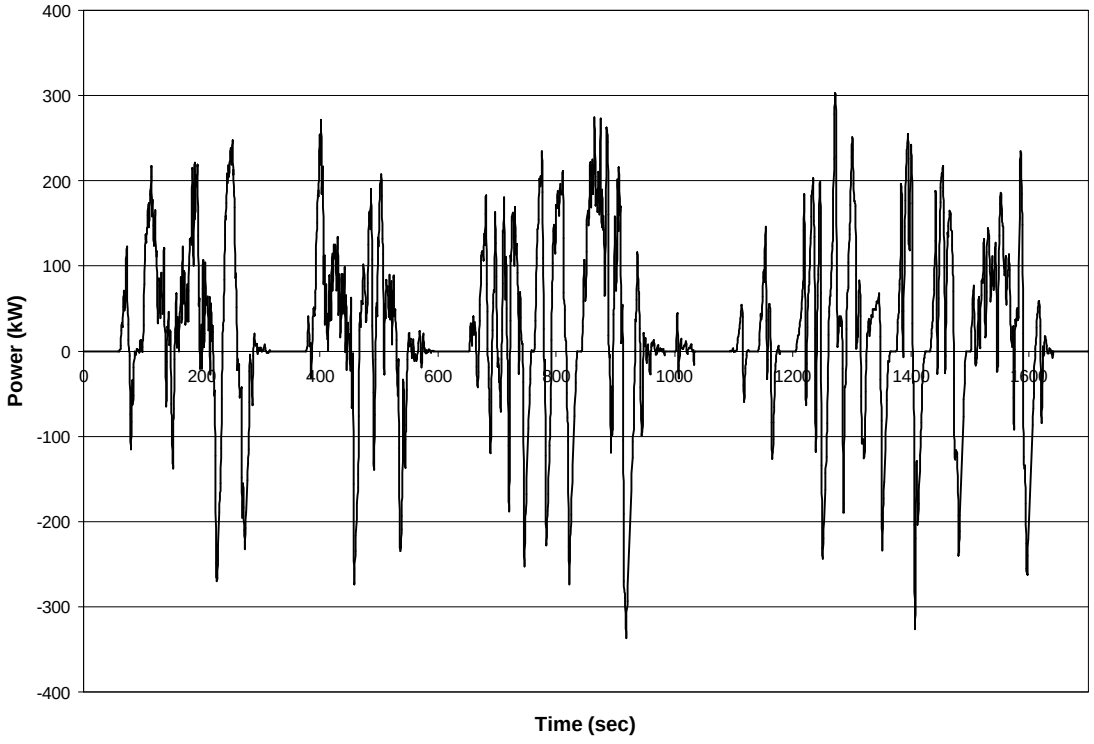

Figure 3.3.6 Power required for Class 8 vehicle over the CSHVC.

Figures 3.3.7 through 3.3.9 show the power requirements for each vehicle over the Yard Cycle. The low speeds and accelerations in this cycle result in extremely low power requirements. This, combined with fairly significant available regenerative braking energy, results in average power requirements close to zero. The Class 2B vehicle requires only 14 kW of peak power to meet the cycle while the Class 6 and 8 vehicles require 40 and 105 kW respectively.

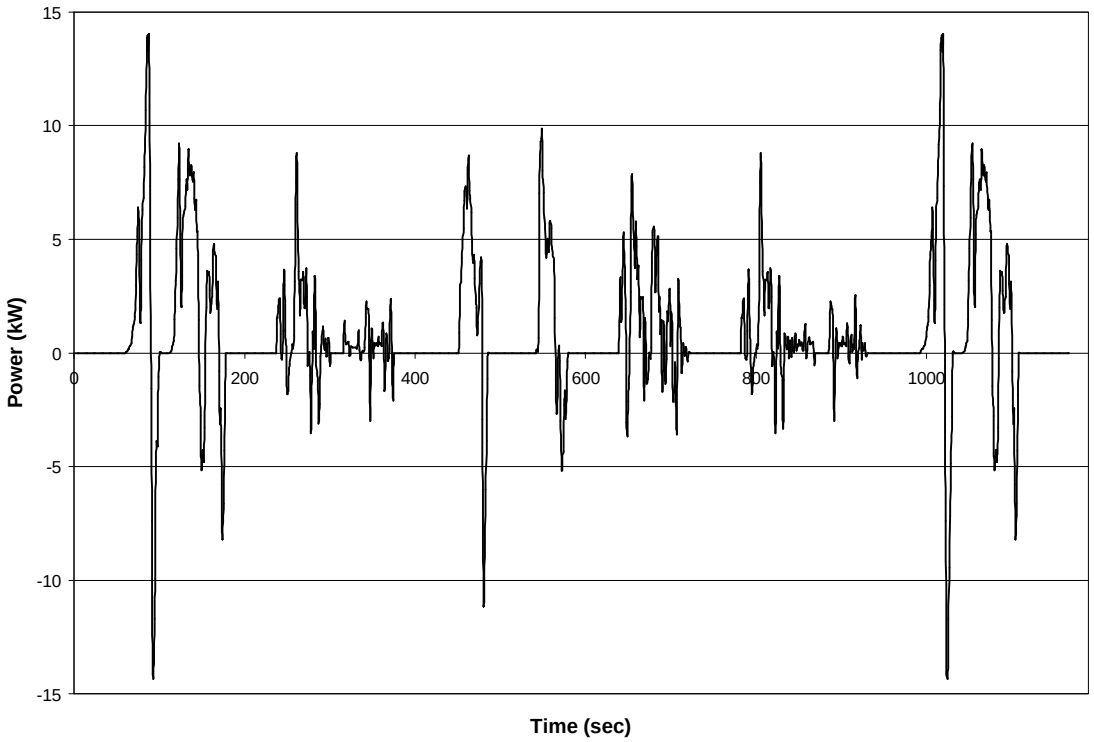

Figure 3.3.7 Power required for Class 2B vehicle over the Yard Cycle.

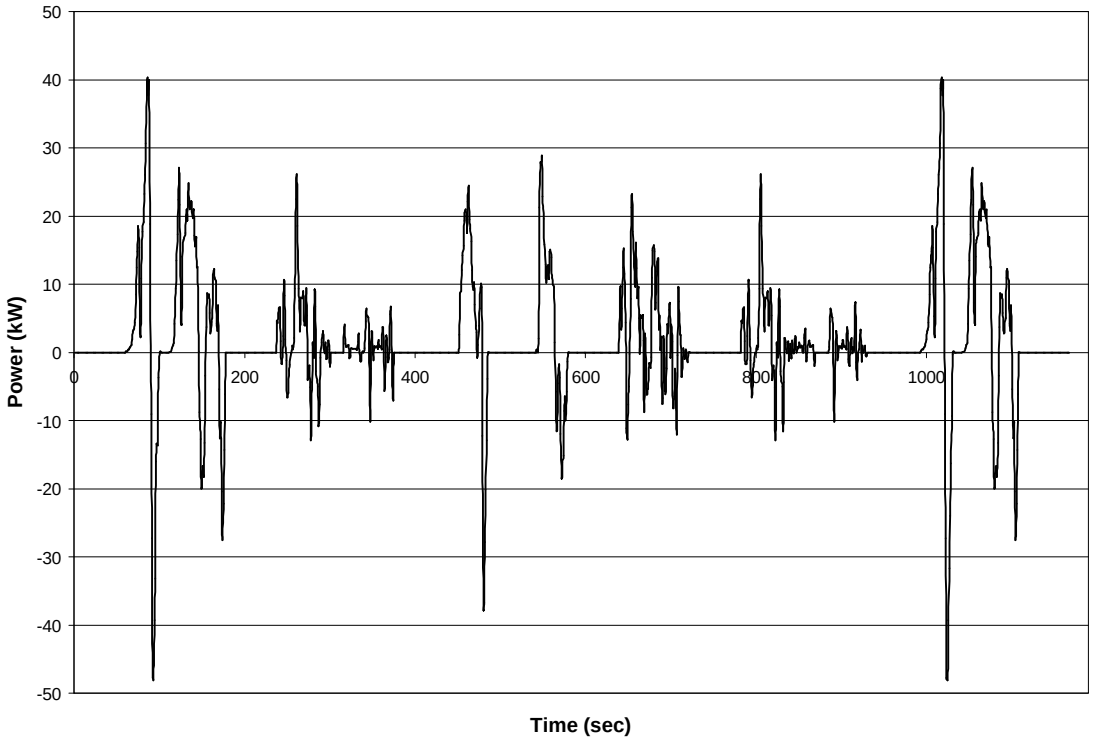

Figure 3.3.8 Power required for Class 6 vehicle over the Yard Cycle.

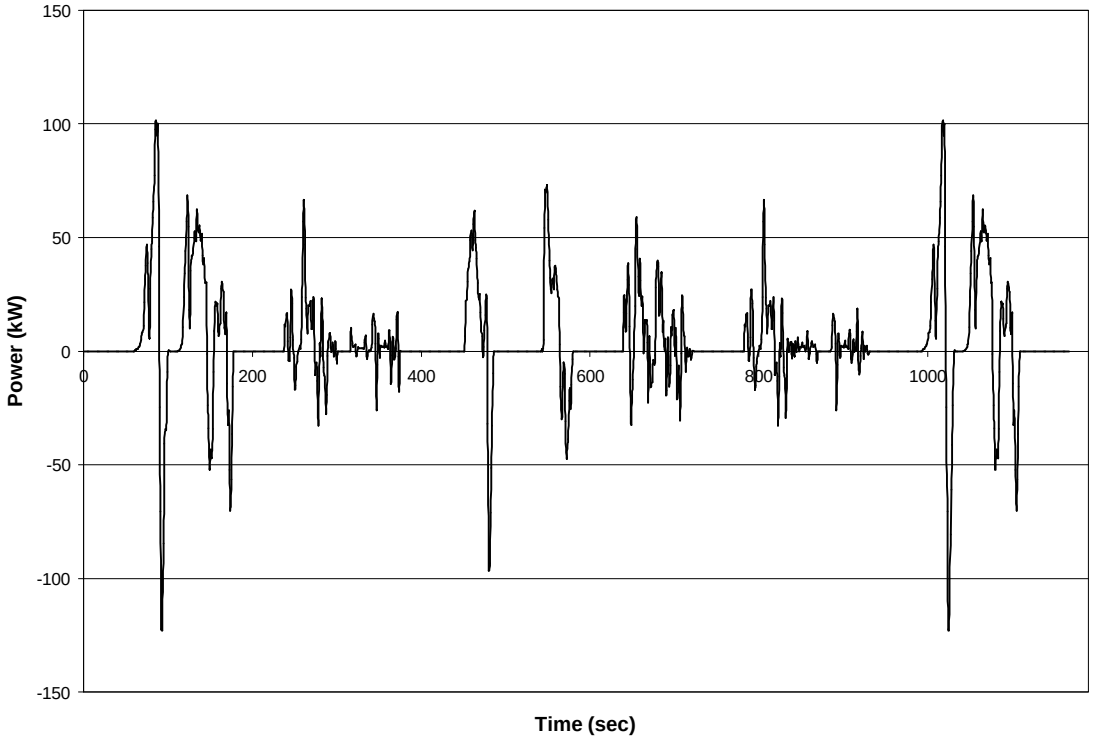

Figure 3.3.9 Power required for Class 8 vehicle over the Yard Cycle.

Figures 3.3.10 through 3.3.12 show the power requirements for each vehicle over the Manhattan Cycle. This cycle is very repetitive in that it follows a pattern of quite similar accelerations and decelerations. This results in a very low average power requirement. While power spikes for the Class 6 and 8 vehicles are over the limits, they are not excessive. The limited power available to the average vehicles would not result in large deviations from the trace.

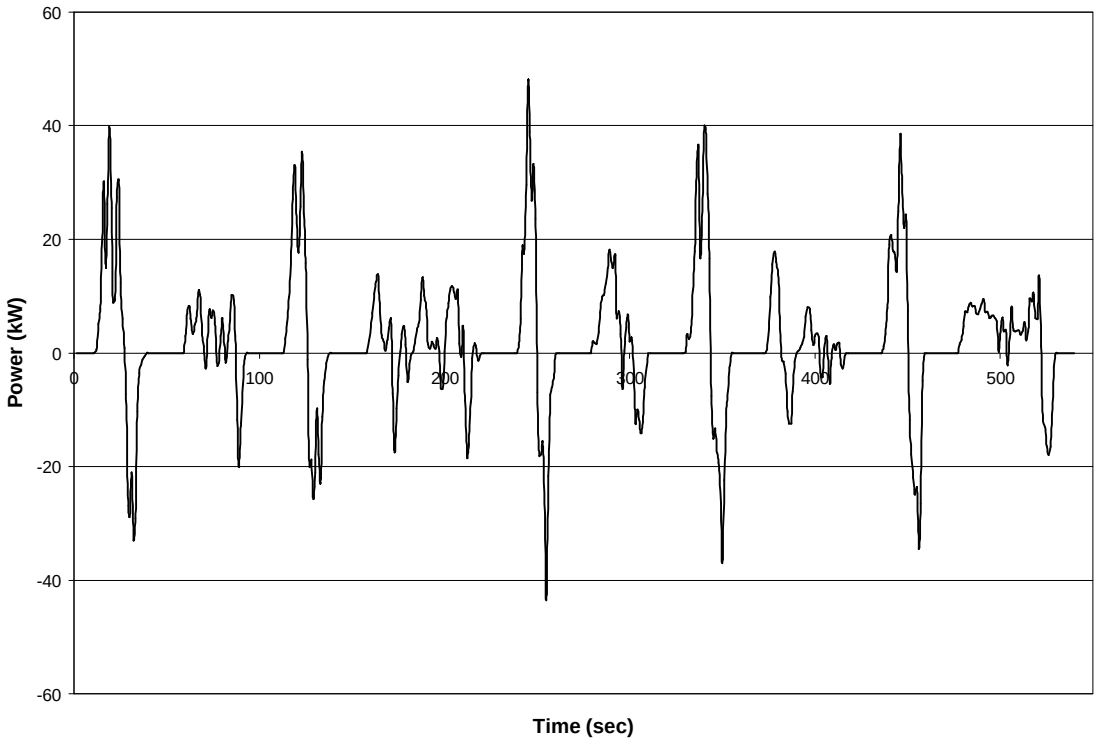

Figure 3.3.10 Power required for Class 2B vehicle over the Manhattan Cycle.

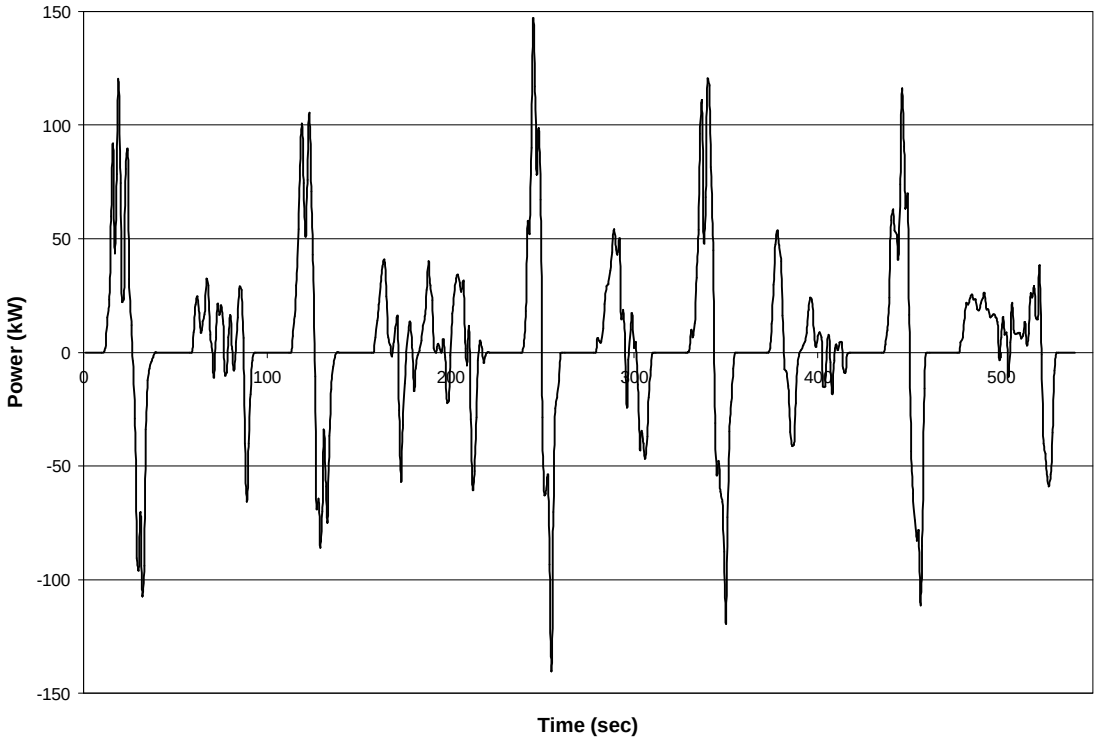

Figure 3.3.11 Power required for Class 6 vehicle over the Manhattan Cycle.

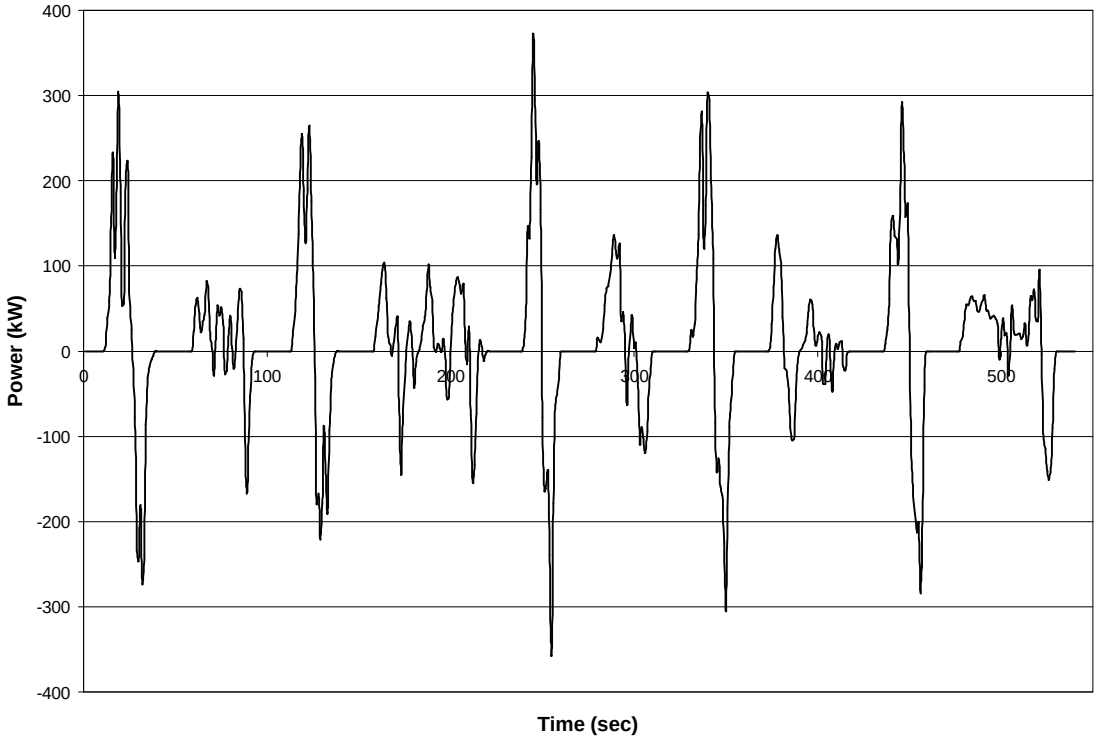

Figure 3.3.12 Power required for Class 8 vehicle over the Manhattan Cycle.

Figures 3.3.13 through 3.3.15 show the power requirements for each vehicle over the Test D Cycle.

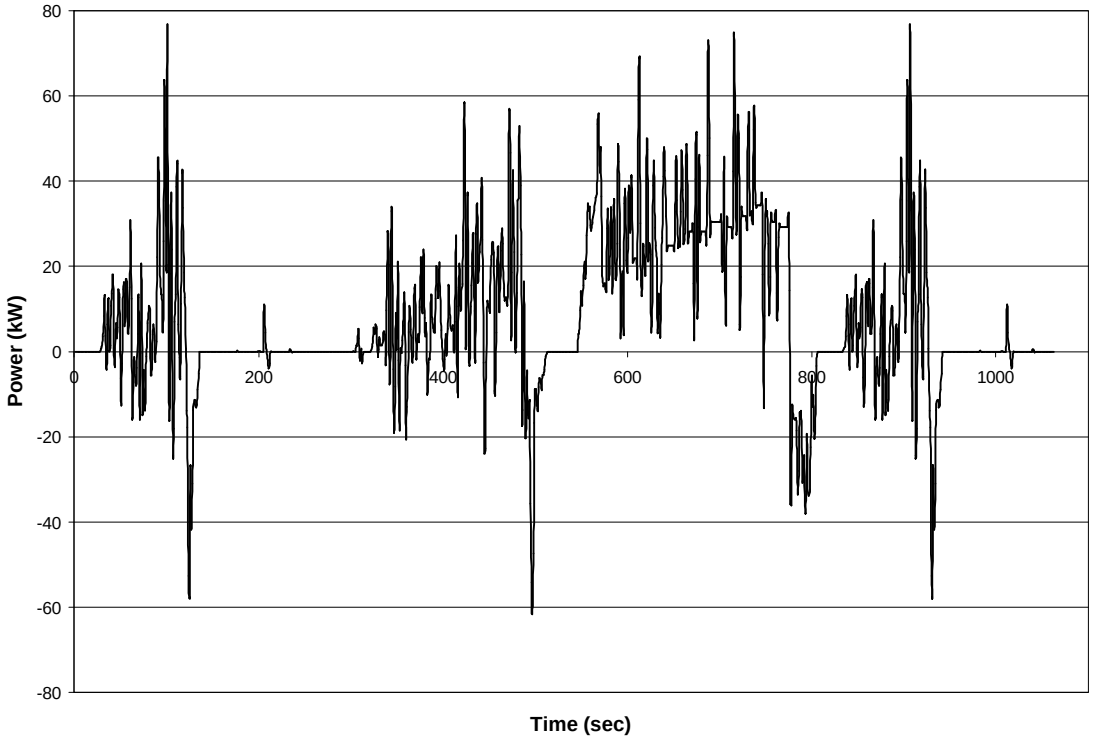

Figure 3.3.13 Power required for Class 2B vehicle over the Test D Cycle.

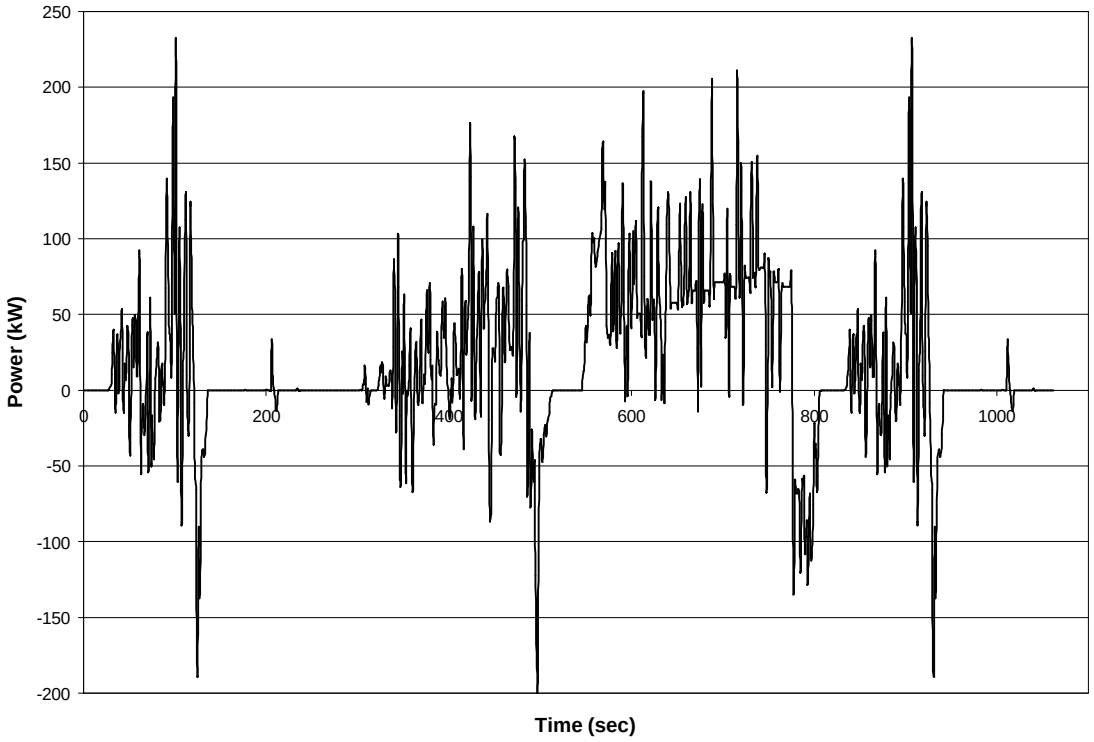

Figure 3.3.14 Power required for Class 6 vehicle over the Test D Cycle.

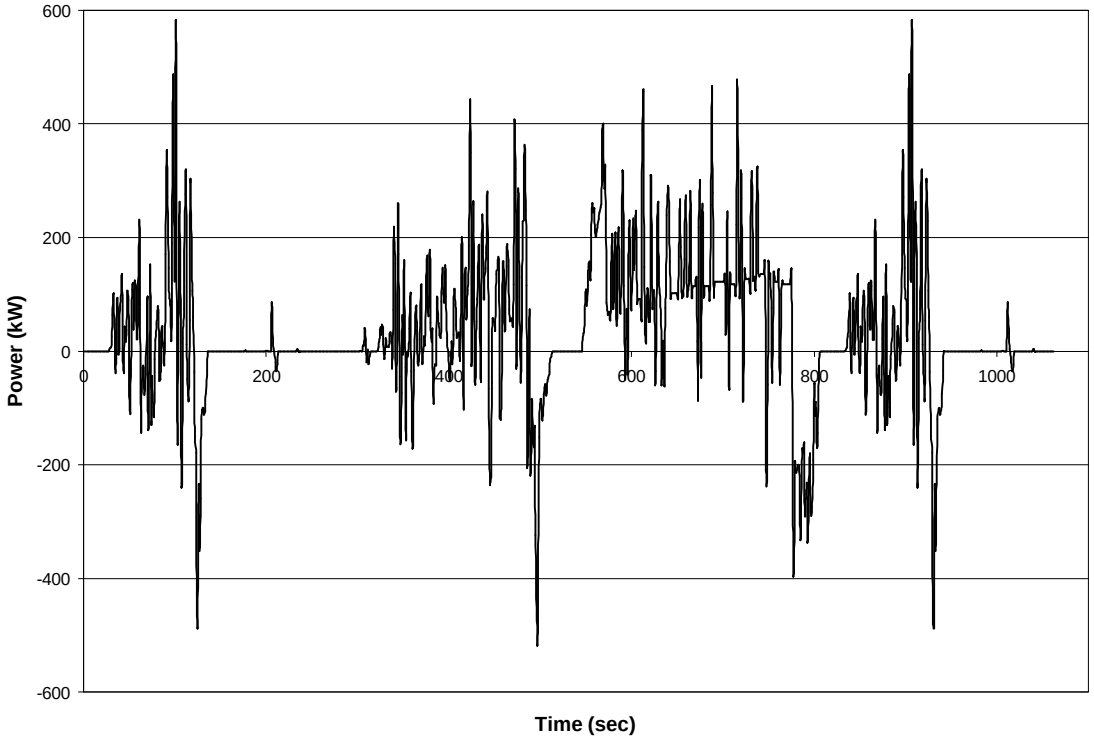

Figure 3.3.15 Power required for Class 8 vehicle over the Test D Cycle.

Figures 3.3.16 through 3.3.18 show the power requirements for each vehicle over the Combined Cycle.

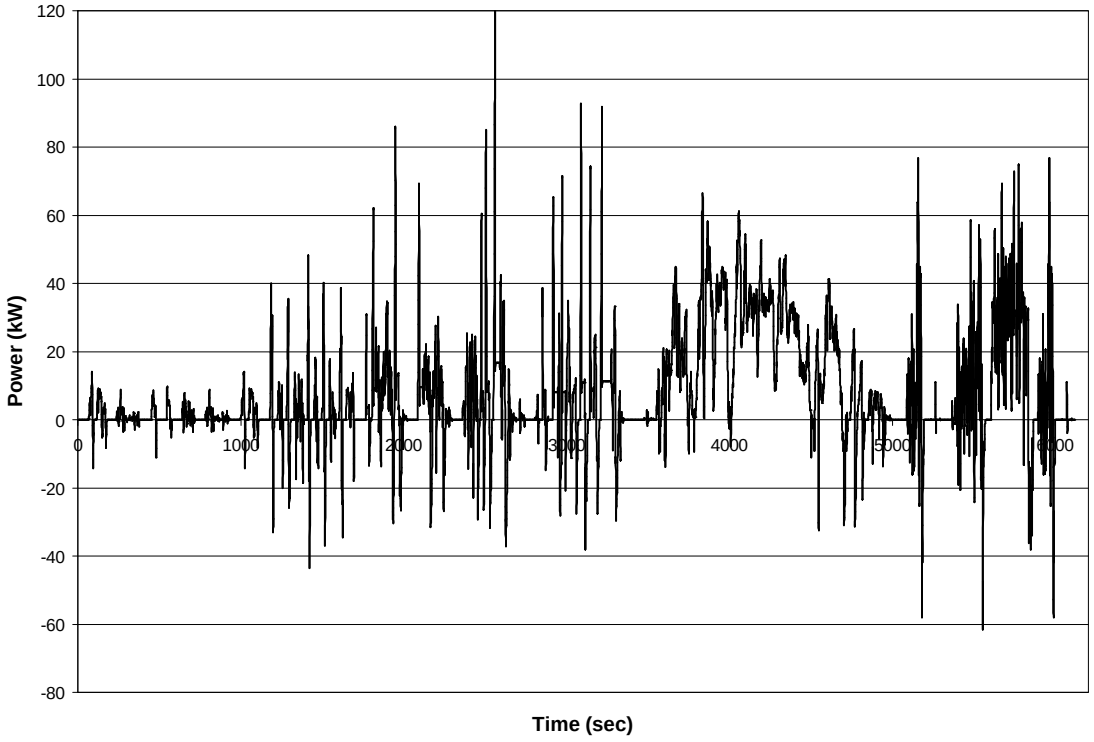

Figure 3.3.16 Power required for Class 2B vehicle over the Combined Cycle.

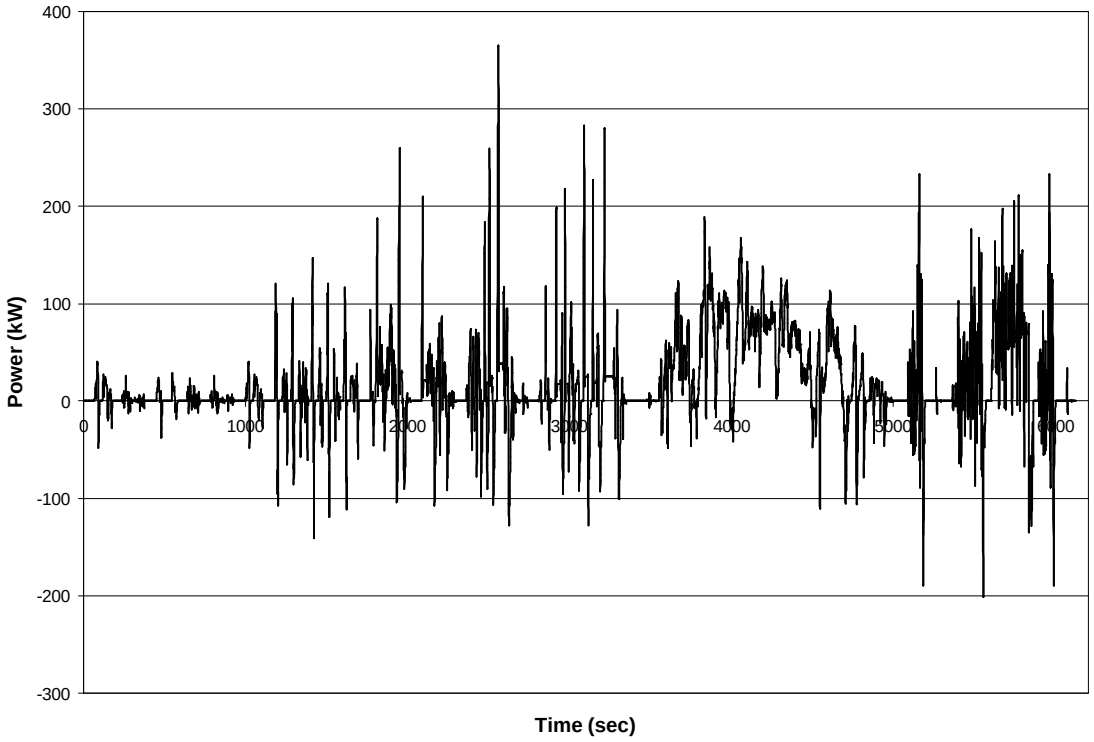

Figure 3.3.17 Power required for Class 6 vehicle over the Combined Cycle.

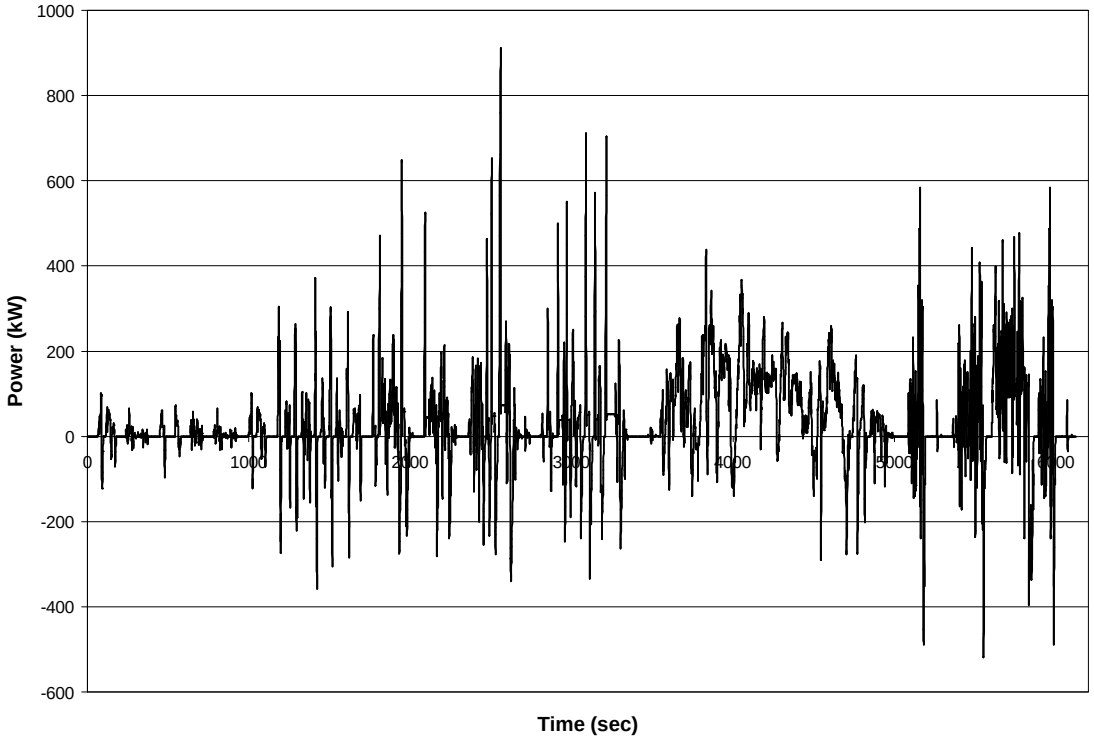

Figure 3.3.18 Power required for Class 8 vehicle over the Combined Cycle.

3.4 Simulation

Given an instantaneous power required at the vehicle wheels determined from the road load equation, the power requirements from the ICE, electric motor, and batteries can be determined. Similar control strategies were used to simulate the series and parallel HEVs.

3.4.1 Series Control Strategy

In the series HEV control strategy, the ICE is run at a constant percentage of the road load power, C_1, plus or minus a State of Charge (SoC) correction factor, as shown in Equation 11 while the electric motor supplies or absorbs the balance of the power required at the wheels.

$$P_e = C_1 P_w - C_2\left(SoC_i - SoC_t\right) \tag{11}$$

The SoC correction factor demands more power from the ICE when the actual SoC falls below the target value and decreases the demand on the ICE when the target SoC is exceeded. This also serves to smooth the power from the ICE relative to the road load power. The power from the ICE is delivered directly to the electric motor through a generator to avoid the losses associated with using the batteries while the electric motor draws power from or delivers power to the batteries. Additionally, the ICE can be set to run at a minimum power to account for any auxiliary loads associated with operating the vehicle.

3.4.2 Parallel Control Strategy

The parallel HEV uses the same control strategy equation as the series vehicle, but the power from the engine is directed to the wheels and accounts for a portion of the power demanded by the road load equation. The balance of the road load power is

provided by the electric motor. As in the series vehicle, a provision is made to account for auxiliary loads.

For the simulation of both the parallel HEV and conventional vehicle, the issue of gear-shifts and turbo lag are avoided. During gear-shifts with a manual transmission, the power delivered from the engine to the wheels briefly drops to zero. During the power drop and during transients from low to high power, turbo lag becomes important. Turbo-charged diesel engines such as those used in most automotive applications use exhaust driven turbines to drive compressors to increase the density of the intake air charge allowing for more fueling and power. At low engine speeds, the flow of exhaust gases is too low to properly spool the turbine and no power gains are seen. There is a brief time constant associated with sudden power demands by the driver through the accelerator pedal and speeding the engine to the point that the turbo-charger becomes effective and the engine delivers the power desired. This is also an issue when the engine speed drops during gear-shifts. Analysis of this issue would affect the results of the simulation.

3.4.3 Battery Model and Simulation

A simplified battery model was used to simulate the flow of power into and out of the batteries. Hawker Genesis G13EP batteries were chosen due to their availability, proper design and hardware for EV and HEV use, and low internal resistance.

Table 3.4.1 Hawker Genesis G13EP Battery Properties. [16]

Product	Hawker Genesis G13EP
Battery Type	Lead-Acid
Capacity	13 Ah
Nominal Full-charge Voltage	12.85 V
Internal Resistance	8.5 mΩ
Weight	4.9 kg

The energy capacity of the batteries in joules can be calculated from

$$E_b = 3600 V_b C_b N_b \tag{12}$$

To achieve the 300-400V operating range of the electric motors typically used in EV and HEV operations, 27 batteries were combined in a resulting in a 324V nominal voltage pack. Three battery packs were used in the Class 6 and 8 HEVs while one pack was used in the Class 2B vehicle.

Once the power required from the electric motor is known from the control strategy, the power demand from the batteries can be calculated. From the SoC of the batteries, a nominal voltage is known based on full charge and an effective empty level.

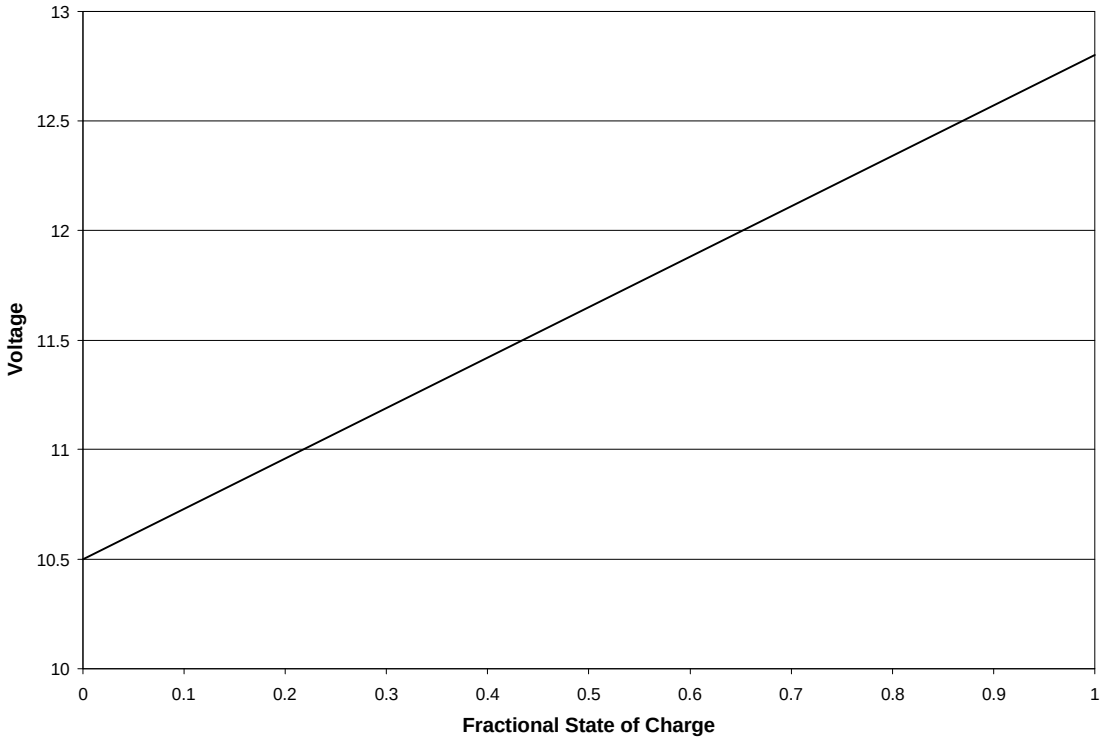

Figure 3.4.1 Battery voltage vs. SoC for Hawker Genesis G13EP. [16]

The SoC of the battery pack at any instant can be calculated from,

$$SoC_i = \frac{3600 V_{bi} C_b N_b}{E_b} \tag{13}$$

This determines the voltage of the battery pack. From this voltage, a current draw can be calculated based on,

$$I_b = \frac{P_m}{V_b} \tag{14}$$

Batteries have internal resistance resulting in power losses during discharge and charging. These losses are approximated based on the current demand on the batteries.

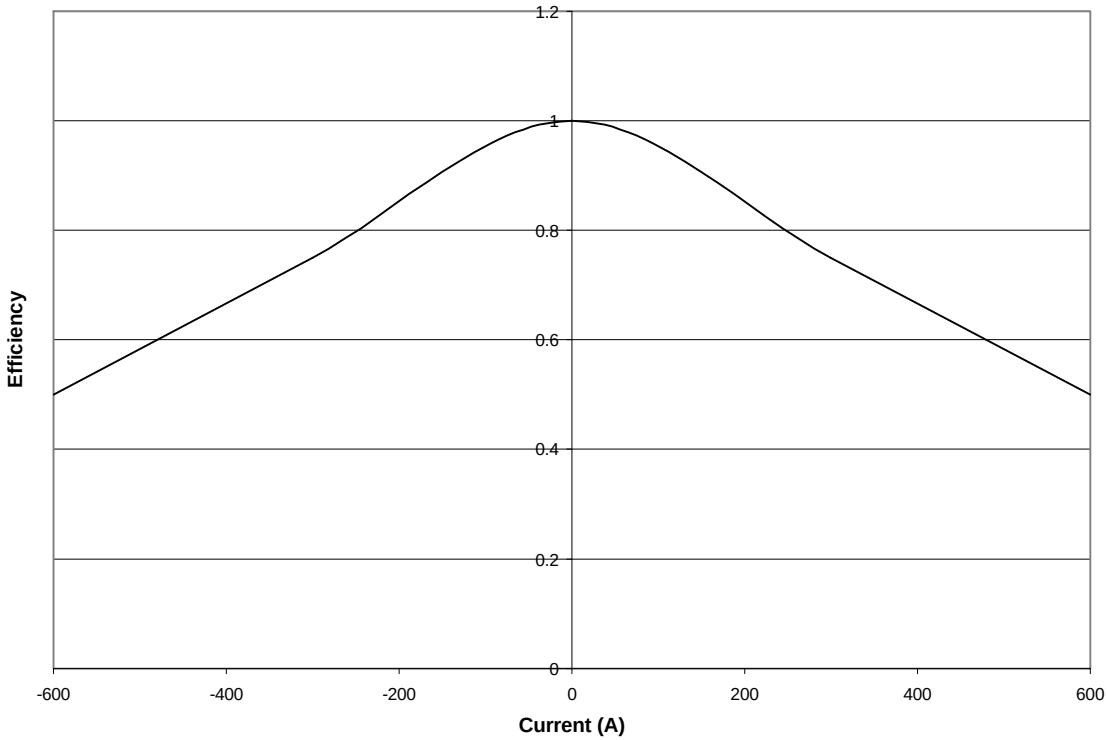

Figure 3.4.2 Battery efficiency vs. current. [17]

When power is demanded from the batteries by the electric motor, this efficiency factor causes a greater power draw from the batteries.

$$P_b = \frac{P_m}{h_b} \tag{15}$$

When power is being delivered to the batteries during regenerative braking or charging while driving, the efficiency factor decreases the power available to the battery below that delivered from the electric motor.

$$P_b = h_b P_m \tag{16}$$

Since the power flow at the batteries is known, and,

$$1\ joule = 1\,\frac{watt}{\sec ond}$$

a new SoC is calculated from,

$$SoC_i = \frac{SoC_{i-1}E_b - E_{bi}}{E_b} = \frac{SoC_{i-1}E_b - P_{bi}}{E_b} \tag{17}$$

Once the new SoC is calculated, the control strategy determines a new power level for the ICE and motor based on the road load power, the target SoC, and the constants, C_1 and C_2.

4. Simulation Results

To allow for comparison of the results for different vehicle configurations and cycle, for each value of C_1, C_2 was adjusted until the battery SoC at the end of the cycle was equal to the initial SoC. This is referred to as charge sustaining operation. C_2 governs the SoC dependence of the engine. If C_2 is high, the engine power will increase a large amount relative to the difference between the SoC and the target SoC. When the SoC climbs above the target SoC, the C_2 correction factor decreases the engine power to increase power demand on the electric motor and batteries. When the SoC falls below the target SoC, the correction factor increases the engine power reducing demand on the batteries and, in some instances, providing energy to the batteries through charging while driving. The initial and target SoC was set at 80% for all simulations. If the initial SoC was set at 100%, not only would this be an unrealistic expectation for a charge sustaining hybrid, but there would be no capacity for recapturing regenerative braking energy until the batteries had been somewhat depleted.

In consideration of the space required to present all the final data from simulation and optimization, only selected figures will be presented. The remaining figures are presented in the Appendix and all of the results will be addressed in discussion.

4.1 Simulation Results

Table 4.1.1 Conventional Vehicle uncorrected fuel economy from simulation.

	w/o auxiliary load			w/ auxiliary load		
Cycle	Class 2B	Class 6	Class 8	Class 2B	Class 6	Class 8
	mpg			mpg		
Freeway	5.30	9.52	5.70	4.20	6.61	3.83
CSHVR	3.55	5.32	3.07	1.99	2.73	1.61
Yard	1.06	1.48	0.93	0.41	0.54	0.33
Manhattan	2.06	3.12	1.89	0.84	1.16	0.71
Test D	4.81	8.24	4.69	2.31	3.35	1.97
Combined	3.97	6.42	3.80	2.23	3.18	1.89

Table 4.1.2 Average Fuel Economy for In-use Conventional Vehicles [18, 19]

	Fuel Economy
	mpg
Class 2	15.0
Class 6	7.3
Class 8	5.5
Class 8 Buses	2.0

Table 4.1.1 and 4.1.2 compare fuel economy for actual in-use and simulated conventional vehicles. If the in-use fuel economy figures for Class 8 are compared to the simulation results for the Freeway Cycle, they agree well. The average fuel economies in Table 4.1.2 are based on the total miles traveled and the total fuel consumed by all the vehicles in that class. The Class 8 average would tend to be weighted toward the fuel economy of OTR tractors due to the high number of miles they accumulate. If the Class 8 numbers are compared to the simulation results from the Freeway Cycle, they agree well. Similarly, the simulation results from the Manhattan Cycle are within 3% of the average Class 8 bus fuel economy. On average, the Class 6 simulation results agree fairly well with the average in-use fuel economy. Although the fuel economy shown for

average in-use Class 2 vehicles is most likely for unloaded vehicles, there is very little agreement between the Class 2B simulation results and the actual vehicle average fuel economy. This is due to the use of driving cycles unsuitable for Class 2B vehicles. The chosen cycles are designed for heavy-duty vehicles and incorporate accelerations and speeds appropriate for their power and weight. As shown in Figure 3.1.4, Class 2B vehicles have a higher power to weight ratio allowing for increased dynamic performance. When these vehicles are simulated over heavy-duty drive cycles, the engine is run at low power and low efficiency resulting in very poor fuel economy prediction.

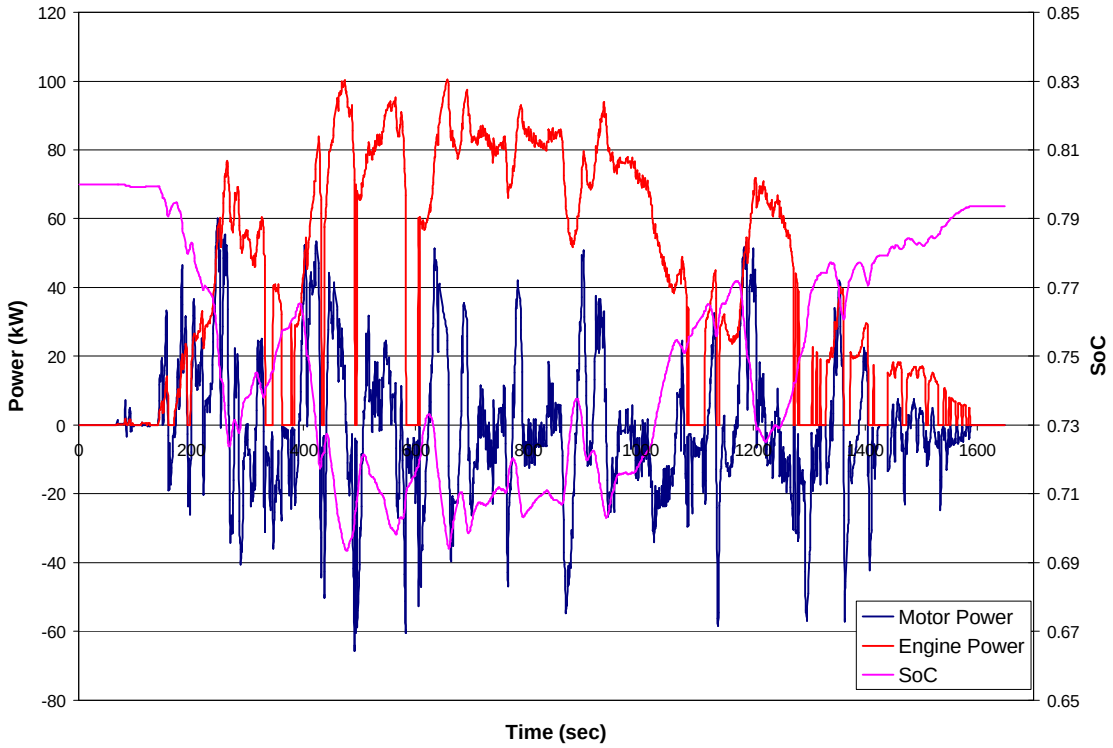

Figure 4.1.1 Class 6 Parallel HEV on Freeway Cycle without auxiliary load, C_1 = 0.2, C_2 = 3500.

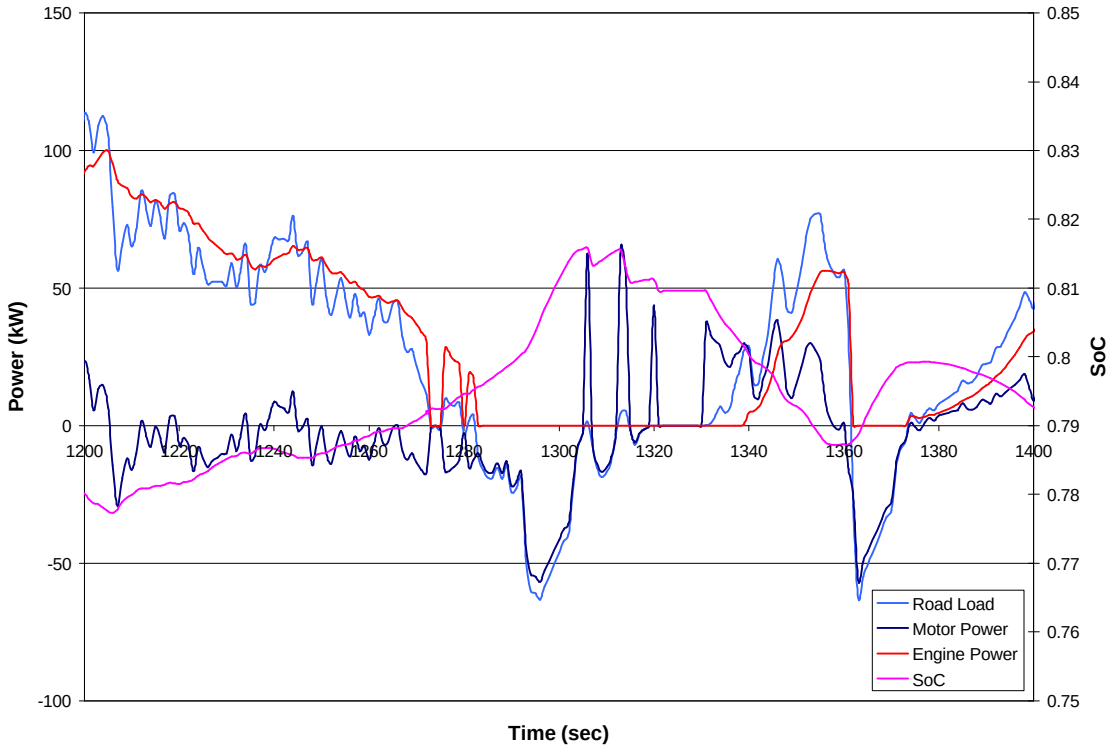

Figure 4.1.2 Expanded portion of Figure 4.1.1 from 1200 to 1400 seconds.

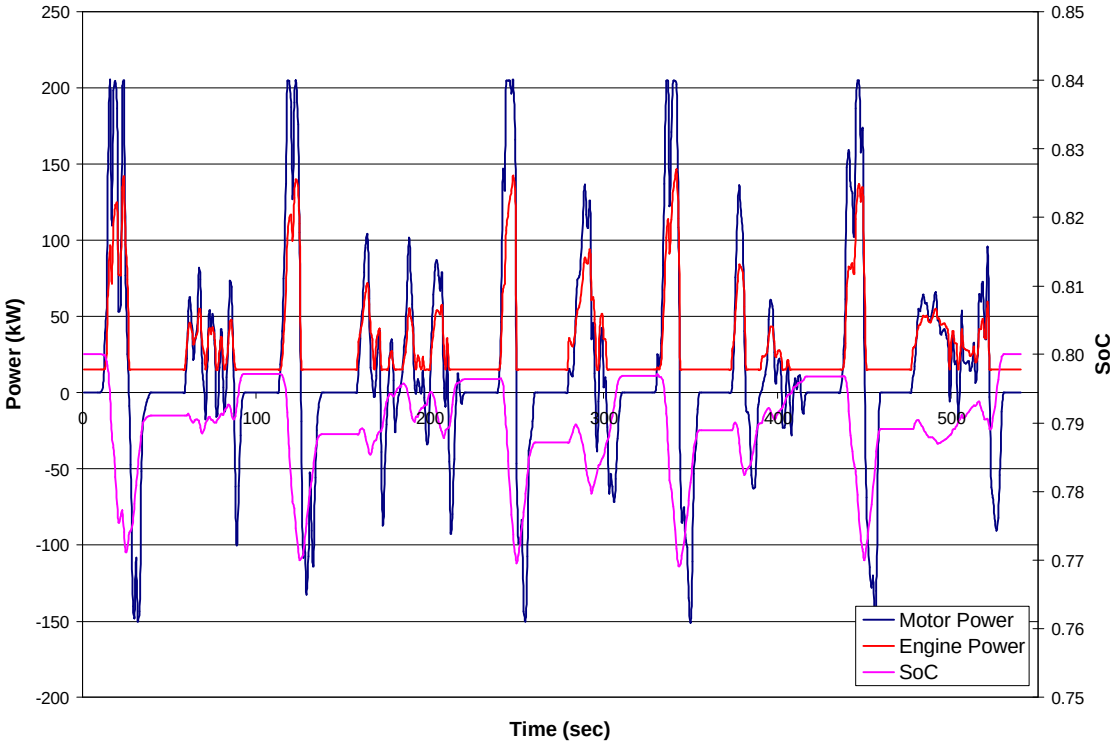

Figure 4.1.3 Class 8 Series HEV on Manhattan Cycle with auxiliary load, C_1 = 0.2, C_2 = 3375.

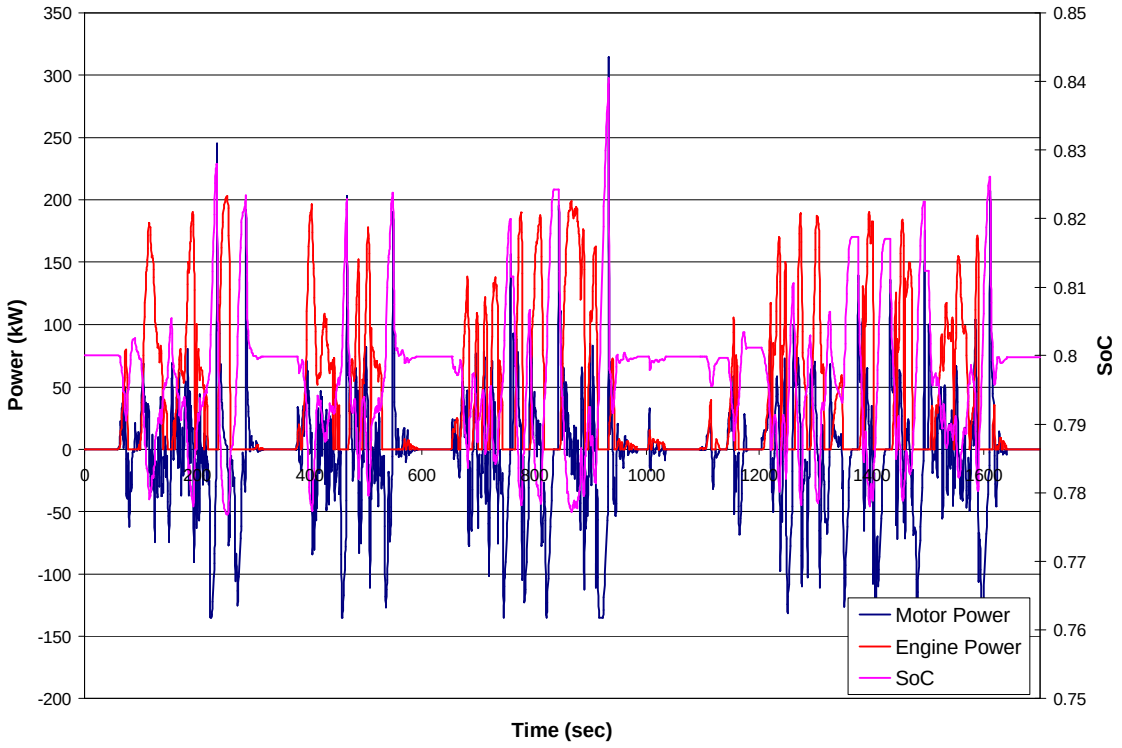

Figure 4.1.4 Class 8 Parallel HEV on CSHVC without auxiliary load, C_1 = 0.2, C_2 = 6800.

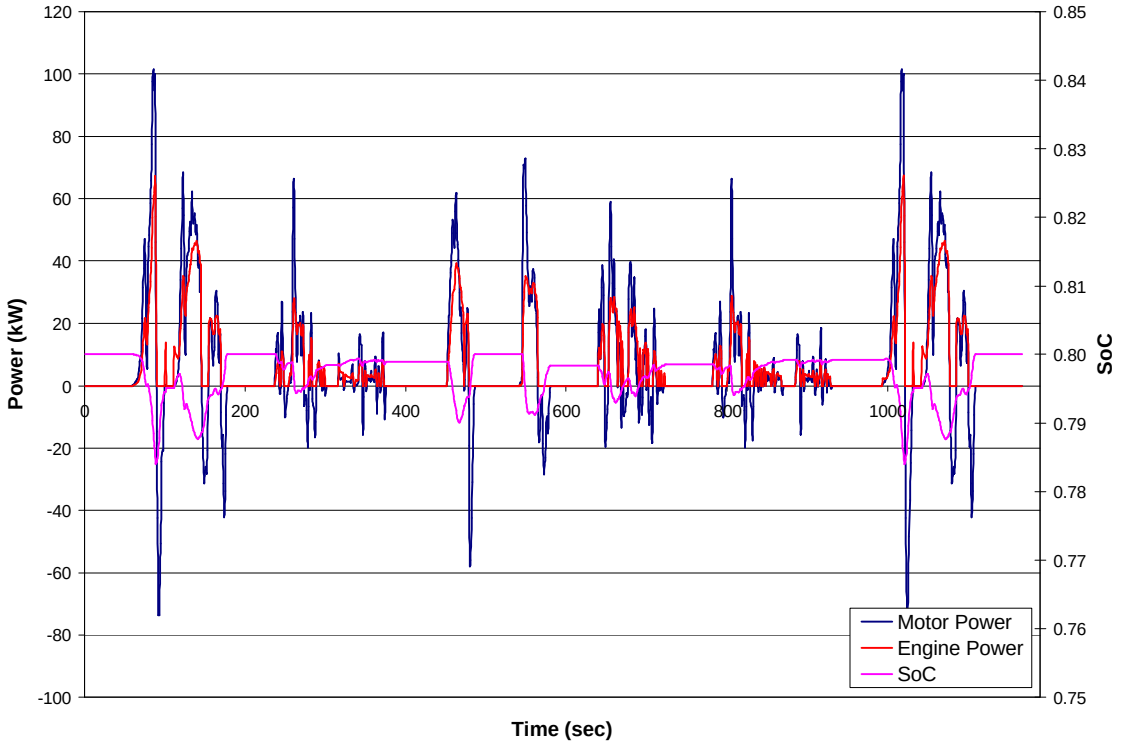

Figure 4.1.5 Class 8 Series HEV on Yard Cycle without auxiliary load, C_1 = 0.3, C_2 = 2550.

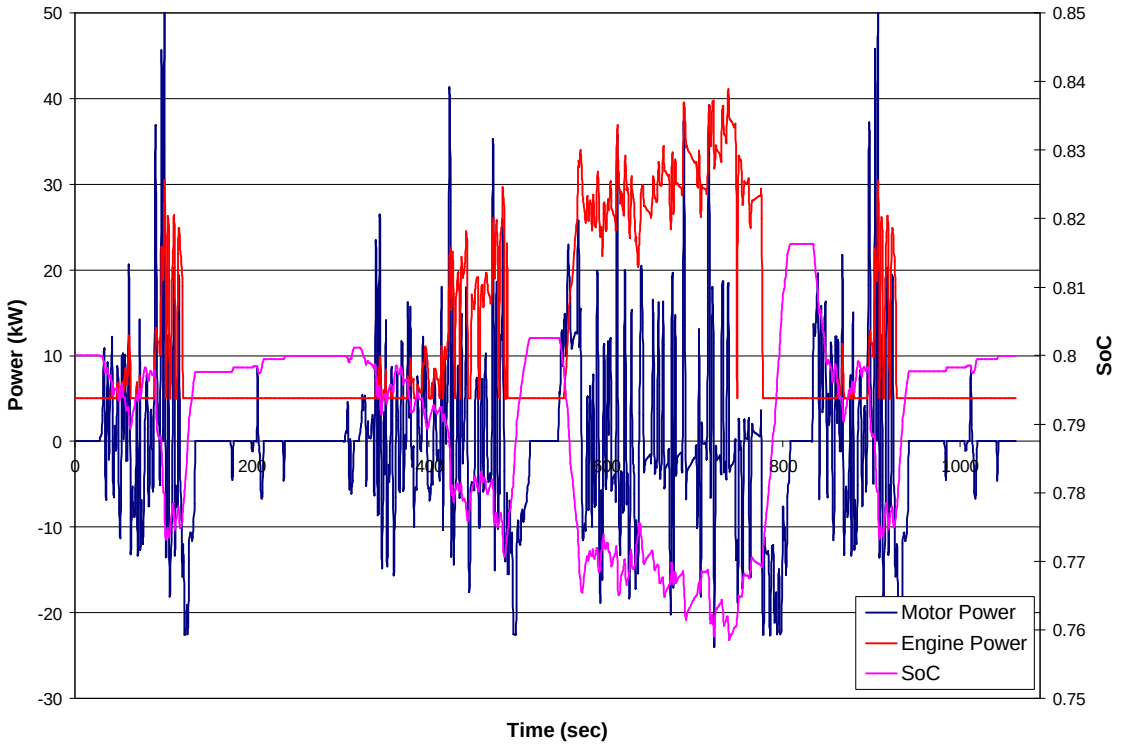

Figure 4.1.6 Class 2B Parallel HEV on Test D Cycle with auxiliary load, C_1 = 0.1, C_2 = 1290.

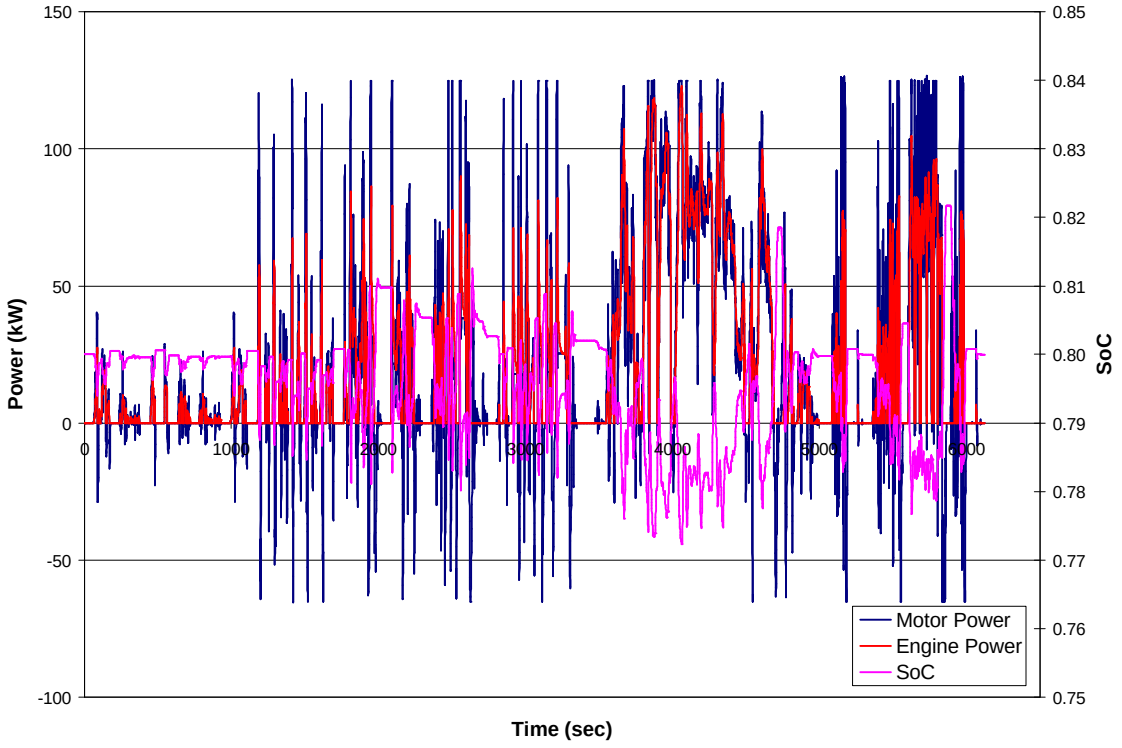

Figure 4.1.7 Class 6 Series HEV on Combined Cycle without auxiliary load, C_1 = 0.2, C_2 = 3550.

4.2 Optimization

Figures 4.2.1 through 4.2.18 show the variation of fuel economy with C_1 for the various vehicle configurations and cycles. While most of the plots are fairly smooth and predictable, a deficiency of the simulation is readily apparent in Figures 4.2.2, 4.2.3 4.2.10, 4.2.15, and 4.2.18. In these figures, some of the fuel economy traces show dramatic changes for small changes in C_1 or are not complete for the entire range of C_1 values. This is due to the control strategy. In situations where C_2 is very large to maintain charge sustaining operation over the cycle, very small changes in SoC can result in large spikes and oscillations in engine power. This is due to the use of a control strategy that is directly proportional to the road load power and the SoC. A solution would be the inclusion of a derivative term shown in Equation 18.

$$P_e = C_1 P_w - C_2\left(SoC_i - SoC_t\right) + C_3 \frac{dP_e}{dt}$$

This modified equation can be used to limit the speed of change in engine power over a period of time and would serve as a damper to smooth out spikes and oscillations. This strategy could be implemented by imposing a maximum rate of change of engine power. C_3 could be sized to set the level of damping required.

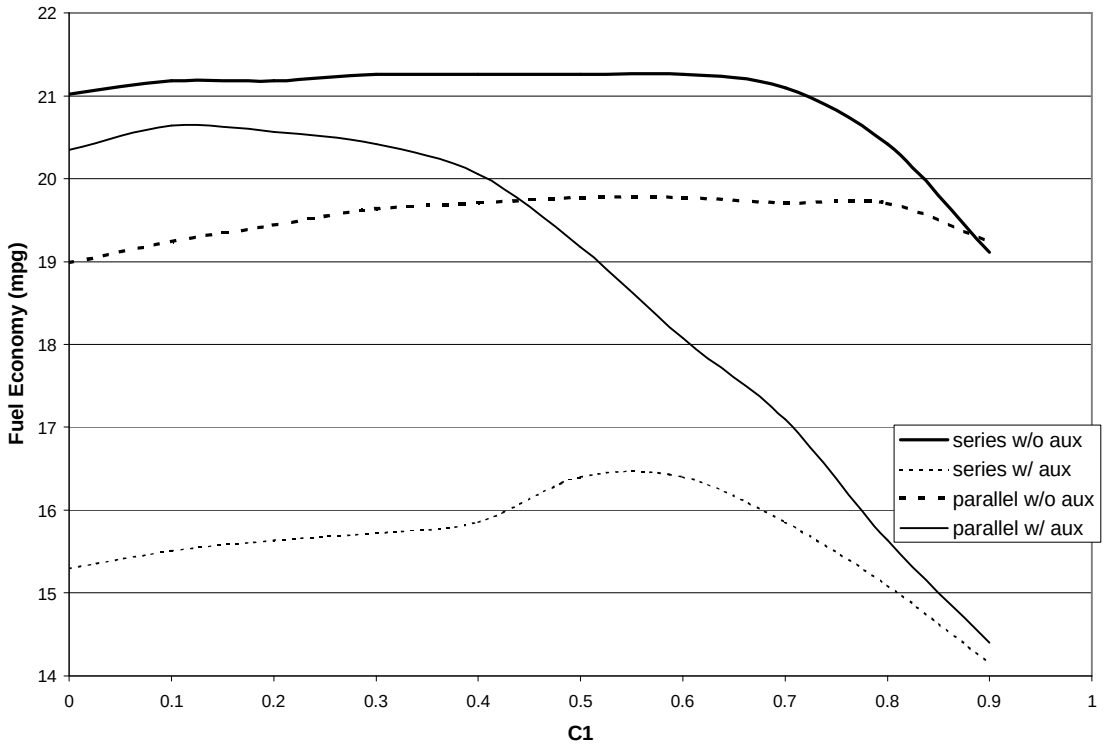

Figure 4.2.1 Class 2B HEV Fuel Economy on Freeway Cycle.

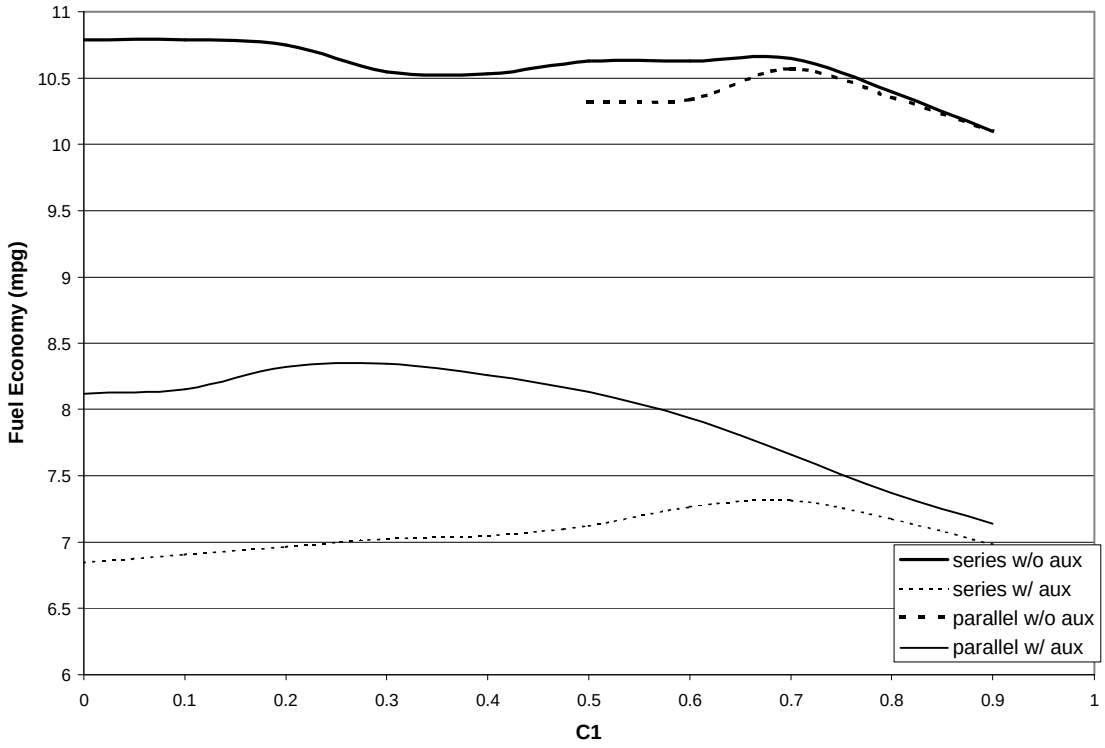

Figure 4.2.2 Class 6 HEV Fuel Economy on Freeway Cycle.

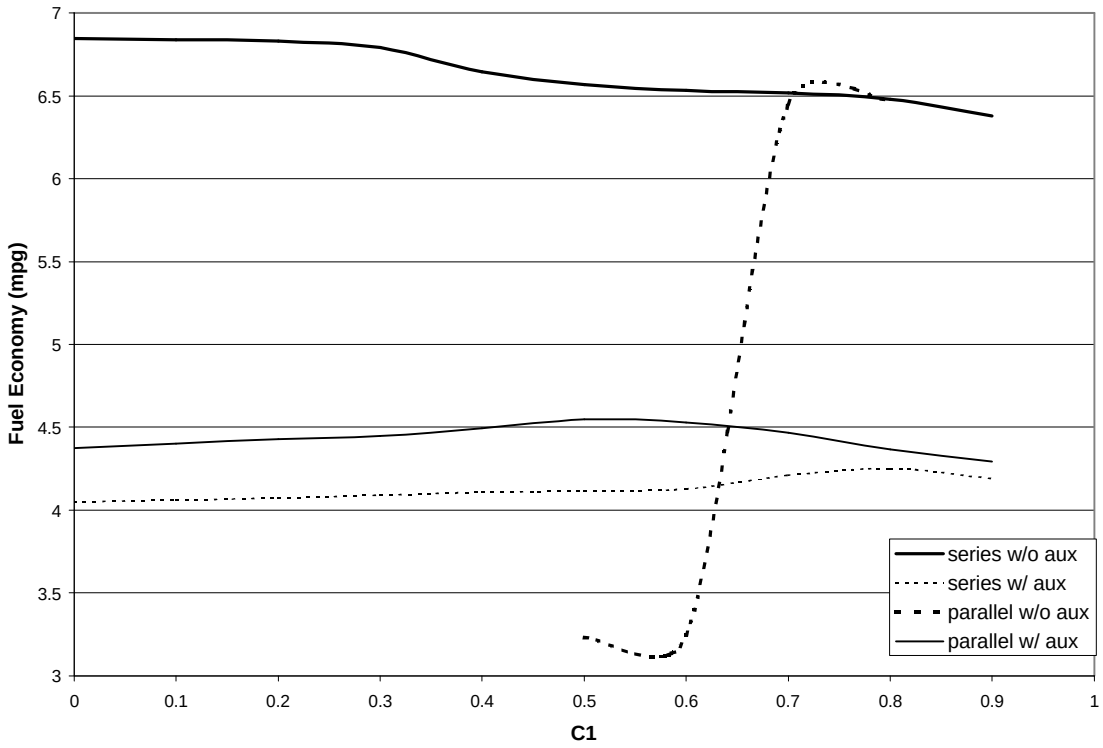

Figure 4.2.3 Class 8 HEV Fuel Economy on Freeway Cycle.

The instability in the parallel HEV without auxiliary load in Figure 4.2.3 as well as the incomplete Class 6 data in Figure 4.2.2 are due to the numerical instability in the simulation discussed at the beginning of this section. Similar instabilities can be seen in the Class 8 and Class 2B HEVs in Figures 4.2.6 and 4.2.7.

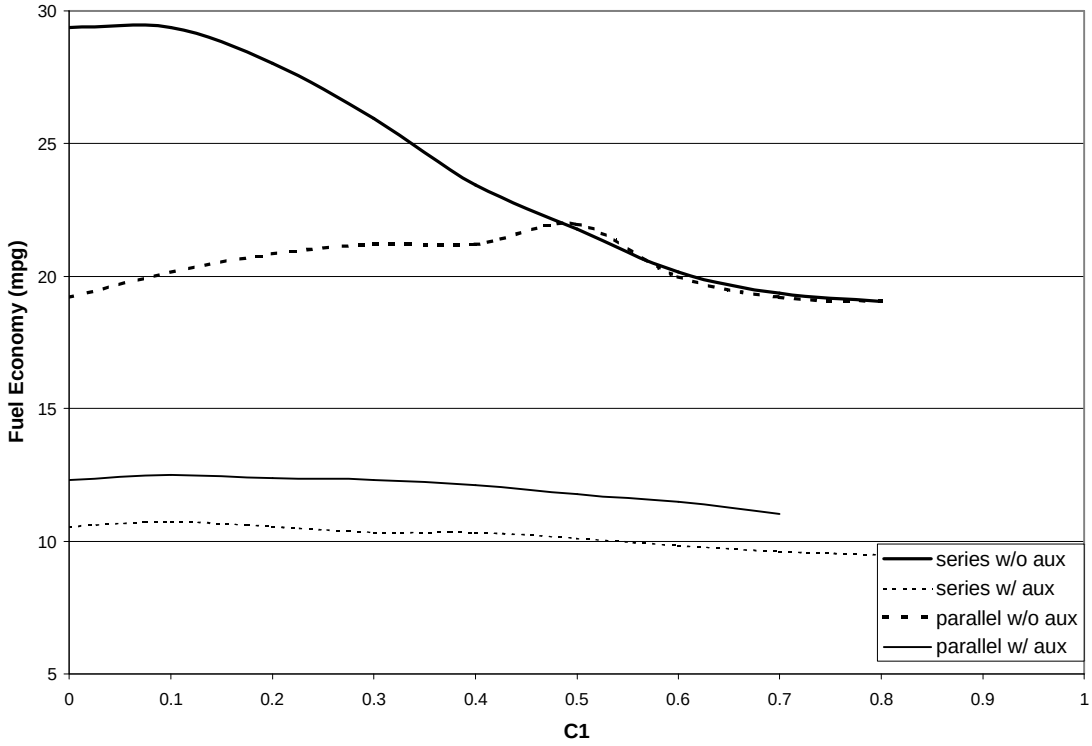

Figure 4.2.4 Class 2B HEV Fuel Economy on CSHVC Cycle.

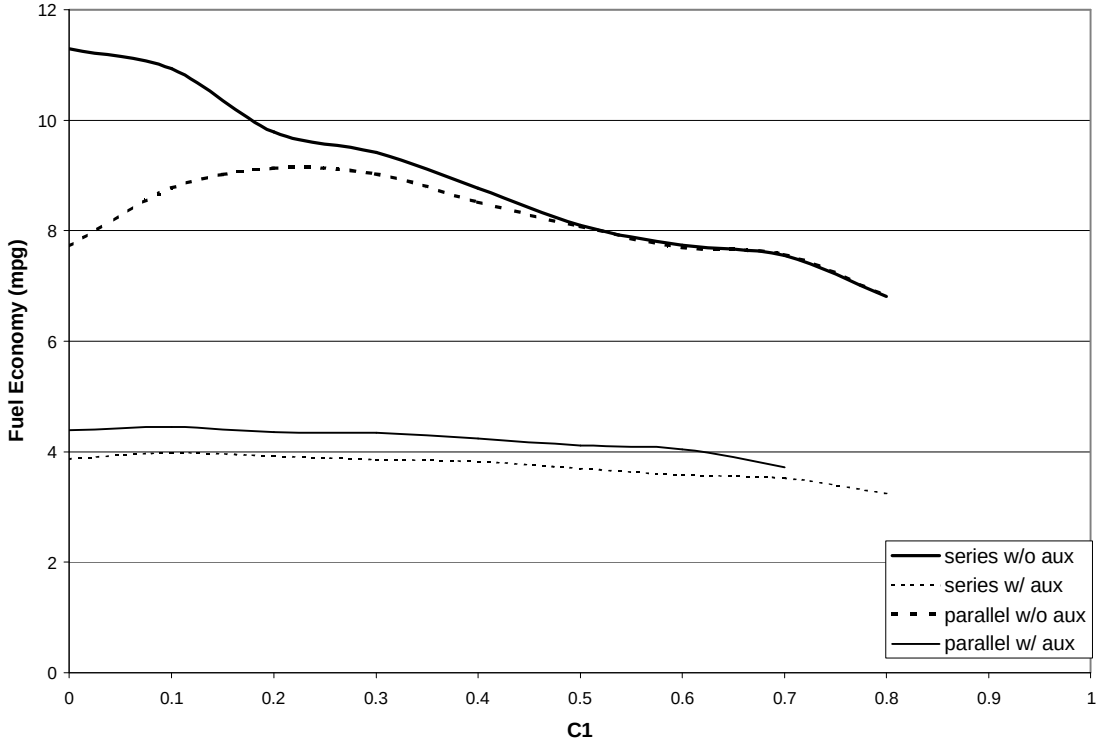

Figure 4.2.5 Class 6 HEV Fuel Economy on CSHVC Cycle.

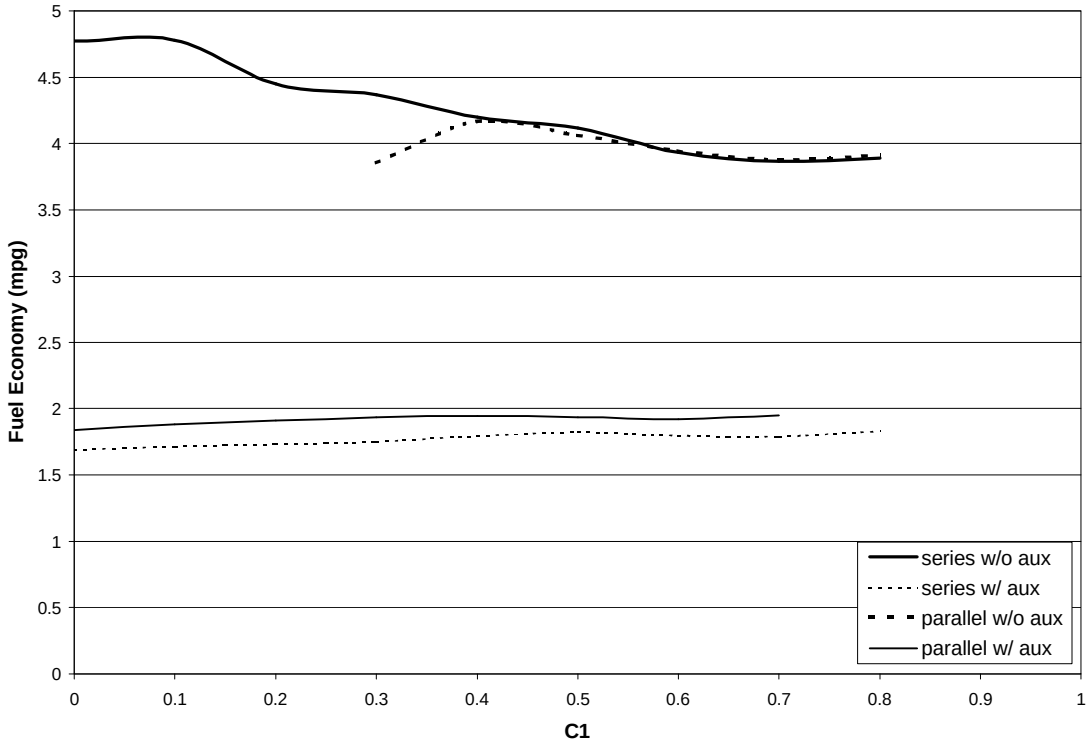

Figure 4.2.6 Class 8 HEV Fuel Economy on CSHVC Cycle.

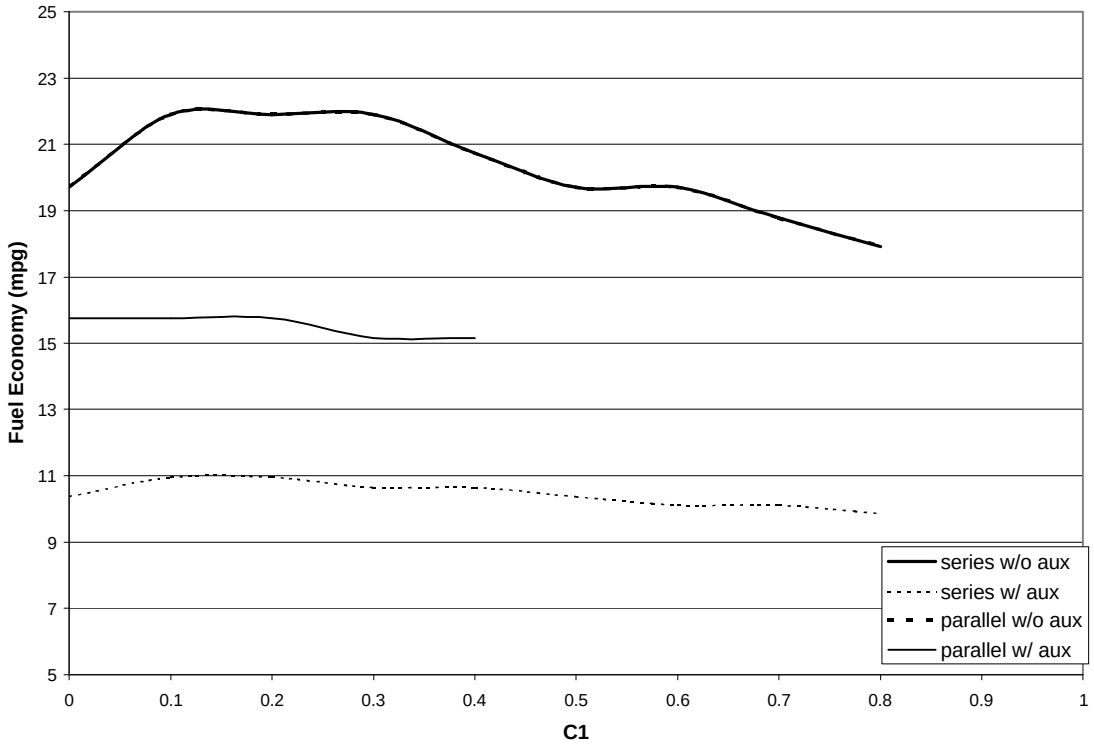

Figure 4.2.7 Class 2B HEV Fuel Economy on Yard Cycle.

The data for the Class 8 parallel HEV in Figure 4.2.7 appears to be missing. This is due to overlapping data from the Class 8 series HEV.

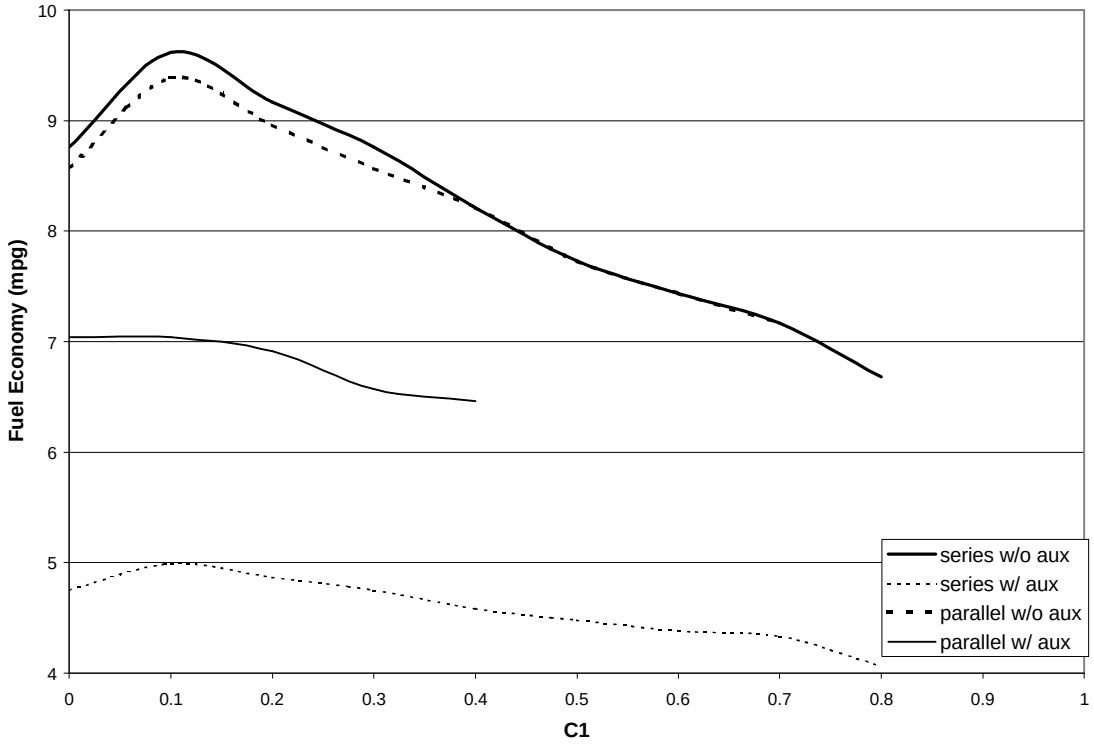

Figure 4.2.8 Class 6 HEV Fuel Economy on Yard Cycle.

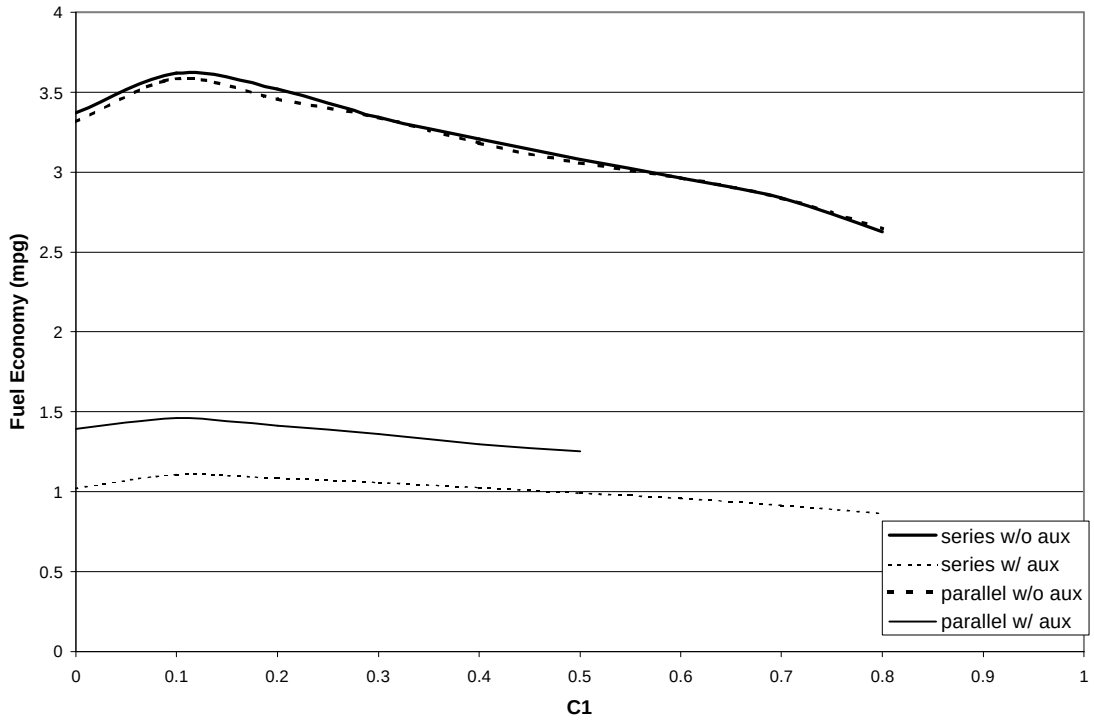

Figure 4.2.9 Class 8 HEV Fuel Economy on Yard Cycle.

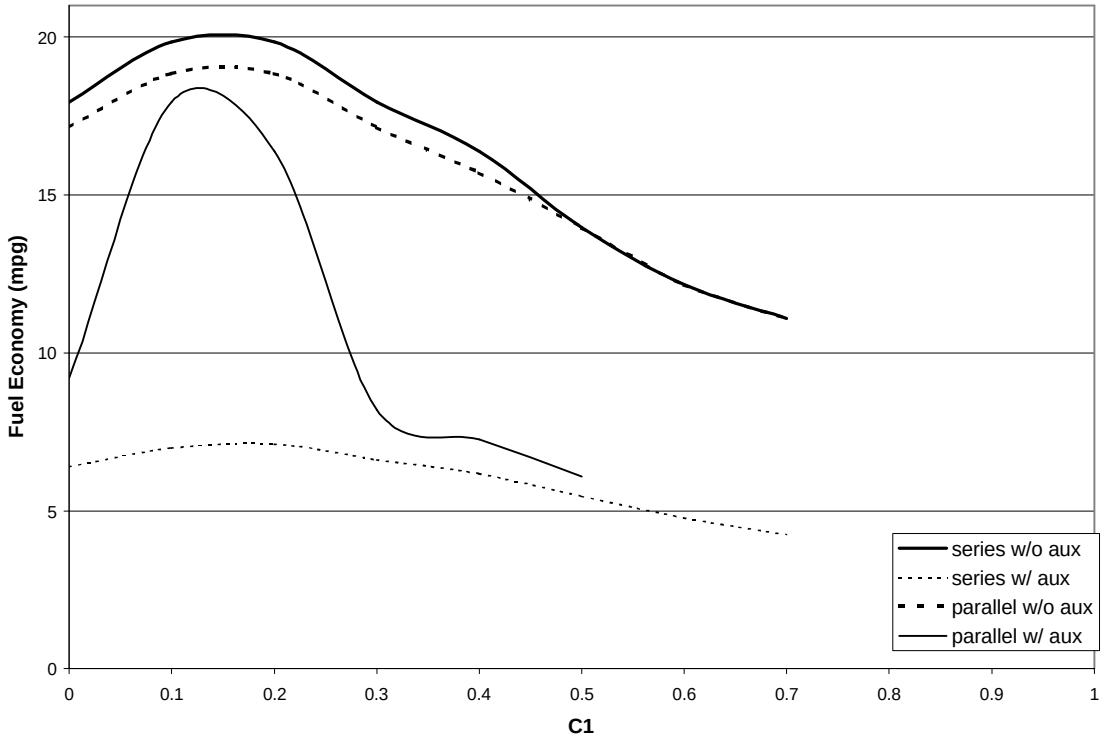

Figure 4.2.10 Class 2B HEV Fuel Economy on Manhattan Cycle.

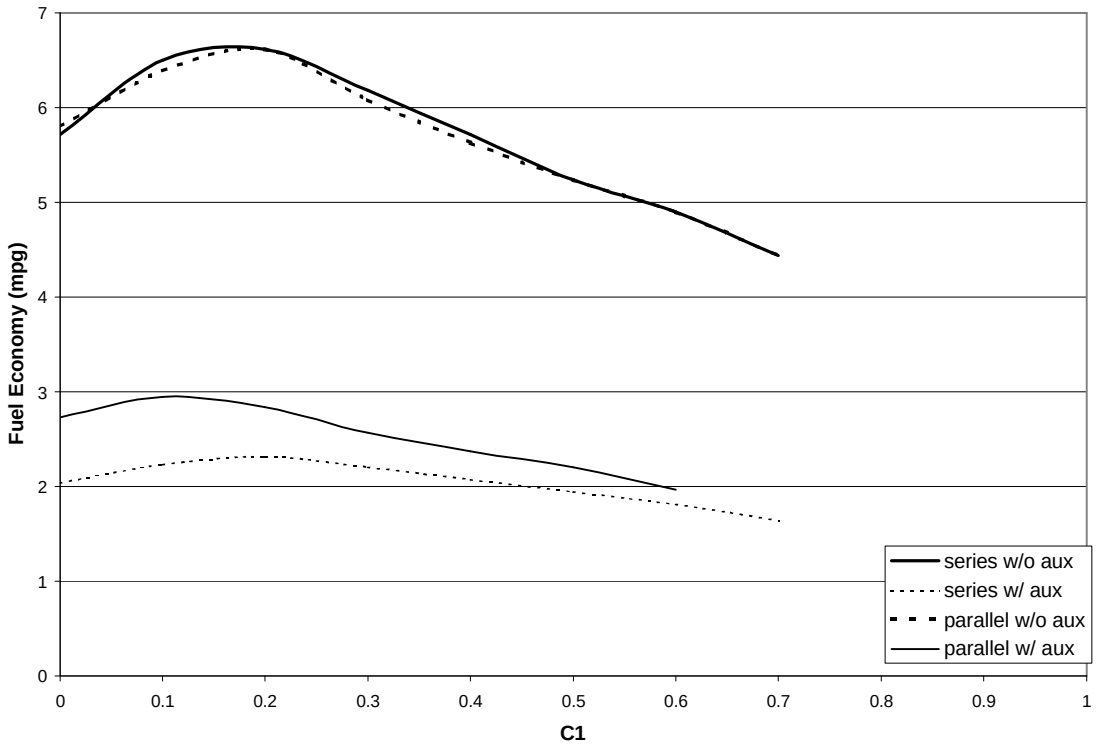

Figure 4.2.11 Class 6 HEV fuel economy on Manhattan Cycle.

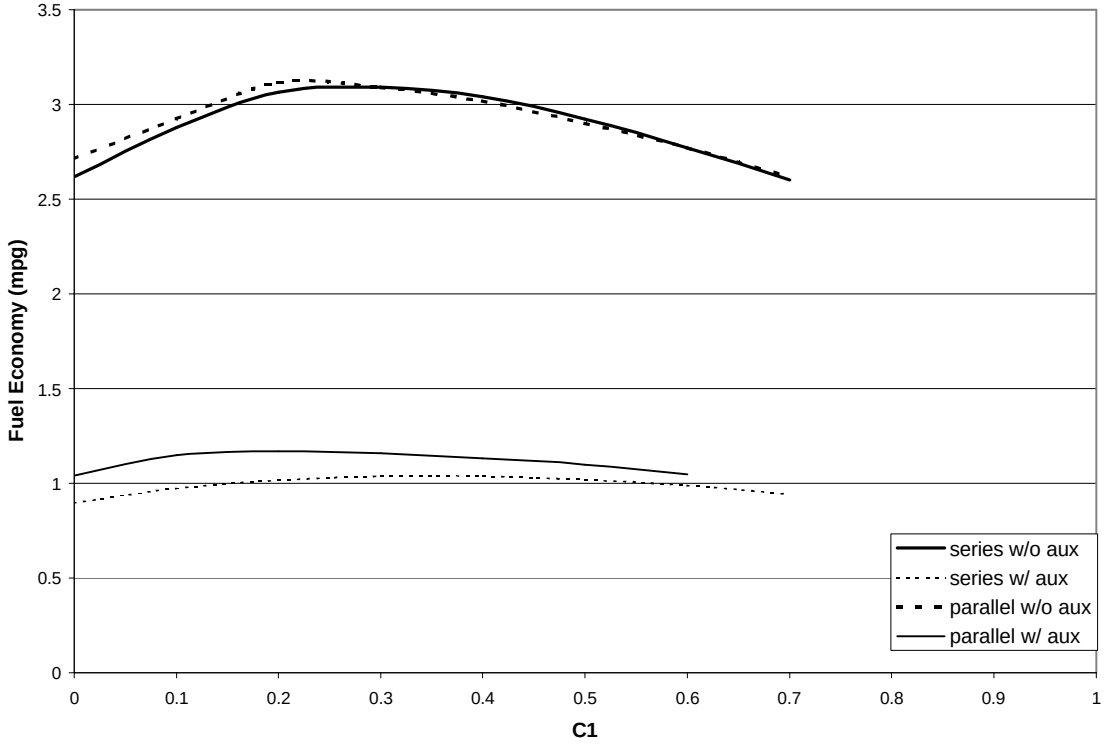

Figure 4.2.12 Class 8 HEV fuel economy on Manhattan Cycle.

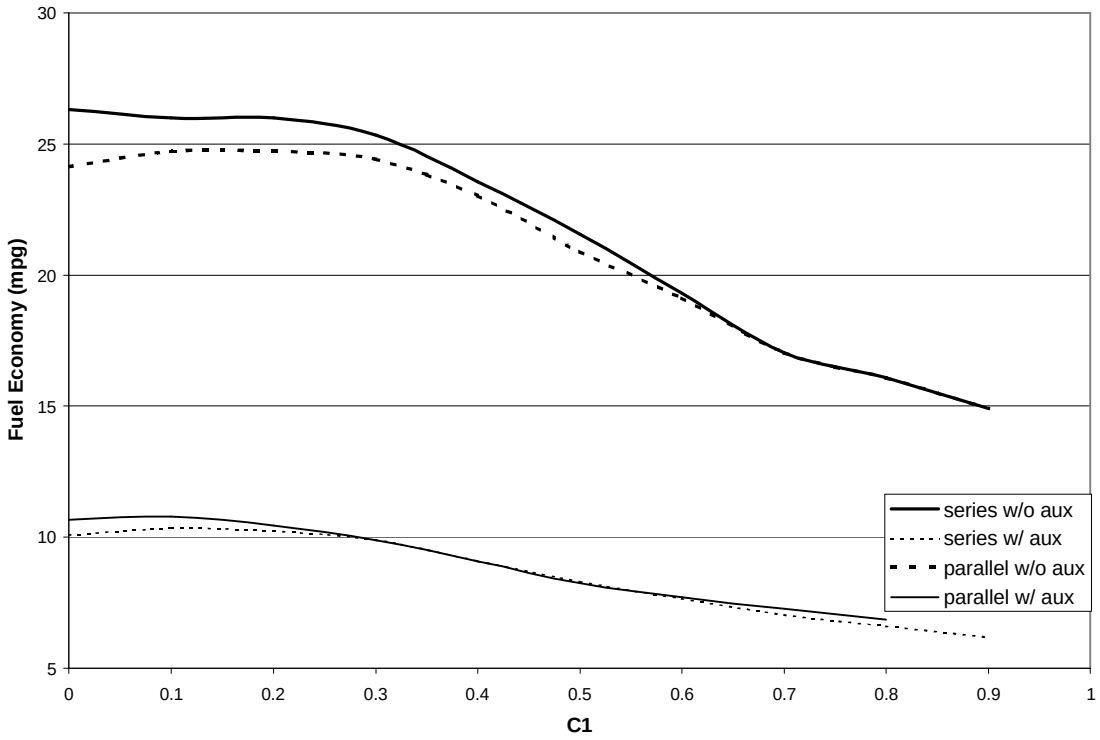

Figure 4.2.13 Class 2B HEV fuel economy on Test D Cycle.

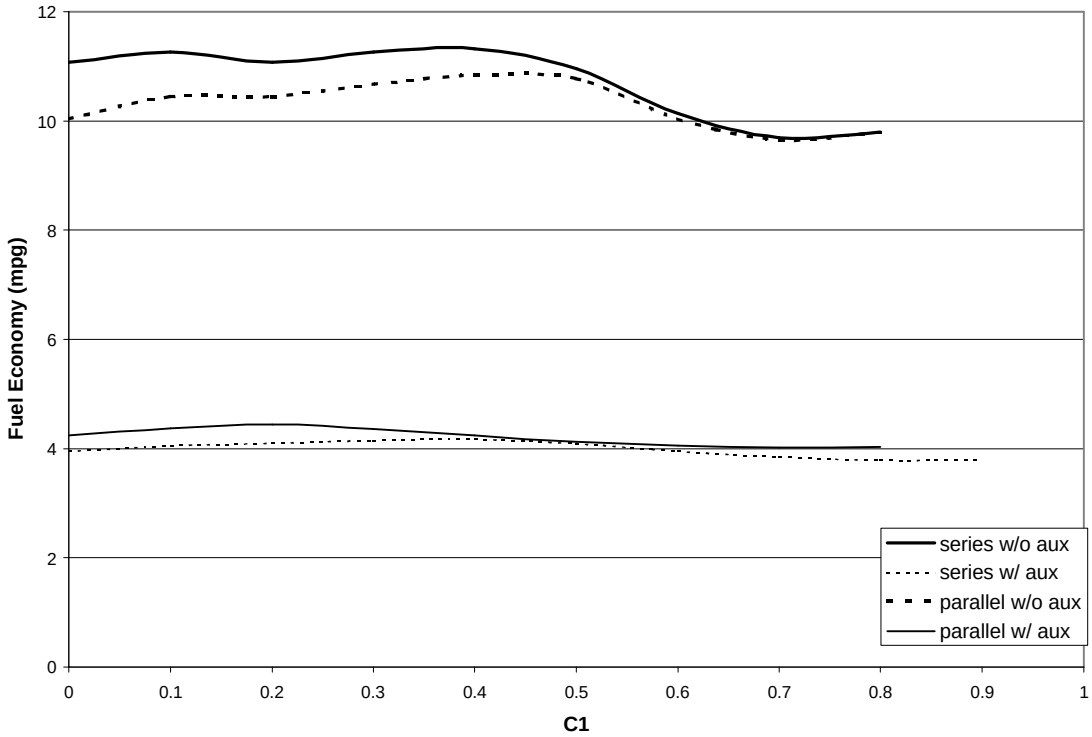

Figure 4.2.14 Class 6 HEV fuel economy on Test D Cycle.

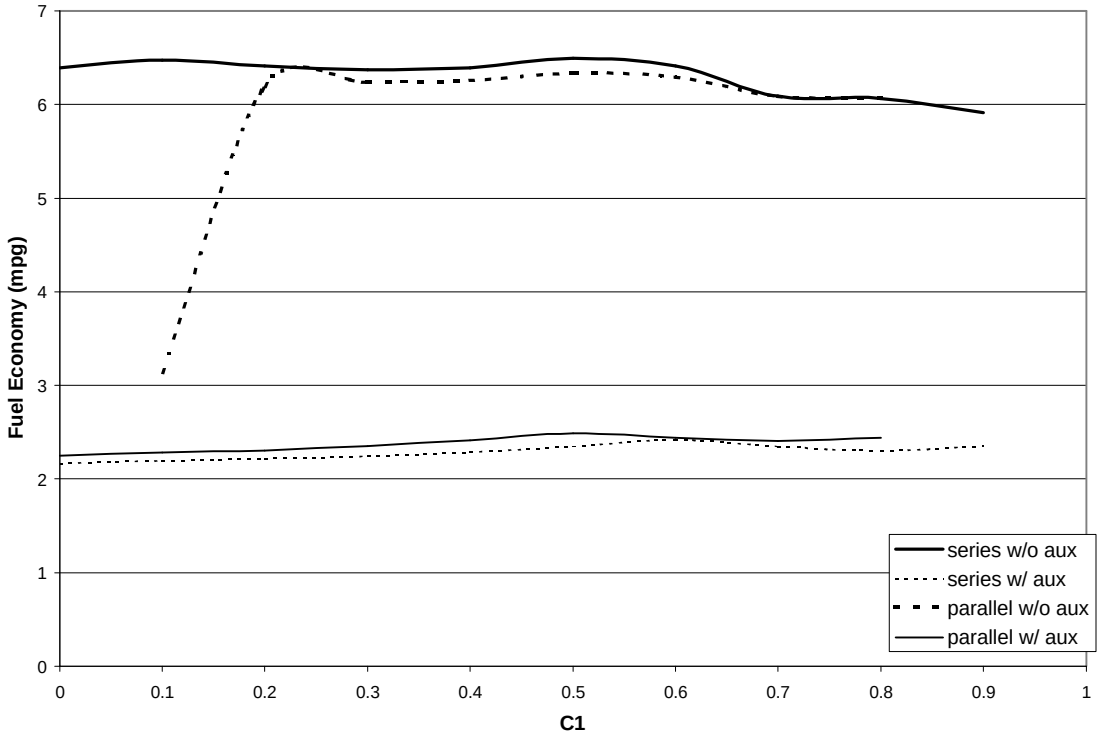

Figure 4.2.15 Class 8 HEV fuel economy on Test D Cycle.

The sudden instability of the parallel HEV without auxiliary loads as C_1 approaches zero in Figures 4.2.15 and 4.1.18 are, again, due to the numerical instabilities in the simulation. Incorporating the changes recommended at the beginning of the section might solve these problems.

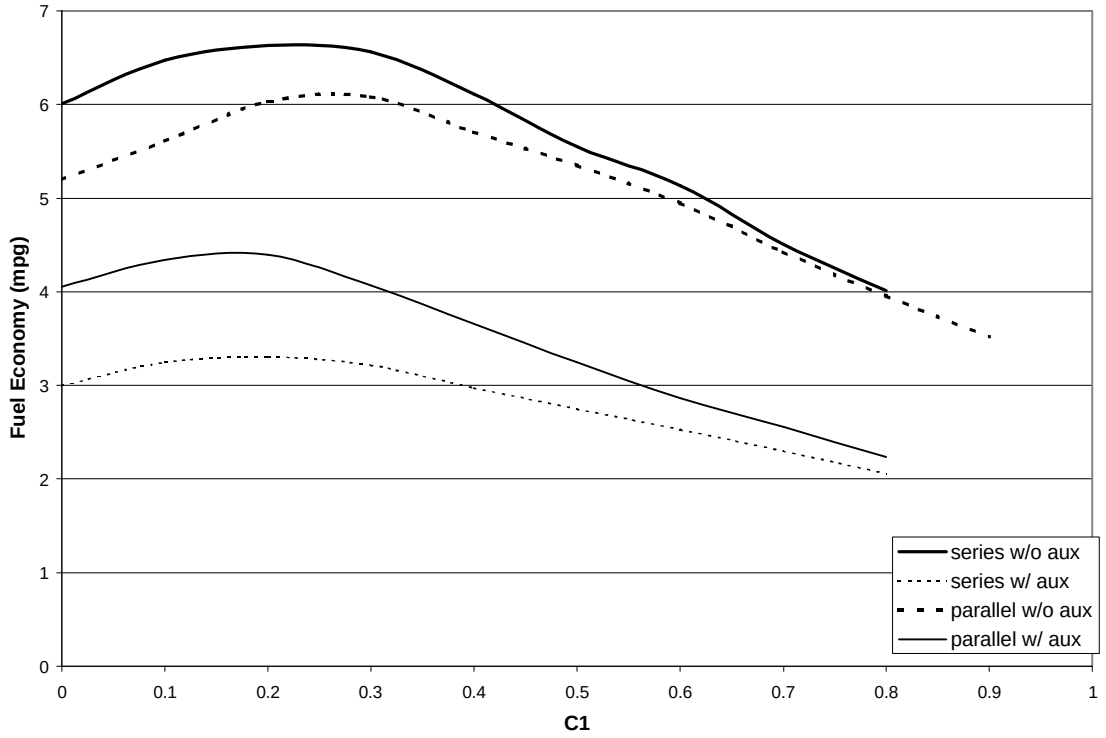

Figure 4.2.16 Class 2B HEV fuel economy on Combined Cycle.

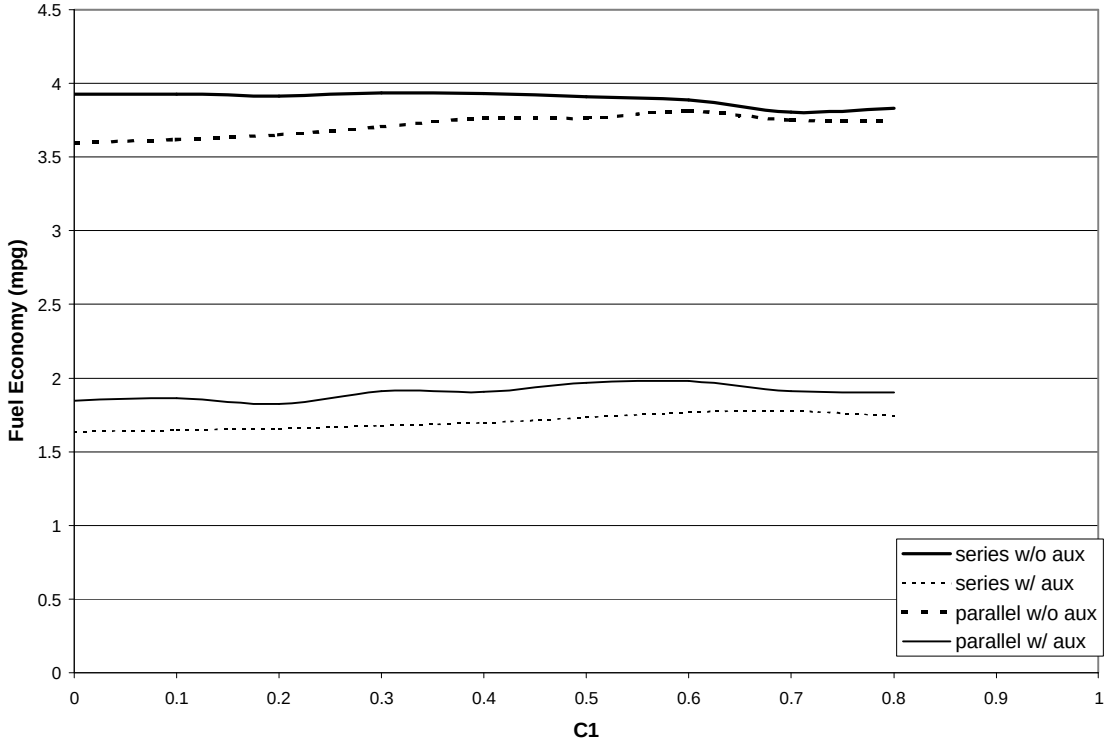

Figure 4.2.17 Class 6 HEV fuel economy on Combined Cycle.

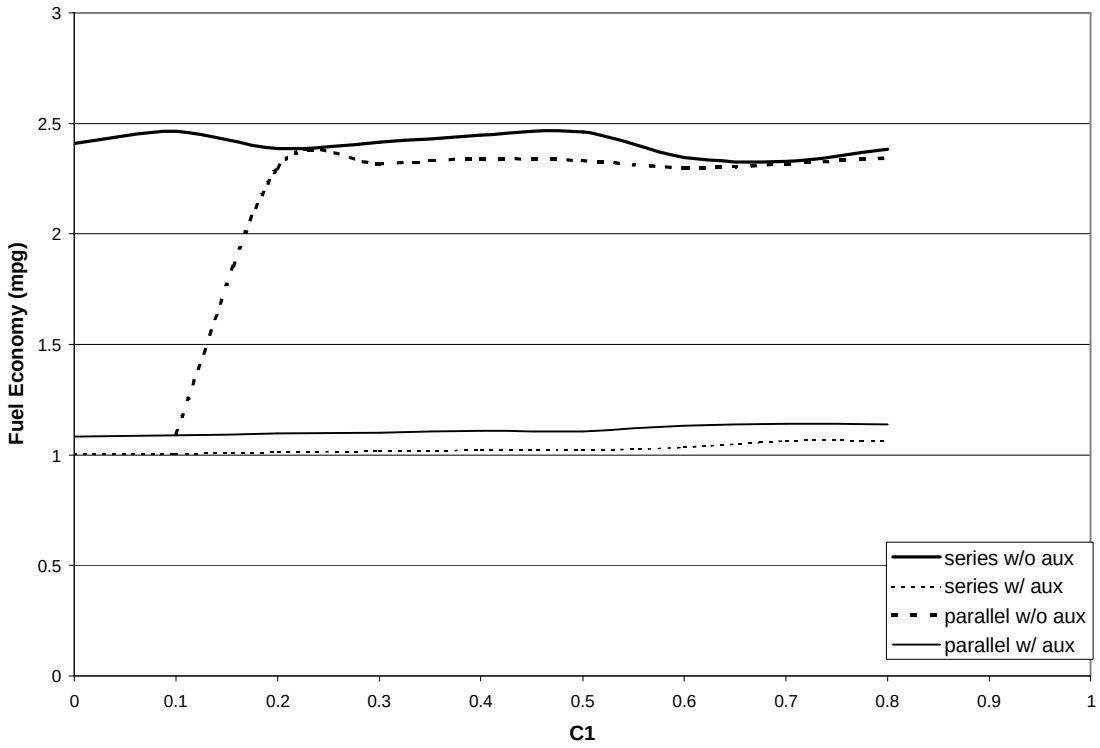

Figure 4.2.18 Class 8 HEV fuel economy on Combined Cycle.

Table 4.2.1 Class 2B optimum HEV without auxiliary load configurations and constants directly from simulation.

Cycle	Best Fuel Economy	Hybrid Configuration	C1, C2	% change from conventional	Engine Power	Motor Power
	mpg				kW	kW
Freeway	21.26	Series	0.5, 2960	301	55	66
CSHVC	29.37	Series	0.1, 1490	90	32	41
Yard	21.90	Parallel	0.3, 1250	1966	7	14
Manhattan	19.84	Series	0.2, 3070	858	21	48
Test D	12.98	Series	0.2, 1230	170	42	77
Combined	6.63	Series	0.2, 1230	67	64	120

Table 4.2.2 Class 2B optimum HEV with auxiliary load configurations and constants directly from simulation.

Cycle	Best Fuel Economy	Hybrid Configuration	C1, C2	% change from conventional	Engine Power	Motor Power
	mpg				kW	kW
Freeway	20.42	Parallel	0.3, 225	396	41	33
CSHVC	12.50	Parallel	0.1, 540	60	28	29
Yard	15.77	Parallel	0.2, 405	3746	5	12
Manhattan	17.95	Parallel	0.1, 660	2037	43	16
Test D	10.45	Parallel	0.2, 750	352	41	52
Combined	4.40	Parallel	0.2, 750	97	51	78

The results of the simulation overstate the percent increase in fuel economy for a Class 2B HEV over a conventional vehicle. While the conventional vehicle fuel

economy determined from simulation of the Class 6 and 8 vehicles is similar to that seen in actual vehicles, the fuel economy for the Class 2B vehicles is far lower that what is expected from actual in-use vehicles due to the use of heavy-duty cycles. If the HEV results from the simulation are compared to more realistic conventional fuel economy, the percent improvement is much lower as shown in Table 4.2.3

Table 4.2.3 Class 2B without auxiliary load simulation results compared to actual vehicle fuel economy.

Cycle	Best Fuel Economy	Hybrid Configuration	C1, C2	% change from conventional	Engine Power	Motor Power
	mpg				kW	kW
Freeway	21.26	Series	0.5, 2960	41	55	66
CSHVC	29.37	Series	0.1, 1490	126	32	41
Yard	21.9	Parallel	0.3, 1250	68	7.4	14
Manhattan	19.84	Series	0.2, 3070	53	21.4	48
Test D	12.98	Series	0.2, 1230	0	42	76.76
Combined	6.63	Series	0.2, 1230	-49	64	120

One of the limitations of this simulation method is evident in the Class 2B results. Since gear ratios are not included, no torque analysis can be done. This results in suggested configurations that are obviously in error. In Table 4.2.2, a parallel configuration with a 5 kW ICE and 12 kW electric motor is recommended. While this combination satisfies the power requirements over the Yard Cycle, an ICE more suited to use in a riding lawnmower would no be capable of producing the torque necessary to contribute to driving a nearly 4000 kg vehicle.

In all of the vehicles, the addition of auxiliary loads was extremely detrimental to the fuel economy. Generally, the fuel economy with auxiliary loads was half the fuel economy without auxiliary loads. This is due to requiring the engine to run inefficiently at low power levels throughout long periods of the cycles. When the vehicle is stopped without auxiliary loads, HEVs commonly allow the engine to shut off greatly reducing

fuel economy over many cycles. The addition of auxiliary loads not only removes this option but also increases the fuel consumption during these periods.

Table 4.2.4 Class 6 optimum HEV without auxiliary load configurations and constants directly from simulation.

Cycle	Best Fuel Economy	Hybrid Configuration	C1, C2	% change from conventional	Engine Power	Motor Power
	mpg				kW	kW
Freeway	10.79	Series	0.2, 5240	13	125	125
CSHVC	11.3	Series	0.1, 3200	112	97	115
Yard	9.61	Series	0.1, 1030	549	25	40
Manhattan	6.61	Parallel / Series	0.2, 2800	113	64	125
Test D	11.32	Series	0.4, 2460	37	102	125
Combined	3.93	Series	0.4, 2475	-39	120	125

Table 4.2.5 Class 6 optimum HEV with auxiliary load configurations and constants directly from simulation.

Cycle	Best Fuel Economy	Hybrid Configuration	C1, C2	% change from conventional	Engine Power	Motor Power
	mpg				kW	kW
Freeway	8.35	Parallel	0.3, 620	26	56	100
CSHVC	4.45	Parallel	0.2, 1650	77	78	78
Yard	7.04	Parallel	0.1, 2080	1228	17	30
Manhattan	2.95	Parallel	0.1, 2025	154	52	105
Test D	4.44	Parallel	0.2, 2420	33	96	100
Combined	1.98	Parallel	0.6, 535	-38	58	110

Results for the Class 6 vehicle appear to be more valid than those for the Class 2B vehicle. The Yard Cycle results are still a fault because the cycle was designed specifically for Class 8 vehicles and the Class 6 conventional vehicle is overpowered. Torque analysis still appears to be a problem with the Yard Cycle with the suggested combination of a 17 kW ICE and a 30 kW electric motor. Interestingly, the HEV achieves poorer fuel economy on the Combined Cycle than the conventional vehicle. This is due to the ordering of the cycles, the control strategy, and the requirement for the vehicle to be perfectly charge sustaining over the cycle. Placing low power demand at the beginning of the cycle and ending it with more aggressive requirements places heavy demand on the batteries. To achieved charge sustaining operation, the ICE must be sized similarly to that used on a conventional vehicle and the control strategy requires a high C_2 to sustain the SoC. The use of a large ICE means that it is forced to run at low power

and poor efficiency during the early portion of the cycle resulting in poor fuel economy. As expected, only modest fuel economy improvement was seen on the Freeway Cycle due to the absence of large amounts of regenerative braking energy and the high average power demand.

Table 4.2.6 Class 8 optimum HEV without auxiliary load configurations and constants directly from simulation.

Cycle	Best Fuel Economy	Hybrid Configuration	C1, C2	% change from conventional	Engine Power	Motor Power
	mpg				kW	kW
Freeway	6.83	Series	0.2, 6000	20	205	205
CSHVC	4.78	Series	0.1, 3900	52	190	205
Yard	3.62	Series	0.1, 3200	289	65	102
Manhattan	3.09	Parallel	0.3, 2675	63	146	135
Test D	6.50	Series	0.5, 1820	39	182	205
Combined	2.46	Series	0.5, 1820	-35	201	205

Table 4.2.7 Class 8 optimum HEV with auxiliary load configurations and constants directly from simulation.

Cycle	Best Fuel Economy	Hybrid Configuration	C1, C2	% change from conventional	Engine Power	Motor Power
	mpg				kW	kW
Freeway	4.55	Parallel	0.5, 600	19	185	81
CSHVC	1.95	Parallel	0.4, 1240	29	173	120
Yard	1.46	Parallel	0.1, 2080	342	53	67
Manhattan	1.16	Parallel	0.3, 2000	63	133	140
Test D	2.49	Parallel	0.5, 1825	26	181	116
Combined	1.14	Parallel	0.7, 325	-40	185	75

Since HEV buses that show significant fuel economy improvement are currently infiltrating the transit bus market, the results on the Manhattan Cycle are expected. Also, the small to moderate gains on the Freeway, CSHVC, and Test D Cycles where higher average speeds and power requirements dominate are expected. The problems evident in the analysis of the Classes 2B and 6 conventional vehicle on the Yard Cycle are not present here. The cycle is designed for heavy-duty vehicles and specifically for Class 8 vehicles. Actual in-use yard spotter trucks are equipped with 175 – 200 kW engines which is approximately the same power used in the average Class 8 vehicle. For these reasons, it appears that the 300% fuel economy increase on the Yard Cycle is valid.

Here, too, the HEV achieves poorer fuel economy than the conventional vehicle over the Combined Cycle for the same reasons as discussed with the Class 6 vehicle.

To further examine the fuel economy of HEVs over varied driving situations, the order of the cycles in the Combined Cycle were reversed and the vehicles were simulated again. A selection of these results is shown in Table 4.2.8.

Table 4.2.8 Simulation results from reversed Combined Cycle.

	Conventional	HEV Configuration	C1, C2	HEV Fuel Economy	% change from conventional
				mpg	
Class 2B	13.00	Series	0.2, 1400	15.78	21
Class 6	9.61	Series	0.2, 1700	11.14	16
Class 8	3.86	Series	0.2, 2900	4.45	15

This variation in fuel economy is due to the way the control strategy forces the vehicle to maintain charge-sustaining operation. In the original Combined Cycle, the high power requirement segments are near the end of the cycle forcing the engine to follow the road load closely throughout the cycle to avoid depleting the batteries. In the reversed cycle, the presence of the high power events near the beginning of the cycle allows the vehicle to recover SoC during the less demanding end portions through charging while driving. This phenomenon is not entirely realistic since requiring an HEV to return to the initial SoC after each use is not always possible.

4.3 Road Grade Effects

All federal test cycles assume that the vehicle is being operated on perfectly flat ground removing the effects of road grade. Obviously, vehicles are expected to operate on a wide variety of terrains and the effects of vehicle operation on hills or mountainous terrain on fuel economy and emissions is an important subject.

Figures 4.3.1 – 4.3.3 show the power requirement for each vehicle class to maintain constant speed on various grades determined from the road load equation (9).

While the Class 2B vehicle can maintain highway speed on a 7% grade without exceeding its maximum power, the Class 6 vehicle would be limited to 30 mph and the Class 8 could maintain 20 mph.

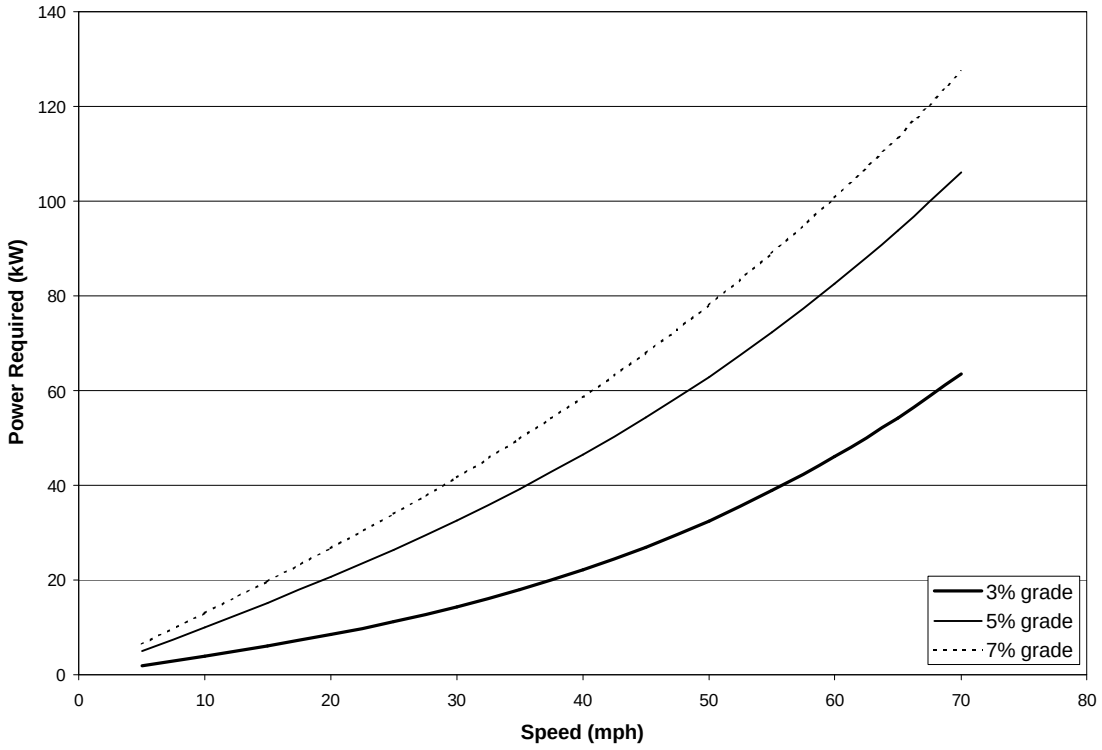

Figure 4.3.1 Power required to maintain constant speed on various grades for Class 2B.

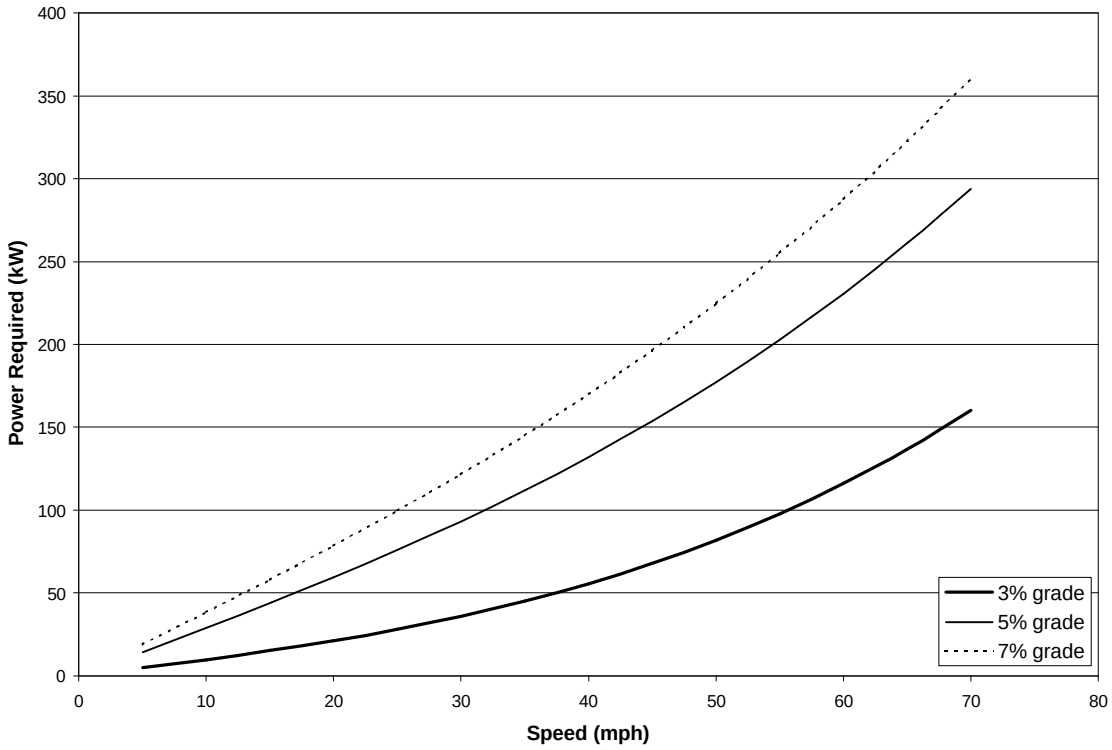

Figure 4.3.2 Power required to maintain constant speed on various grades for Class 2B.

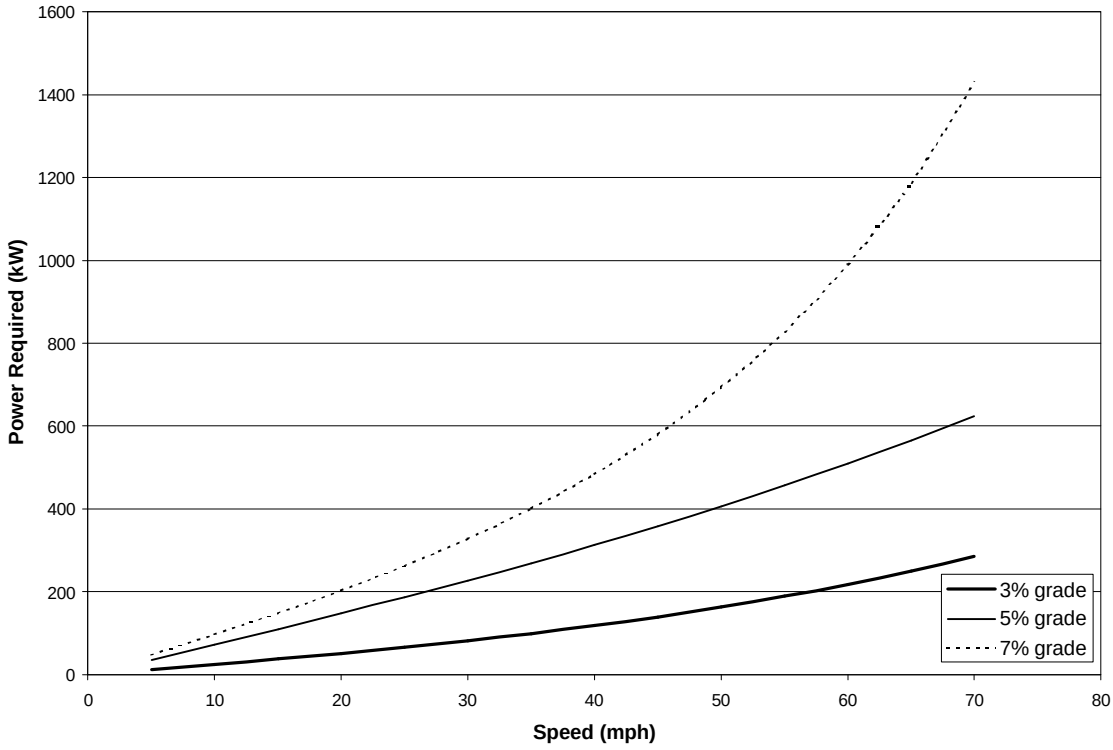

Figure 4.3.3 Power required to maintain constant speed on various grades for Class 8.

Figure 4.3.4 shows the effect of superimposing a sinusoidal terrain with a maximum 2% grade on the Freeway Cycle. When adding road grade to a cycle, the phase of the road grade is very important. Here, the varying terrain results in very little change in the positive and negative power peaks, but shifting it slightly would cause a dramatic increase in the magnitude of the peaks. This demonstrates one of the problems with analyzing the effects of road grade. Real terrain is not perfectly sinusoidal and is difficult to integrate with existing cycles. In the Figure 4.3.4, a series HEV shows a 16% increase in fuel economy over a conventional vehicle, 3% higher than the increase when road grade is not considered, but these results are valid only for this specific trace. Any change in the phase of the terrain would dramatically affect the fuel economy.

The stop and start points of a cycle including road grade are very important. If the vehicle begins at the bottom of a hill and stops at the top, it has no chance of being charge sustaining and is not allowed to take advantage of the regenerative braking energy available while descending the hill. Similarly, if a cycle begins at the top of a hill and ends at the bottom, the power requirements over the cycle will be artificially low and a vehicle designed specifically to meet these requirements would be totally unsuited to climbing the same hill.

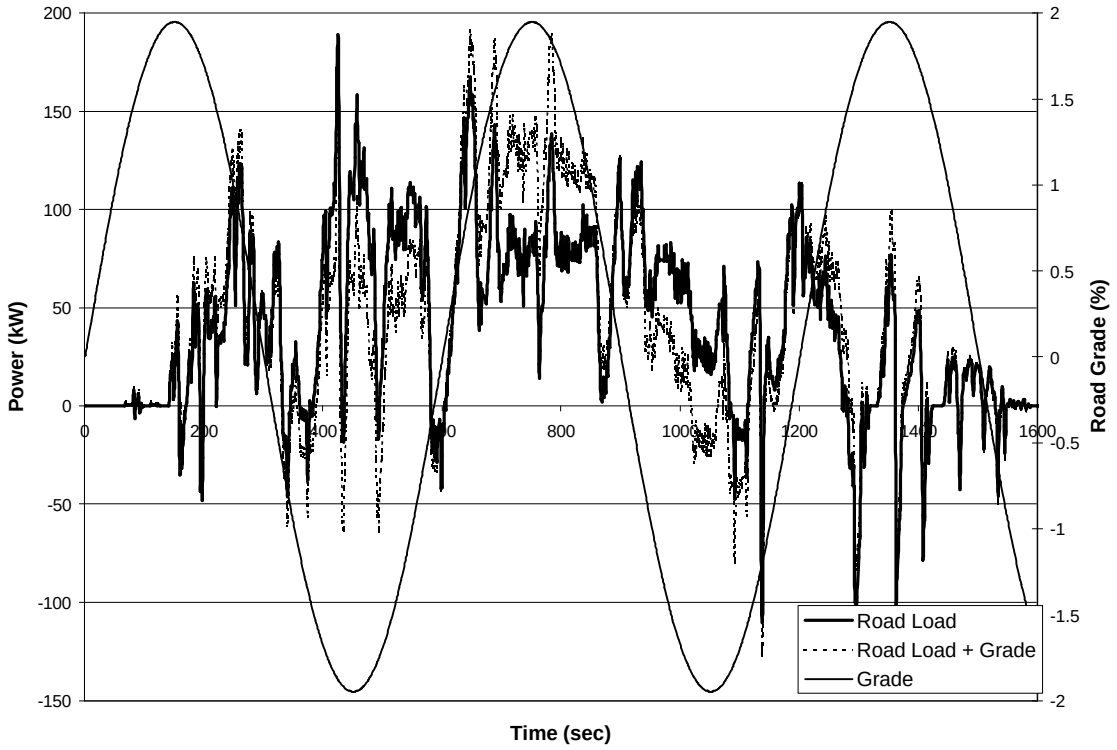

Figure 4.3.4 Power required for Class 6 vehicle over Freeway Cycle with and without road grade.

4.4 Niche Markets

A niche market for any vehicle is a specialized area of vehicle operation that allows the vehicles to be specifically tailored to that type of operation. Niche markets are especially suited to the application of HEV technology. Since HEVs can be extremely specialized through selection of components and control strategy, they can be heavily optimized for specific operations. A few of these include transit buses, yard spotters, and 'cubage' limited vehicles.

4.4.1 Transit Buses

Manufacturers of hybrid electric vehicles are already exploiting the transit bus niche market. The highly transient nature of their operation results in the availability of large amounts of regenerative braking energy. Moderate dynamic requirements, and low

average power and speed make this market especially suited to series HEVs. Since the buses are never expected to leave their regular operating range, they can be specifically designed for urban operation without fear of making them unsuitable for other operation.

4.4.2 Yard Spotters

Yard spotters are another niche market that has been somewhat exploited by conventional vehicle manufacturers but has yet to attract interest from HEV manufacturers. Yard spotting consists of moving empty or loaded trailers from position to position either for storage, loading, or pickup. As seen in the Yard Cycle, developed from these types of operations, yard trucks operate a low speed and power making them suitable for HEV application. The low acceleration demands would minimize the effects of the battery, motor, and controller 'dead weight' on the vehicle's fuel economy. As with the transit buses, yard spotters are never expected to leave their home operating area allowing them to be very specialized. The low average power requirement would make these vehicles especially suited to a series HEV drivetrain with a very small ICE being used as a generator. The dynamic performance of such an HEV should be superior to a conventional vehicle due to the speed - torque characteristics of electric motors providing maximum torque at low speed.

4.4.3 Cubage Limited Vehicles

Hybrid electric powertrains are quite heavy. In the simulated Class 8 vehicle, the batteries along with the battery box and electronics, electric motor, and controller weigh 500 kg. While this is only 1.5% of the GVW of the average Class 8 vehicle, commercial vehicles operate on very small profit margins and, if the vehicle's payload is limited by the GVW, the weight of the payload, hence the profit, is decreased by the weight of the

hybrid powertrain. Many vehicles are not loaded to the GVW during operation. For example, a truck hauling bread will be limited by the available volume rather than weight. In this case, the weight penalty from of the hybrid powertrain will be based on the inertial penalty in the road load equation but will not cut into the profit margin of the operator and the benefits of improved fuel economy become more substantial.

5. Conclusions

If used correctly, hybrid electric technology has the potential to significantly increase the fuel economy of heavy-duty vehicles. This is especially true in niche markets where the advantages of HEV drivetrains can be maximized through specialization. A potential 300% increase in fuel economy for Class 8 HEV yard spotters is a particularly interesting. Cubage limited vehicles also show the potential for a highly profitable HEV market. Incorrectly applied hybrid powertrains can also lead to poorer fuel economy than in conventional vehicles as shown in the 40% decrease in fuel economy for a Class 8 HEV over the Combined Cycle.

The dependence of HEV fuel economy on the order of events in a cycle was shown to be very significant by reversing the order of the cycles in the Combined Cycle. The Class 6 vehicle went from a 39% decrease in fuel economy on the Combined Cycle to a 16% increase on the reversed cycle.

Removing auxiliary loads from the engines on HEVs and even conventional vehicles, where possible, by making them electrically driven would greatly improve fuel economy. Not only would the load on the engine be decreased, but also the overall engine efficiency over a driving cycle would be increased.

Further refinement of the Excel simulation would only increase the reliability of the results, but, as features such as gear ratios, shifts, engine and motor maps, and torque analysis are included, the opportunity for user error and for producing highly subjective results is increased.

Further investigation might include an overview of the process of selecting an appropriate HEV for a given application. A potential HEV customer would be expected to analyze the vehicles in his or her fleet examining both the vehicles and their typical operational modes. After an optimum configuration and component sizes were found, the fuel economy and additional vehicle cost of the resulting HEV could be compared to the fuel economy and cost of a conventional vehicle to determine the potential savings. If these savings were significant, the customer would be advised to purchase and operate HEVs.

References

[1] http://www.ta.doc.gov/pngv/ (4/29/2001)

[2] http://www.osti.gov/hvt/21stcenturytruck.pdf (5/2/2001)

[3] Tóth-Nagy, Csaba, "Investigation and Simulation of the Planetary Combination Hybrid Electric Vehicle", Masters Thesis, West Virginia University, 2000.

[4] Parsley, William, "New York City Transit Operating Experience with Hybrid Transit Buses", SAE / NESEA Hybrid Electric Vehicles in the Bus and Truck Markets TOPTEC: New Ways of Building Better Heavy Duty Vehicles, May 11-12, 2000.

[5] An, F., Stodolsky, F., Vyas, A., Cuenca, R., "Scenario Analysis of Hybrid Class 3 – 7 Heavy Vehicles", SAE Paper 2000-01-0989.

[6] http://www.dieselnet.com

[7] Wang, M., Vehicle Greenhouse Gas Emissions: The Role of Fuel-Cycle Analysis, FutureTruck 2000 Workshop, Pontiac, MI, Sept. 20, 1999.

[8] http://www.gmc.com/

[9] http://www.4adodge.com/

[10] http://www.fordvehicles.com/common/home2.asp

[11] West Virginia University Transportable Heavy-Duty Emissions Testing Laboratory Database, Mechanical and Aerospace Engineering Dept., College of Engineering and Mineral Resources, West Virginia University, January 2001.

[12] Clark, N. N., Daley, J. J., Nine, R. D., Atkinson, C. M., "Application of the New City-Suburban Heavy Vehicle Route (CSHVR) to Truck Emissions

Characterization", SAE Fuels and Lubricants Meeting, SAE Paper 1999-01-1467, Dearborn, MI, May 3-6, 1999.

[13] Clark, N. N. , McKain, D. L., Balon, T. H., Moynihan, P. J., Lynch, S. A., Webb, T. C., "Characterization of Emissions from Hybrid-Electric and Conventional Buses", SAE Fuels and Lubricants Meeting, SAE Paper 2000-01-2011, Paris, France, June 19-22, 2000.

[14] Nine, R. D., Clark, N. N., Daley, J. J., Atkinson, C. M., "Development of a Heavy-Duty Chassis Dynamometer Driving Route", Department of Mechanical and Aerospace Engineering, West Virginia University, Morgantown, WV, 1999.

[15] Gillespie, T. D., Fundamentals of Vehicle Dynamics, SAE, Warrendale, PA, 1992.

[16] http://www.hepi.com/

[17] Kellermeyer, W. F., "Development and Validation of a Modular Hybrid Electric Vehicle Simulation Model", Masters Thesis, West Virginia University, 1998.

[18] Davis, S. C., "Transportation Energy Data Book: Edition 19", Oak Ridge National Laboratory, Oak Ridge, TN, September 1999.

[19] "Hybrid-Electric Drive Heavy-Duty Vehicle Testing Project – Final Emissions Report", NAVC, DARPA, Northeast Advanced Vehicle Consortium, M. J. Bradley & Associates, Inc., and West Virginia University, 2000.

Appendix

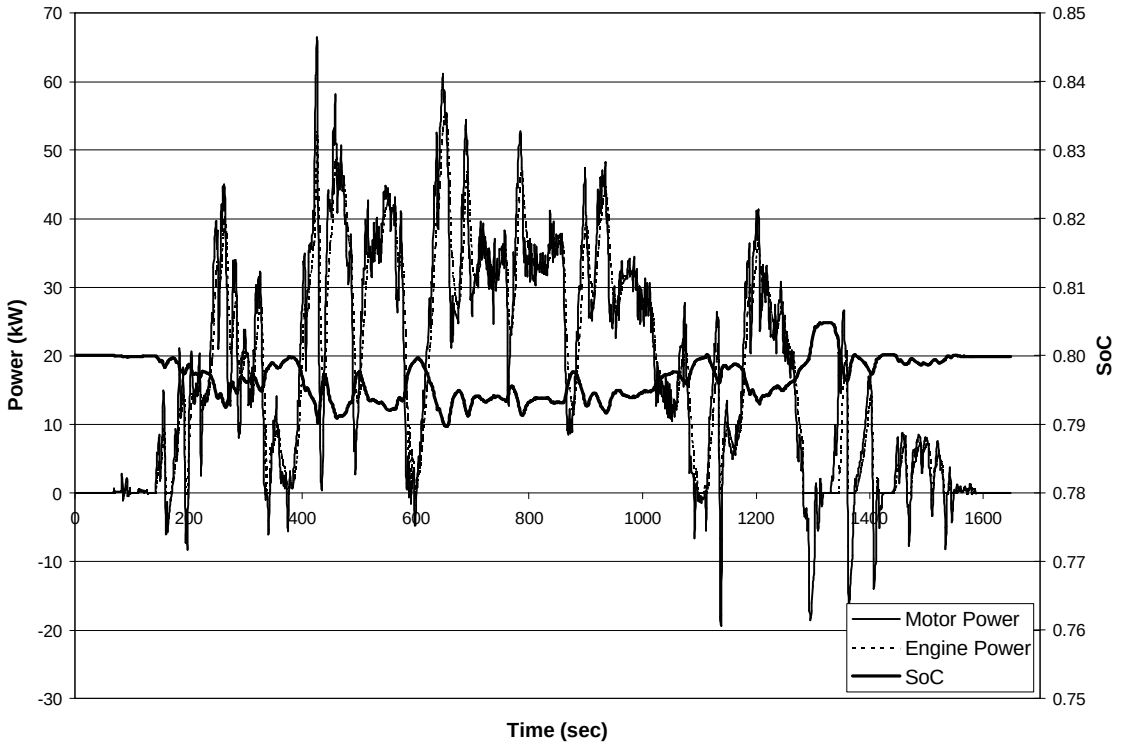

Figure A.1 Class 2B Series HEV on Freeway Cycle without auxiliary load.

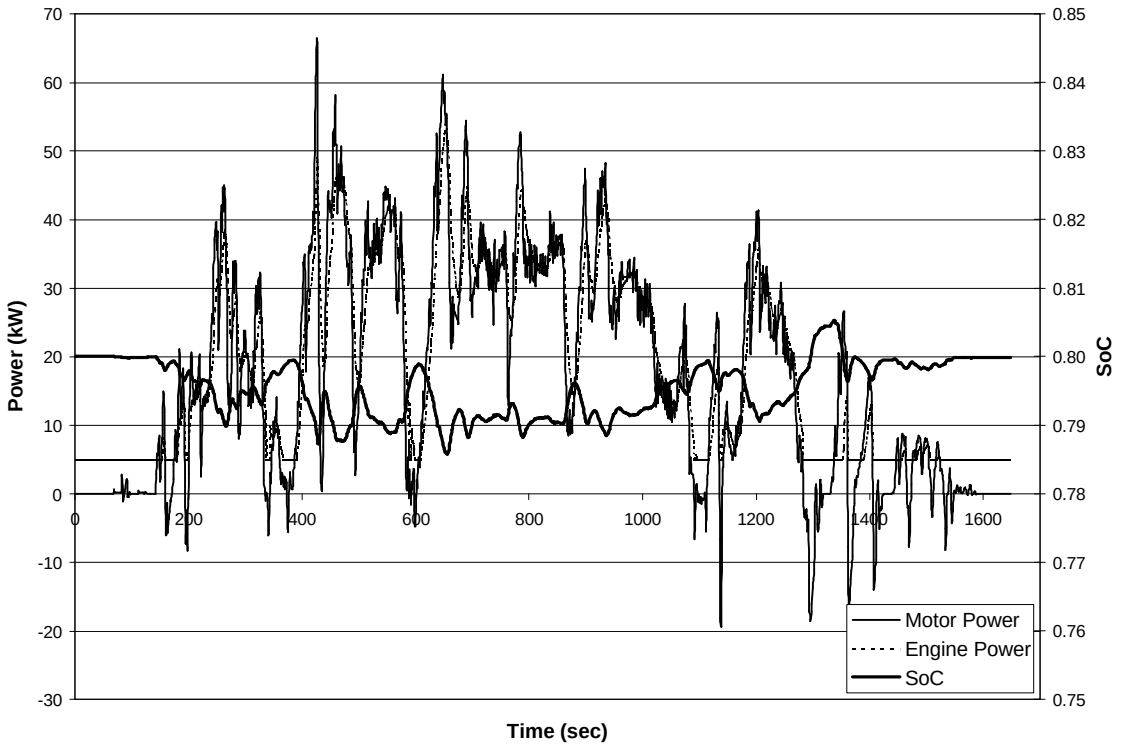

Figure A.2 Class 2B Series HEV on Freeway Cycle with auxiliary load.

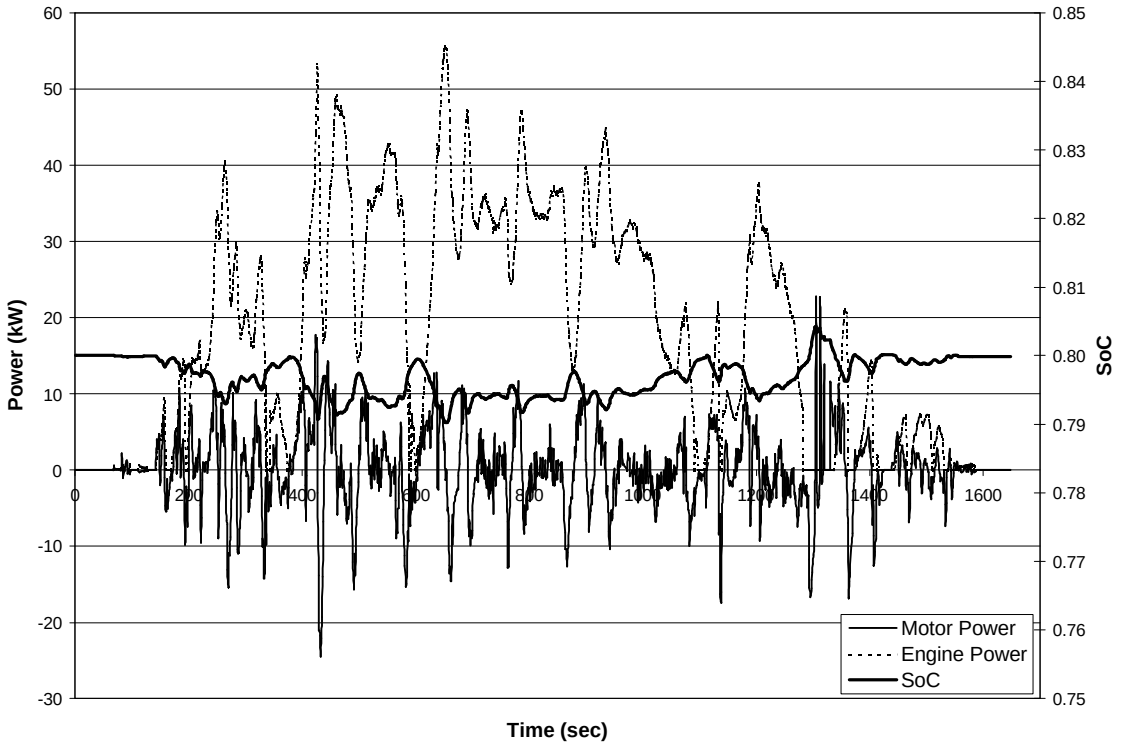

Figure A.3 Class 2B Parallel HEV on Freeway Cycle without auxiliary load.

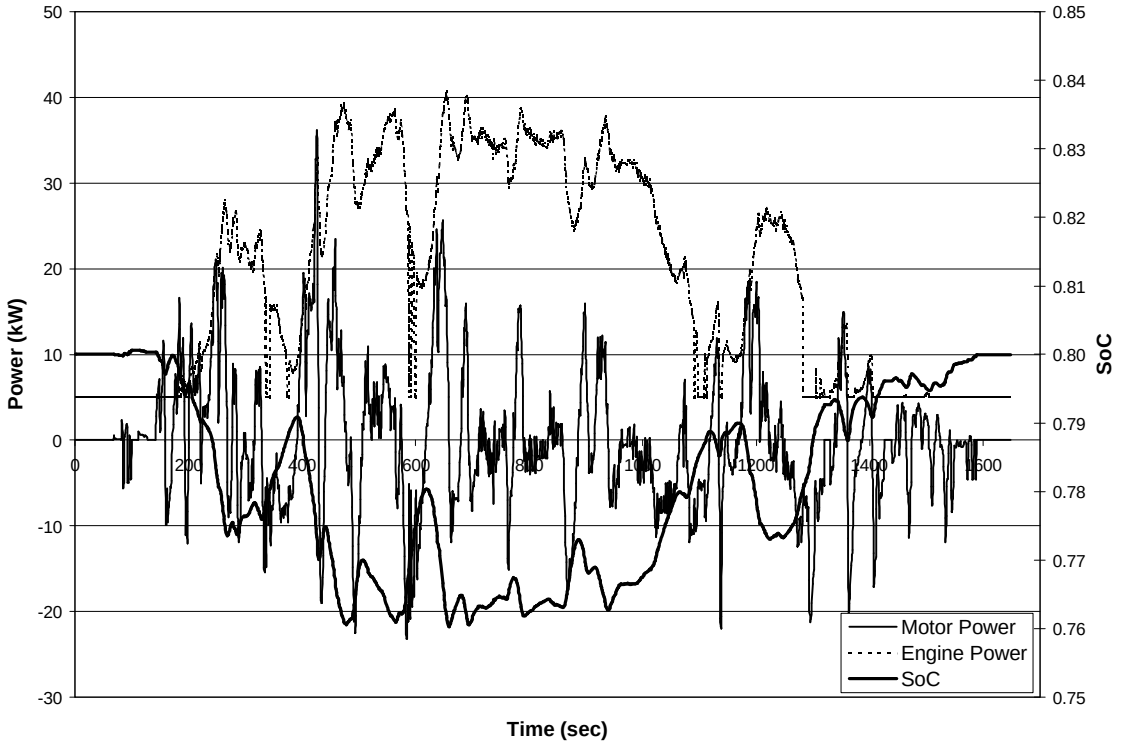

Figure A.4 Class 2B Parallel HEV on Freeway Cycle with auxiliary load.

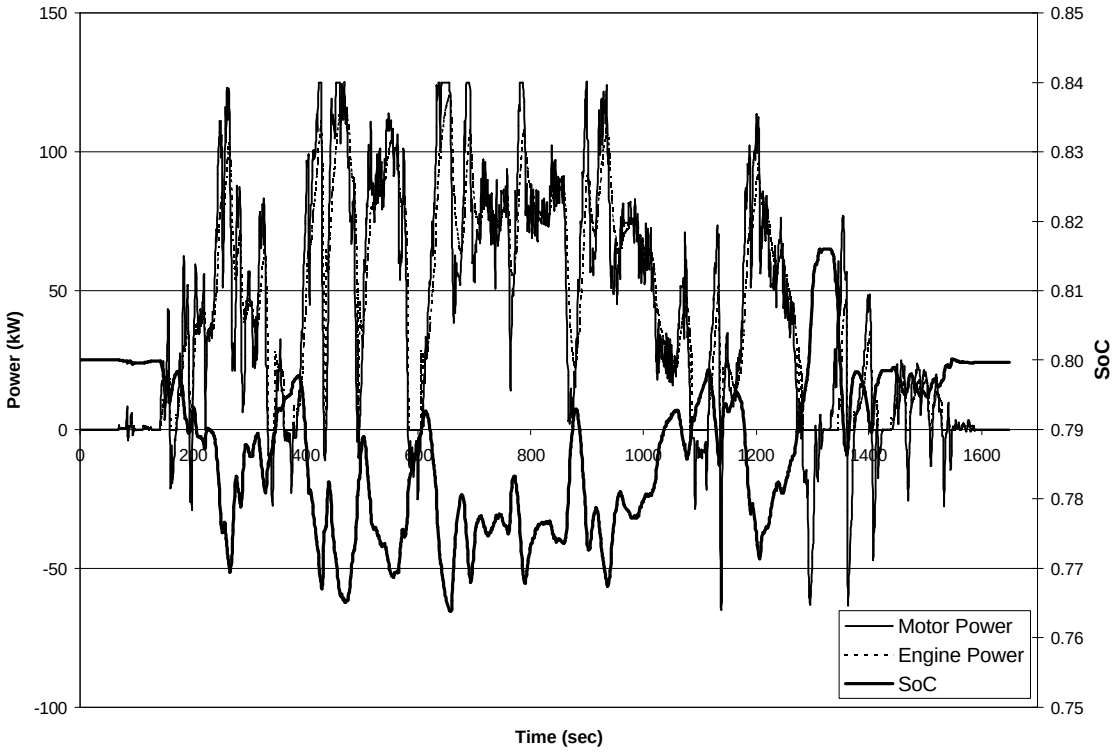

Figure A.5 Class 6 Series HEV on Freeway cycle without auxiliary load.

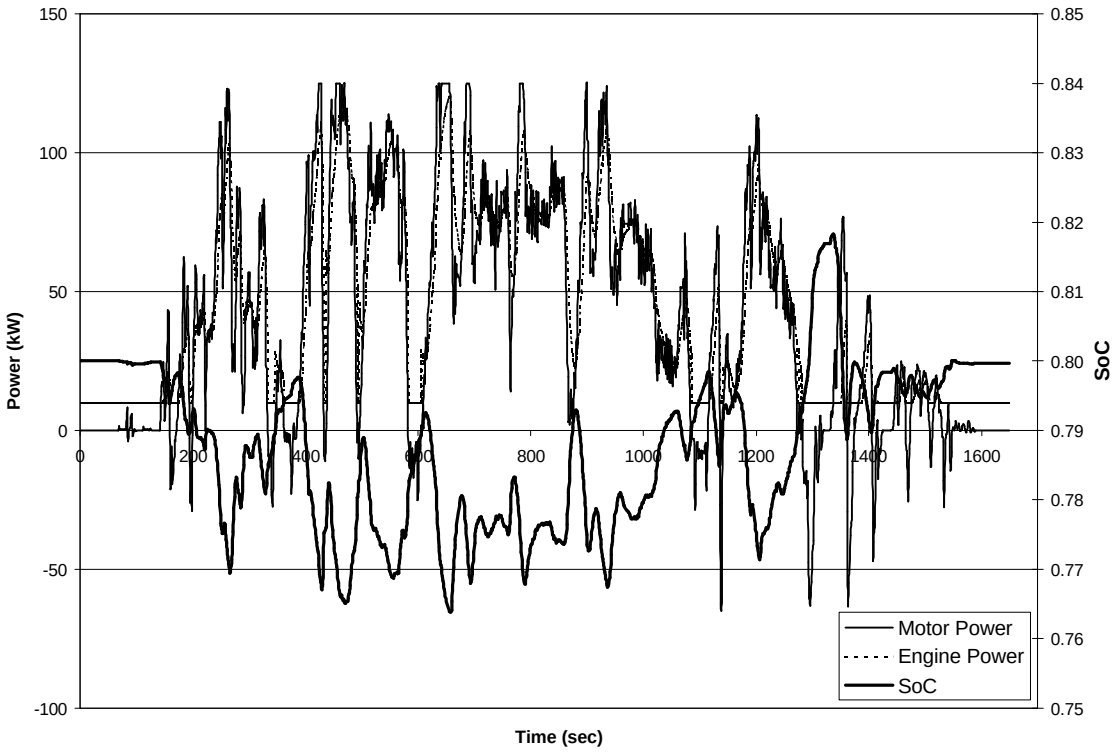

Figure A.6 Class 6 Series HEV on Freeway Cycle with auxiliary load.

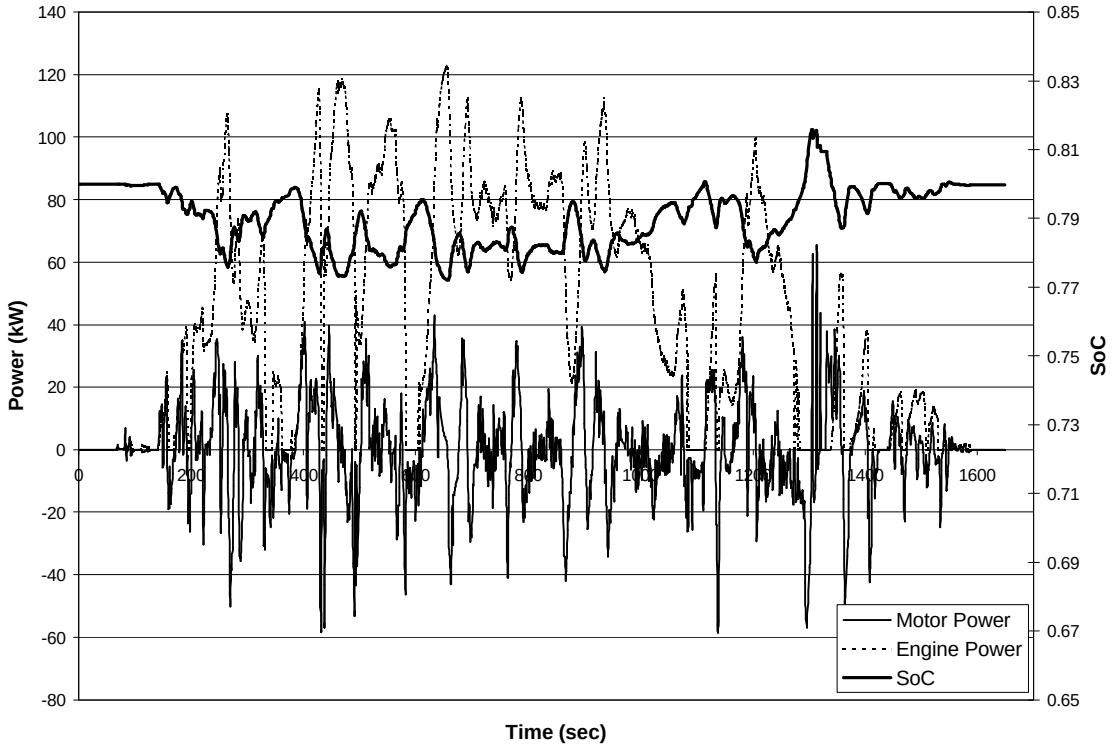

Figure A.7 Class 6 Parallel HEV on Freeway Cycle without auxiliary load.

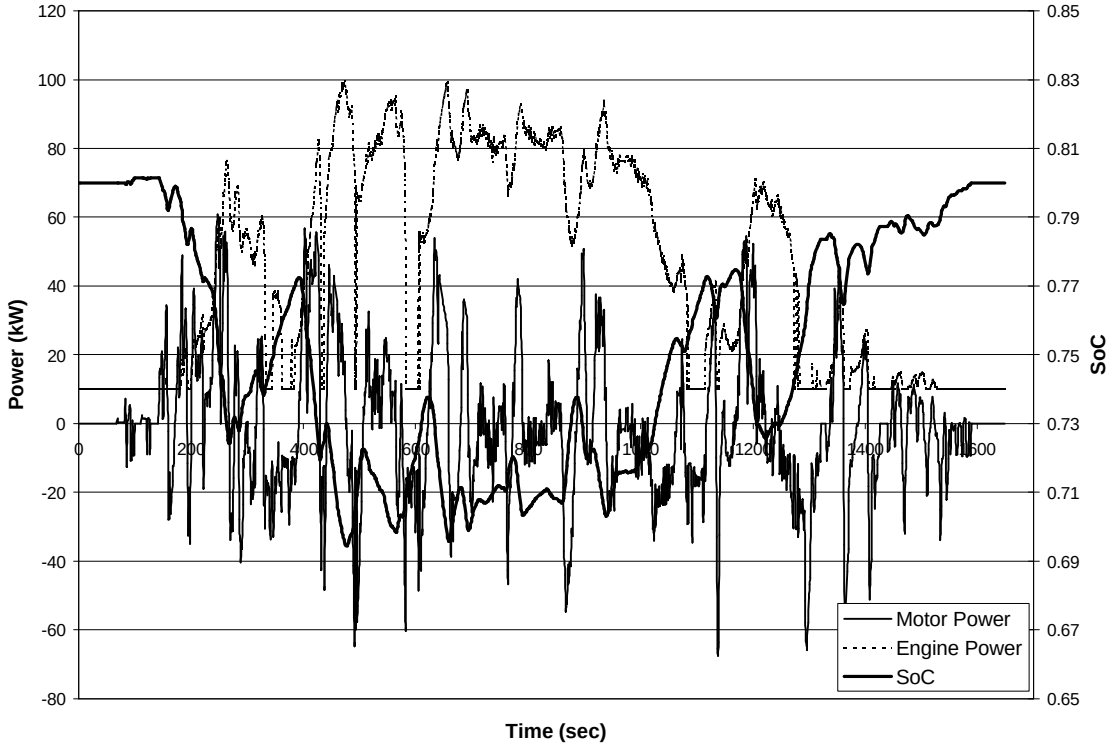

Figure A.8 Class 6 Parallel HEV on Freeway Cycle with auxiliary load.

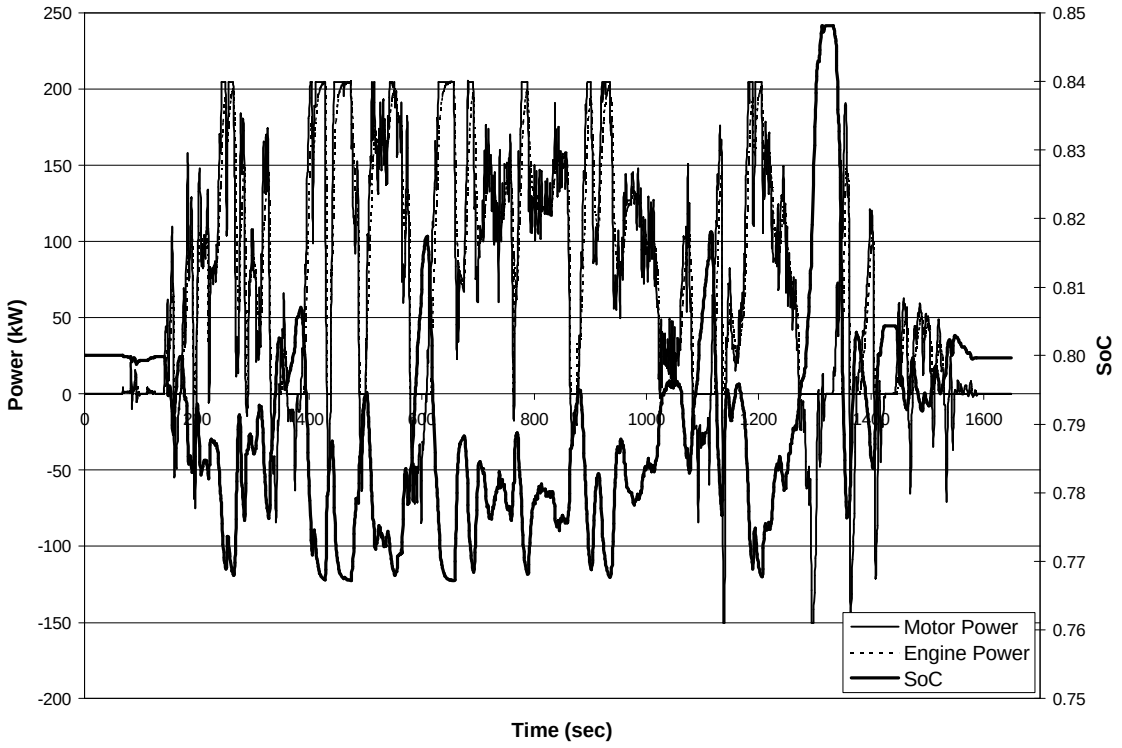

Figure A.9 Class 8 Series HEV on Freeway Cycle without auxiliary load.

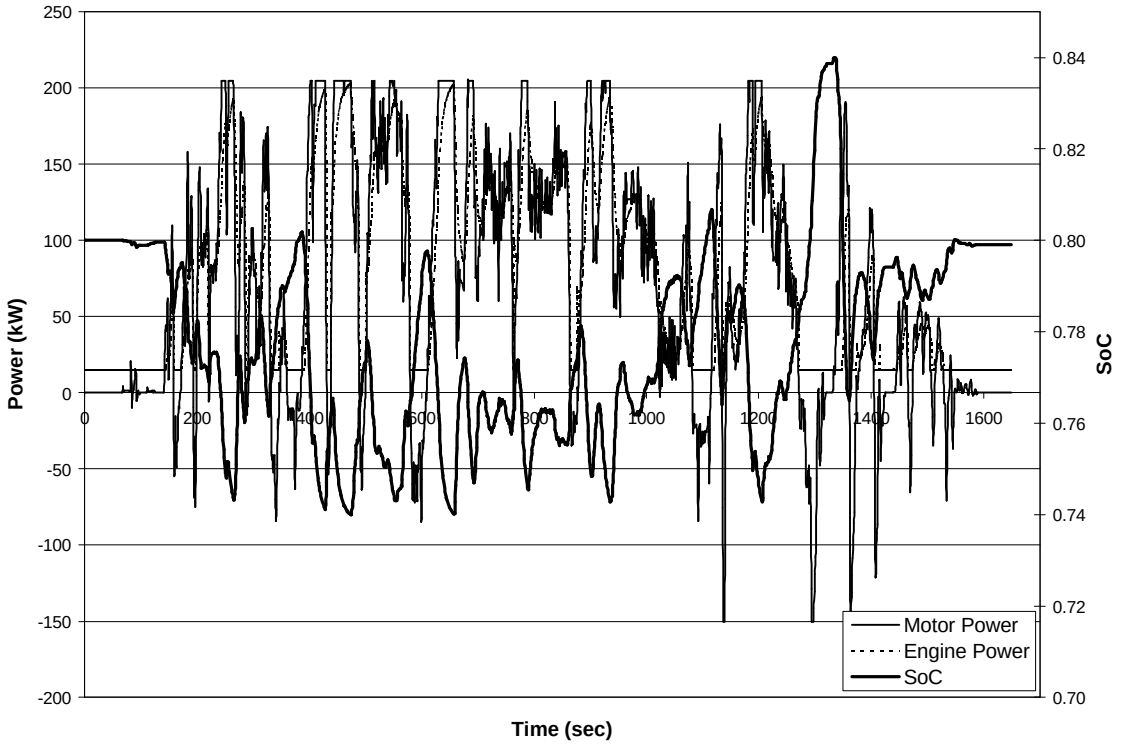

Figure A.10 Class 8 Series HEV on Freeway Cycle with auxiliary load.

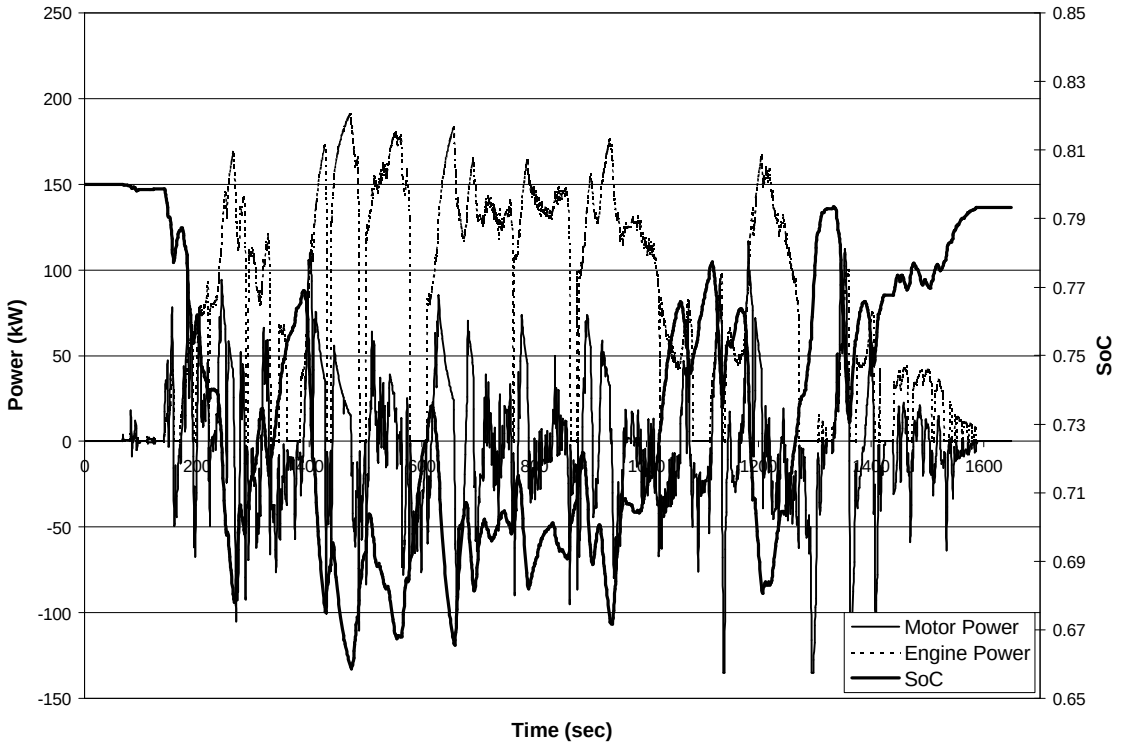

Figure A.11 Class 8 Parallel HEV on Freeway Cycle without auxiliary load.

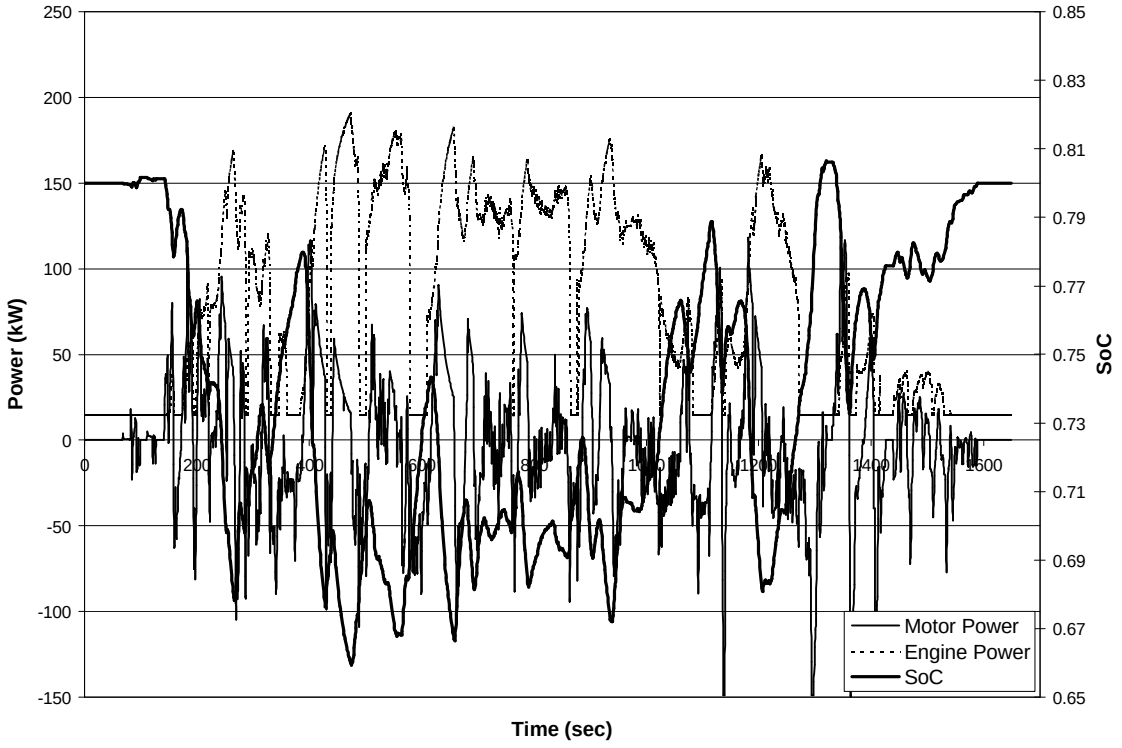

Figure A.12 Class 8 Parallel HEV on Freeway Cycle with auxiliary load.

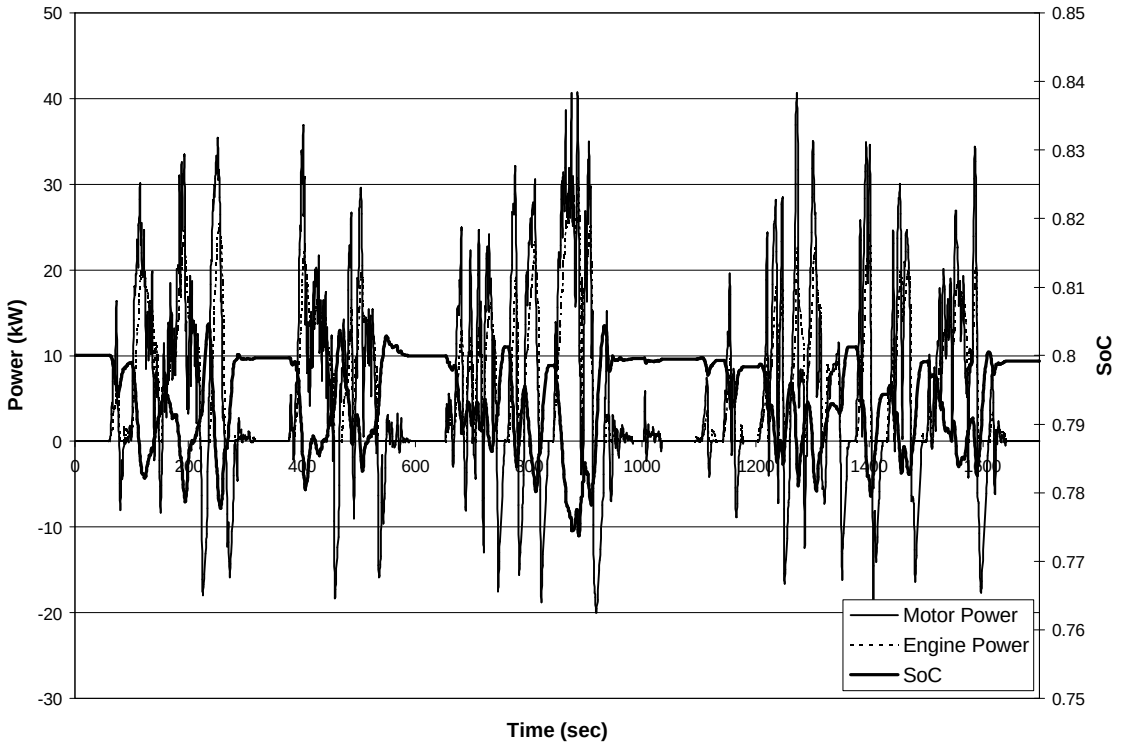

Figure A.13 Class 2B Series HEV on CSHVC without auxiliary load.

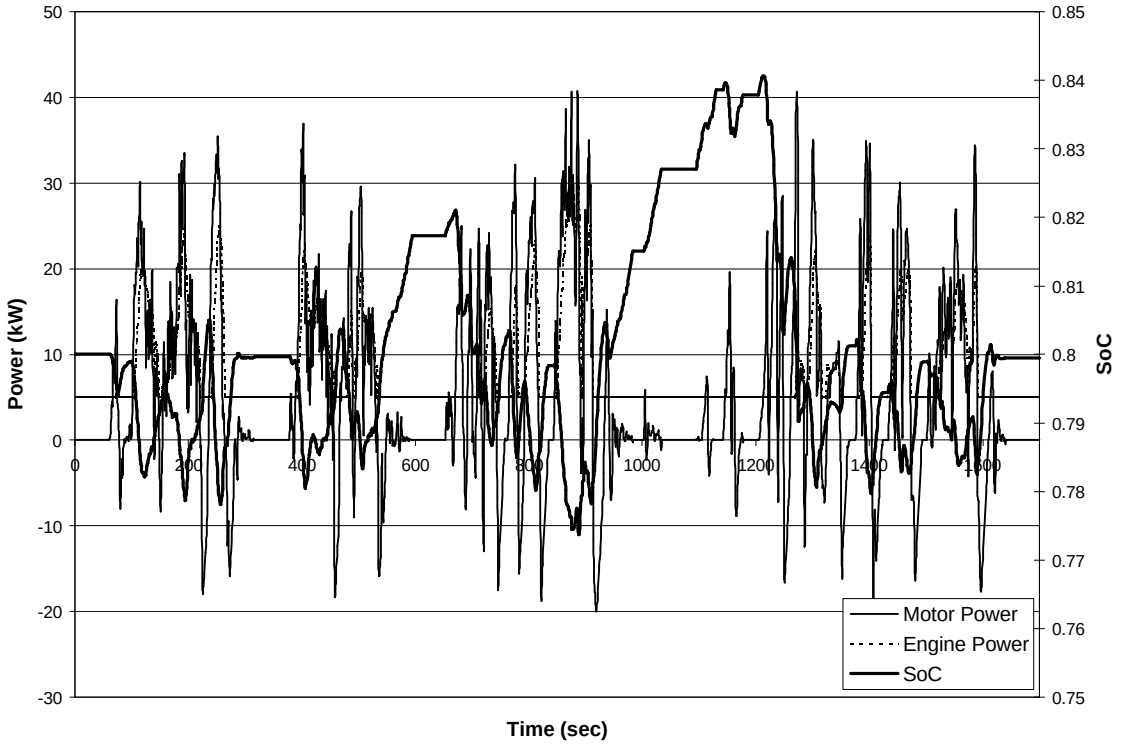

Figure A.14 Class 2B Series HEV on CSHVC with auxiliary load.

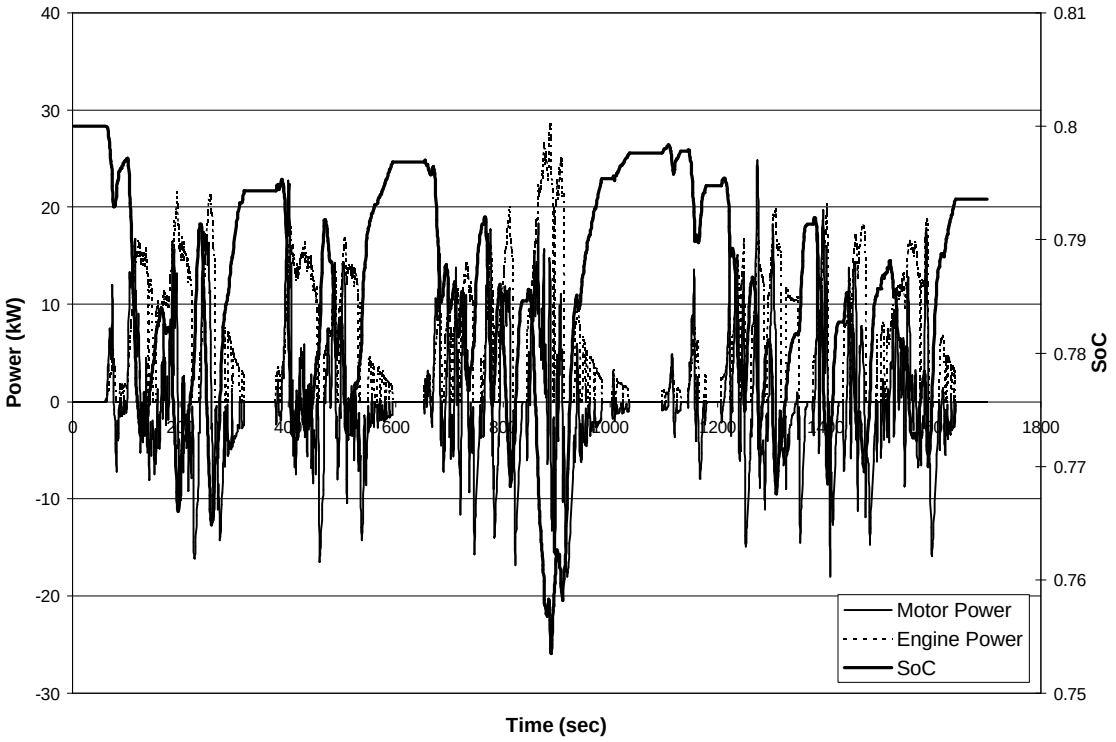

Figure A.15 Class 2B Parallel HEV on CSHVC without auxiliary load.

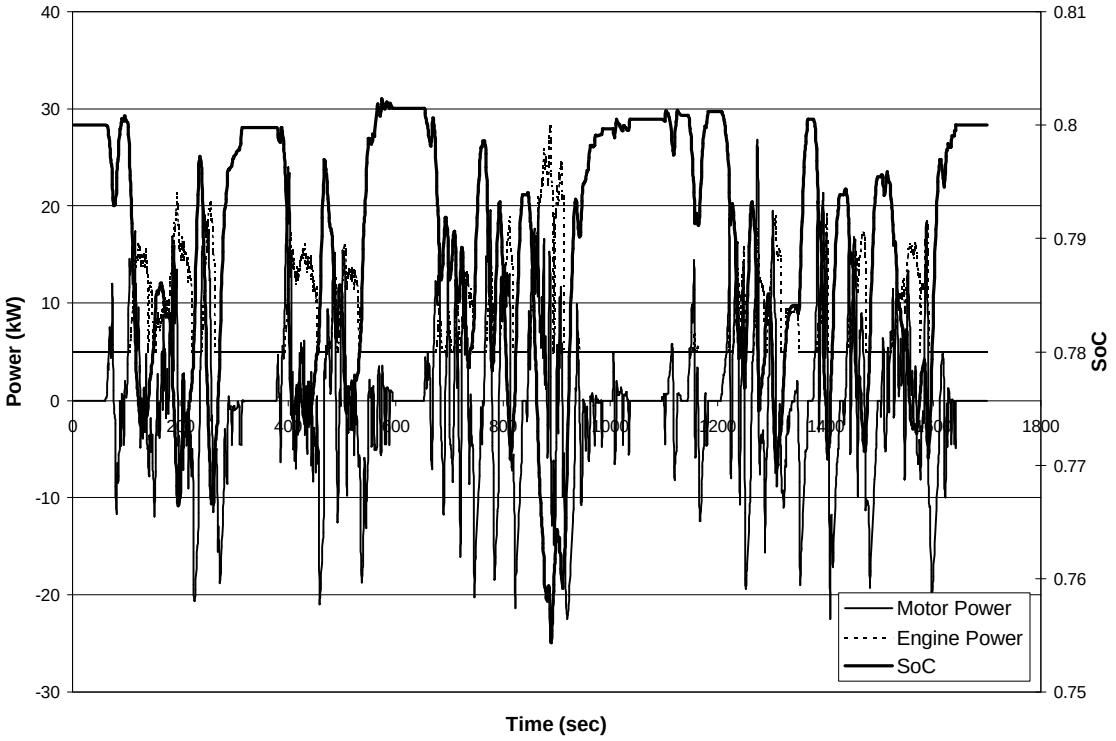

Figure A.16 Class 2B Parallel HEV on CSHVC with auxiliary load.

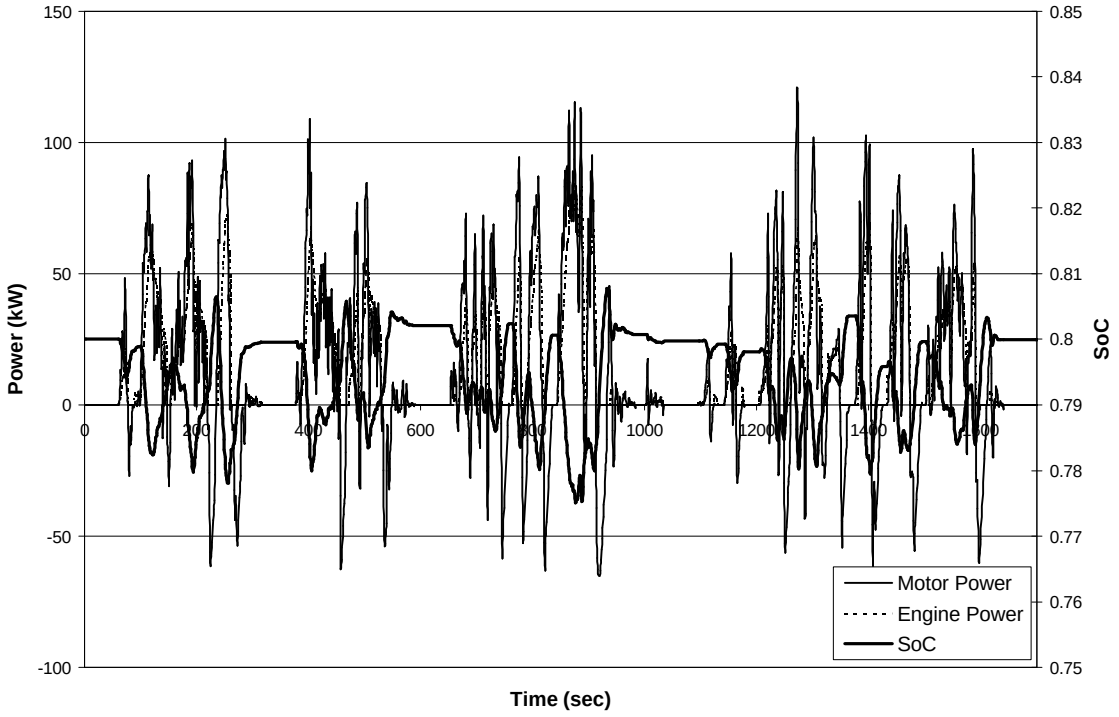

Figure A.17 Class 6 Series HEV on CSHVC without auxiliary load.

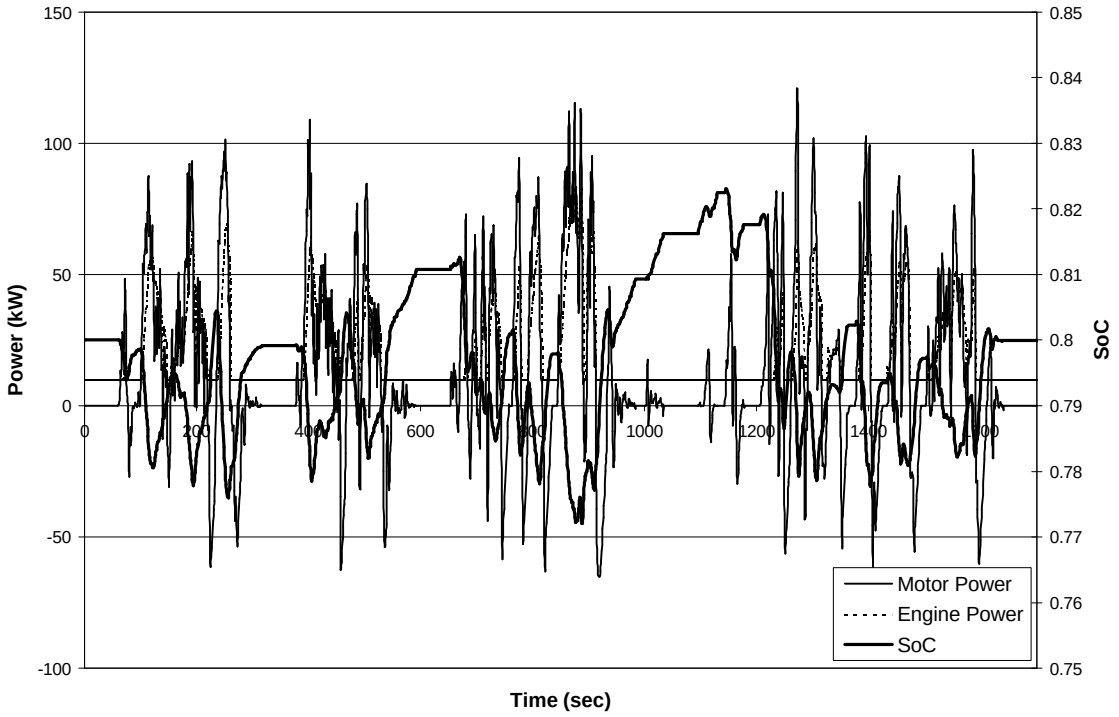

Figure A.18 Class 6 Series HEV on CSHVC with auxiliary load.

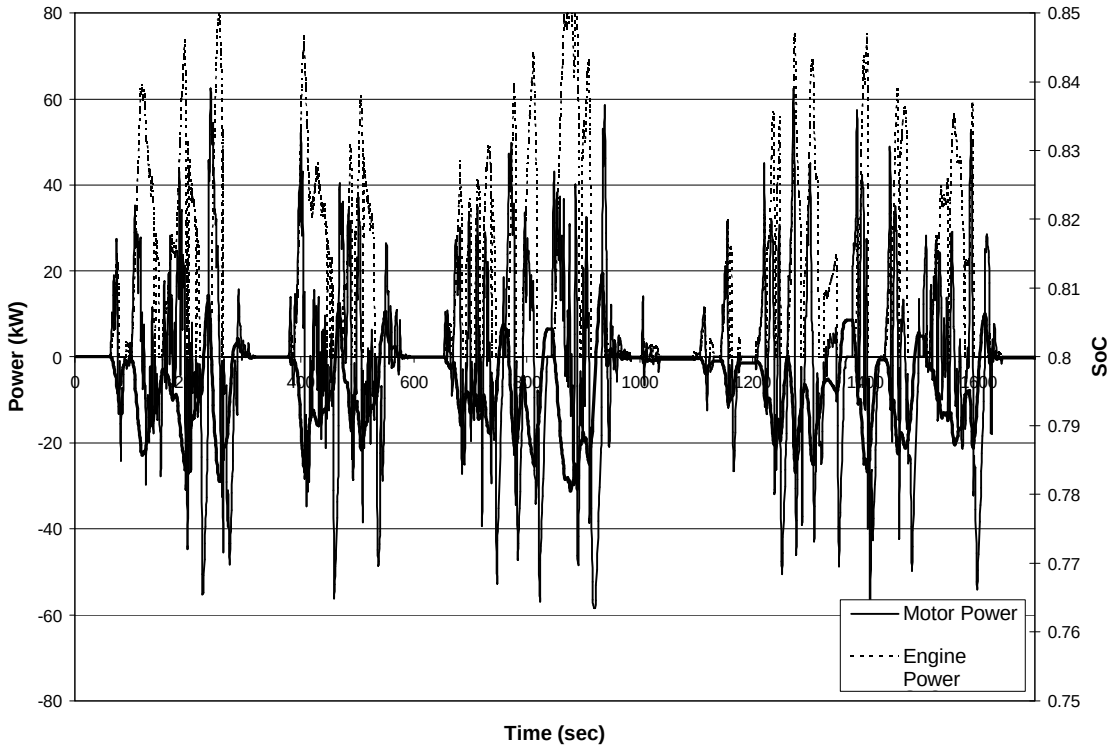

Figure A.19 Class 6 Parallel HEV on CSHVC without auxiliary load.

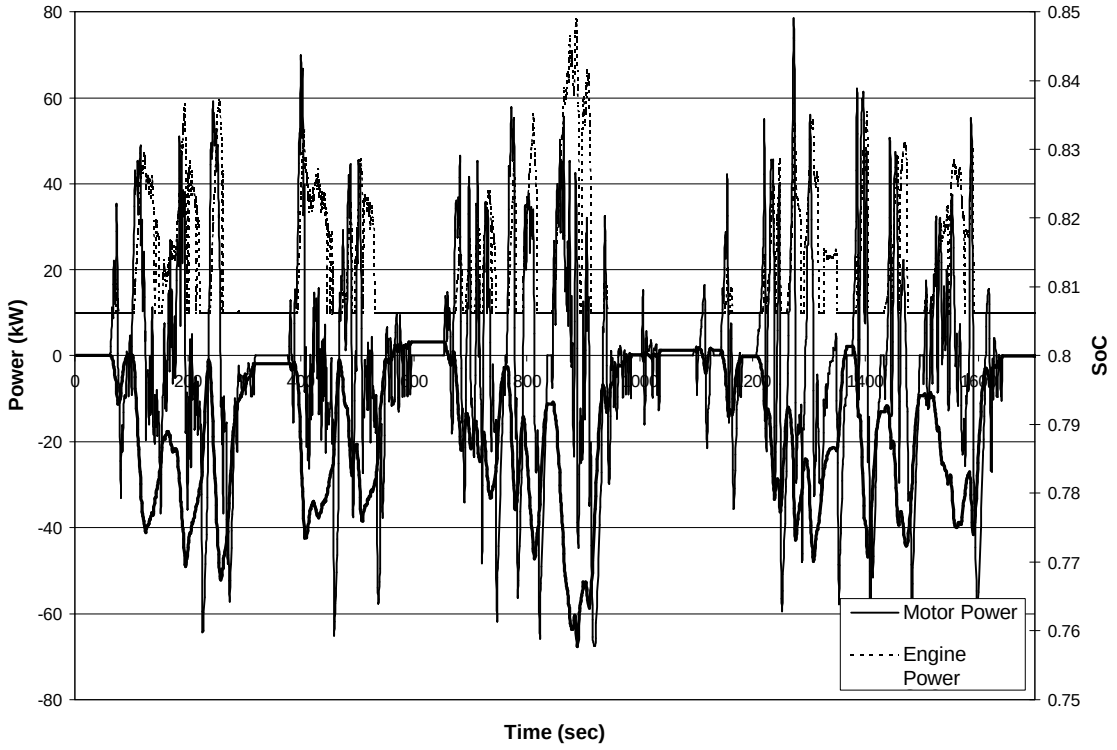

Figure A.20 Class 6 Parallel HEV on CSHVC with auxiliary load.

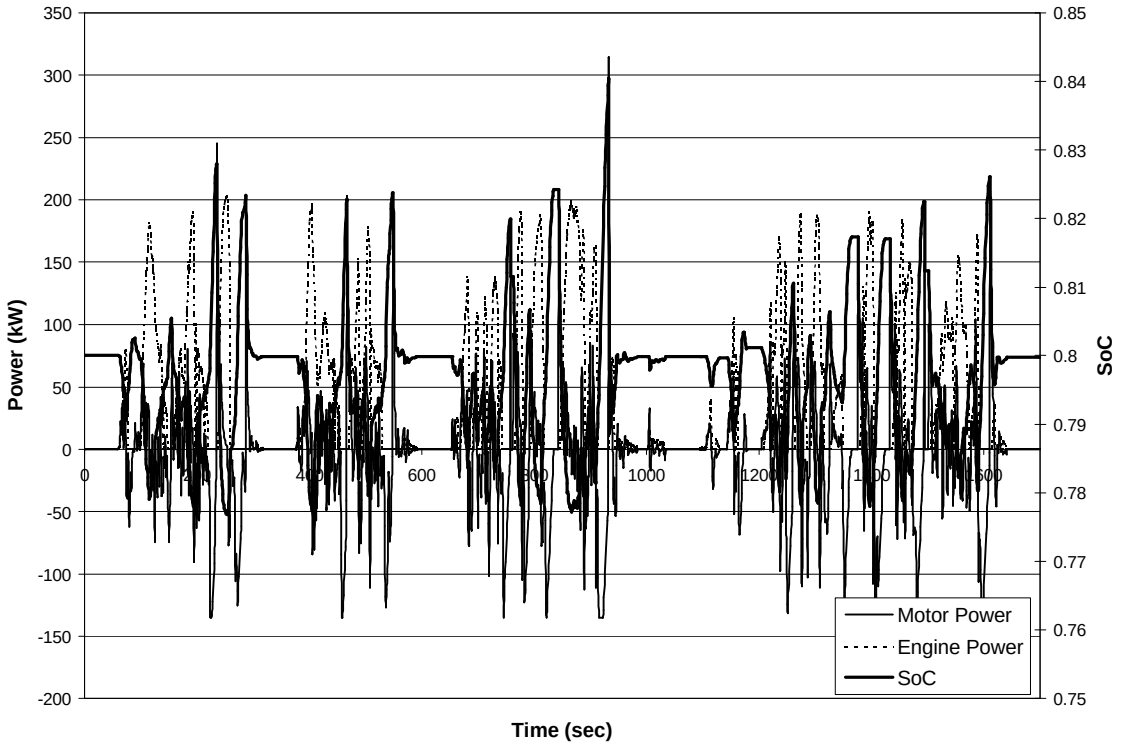

Figure A.21 Class 8 Series HEV on CSHVC without auxiliary load.

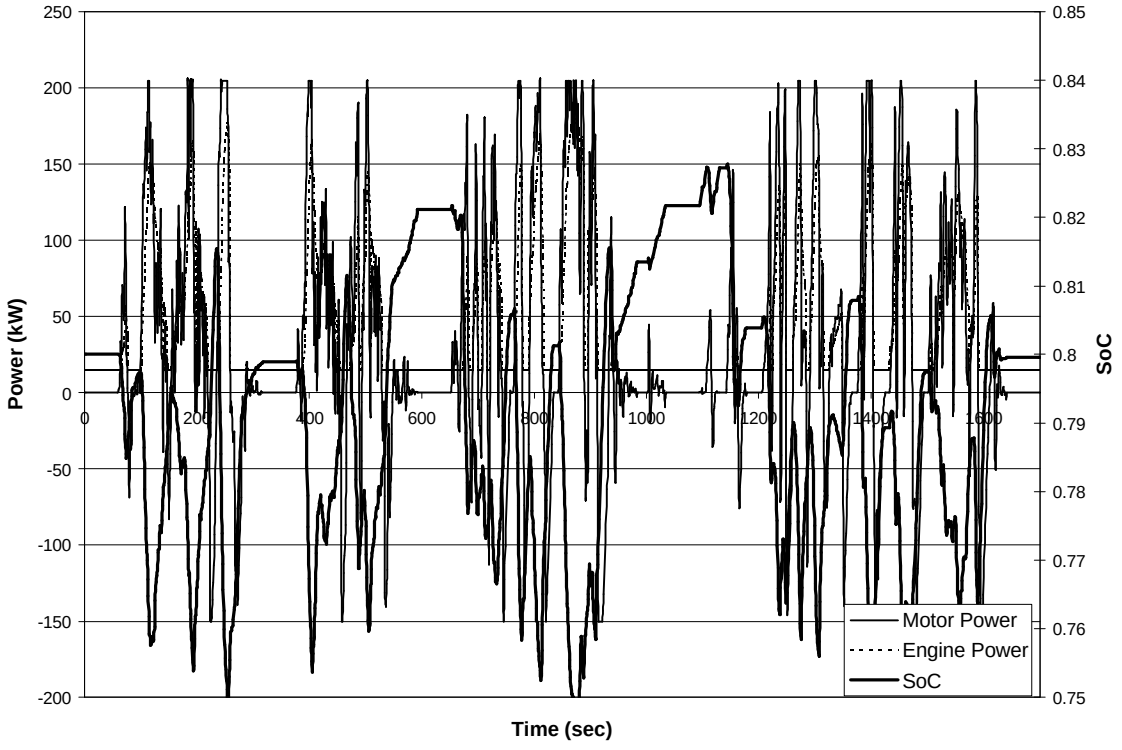

Figure A.22 Class 8 Series HEV on CSHVC with auxiliary load.

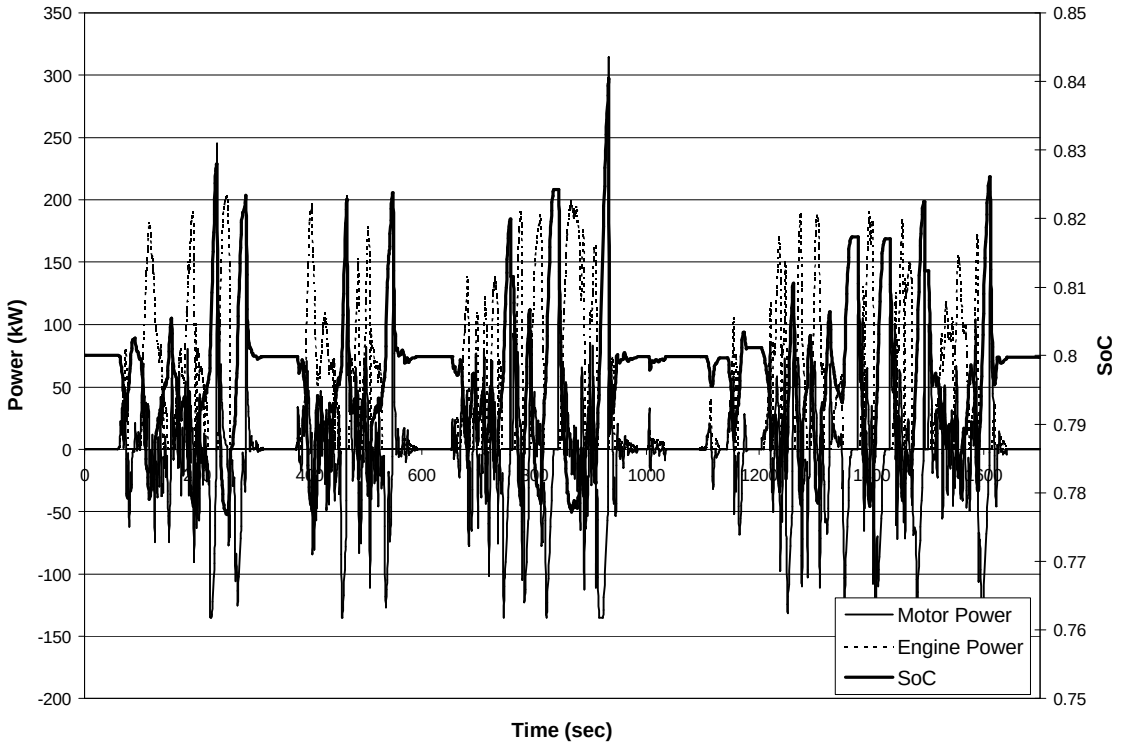

Figure A.23 Class 8 Parallel HEV on CSHVC without auxiliary load.

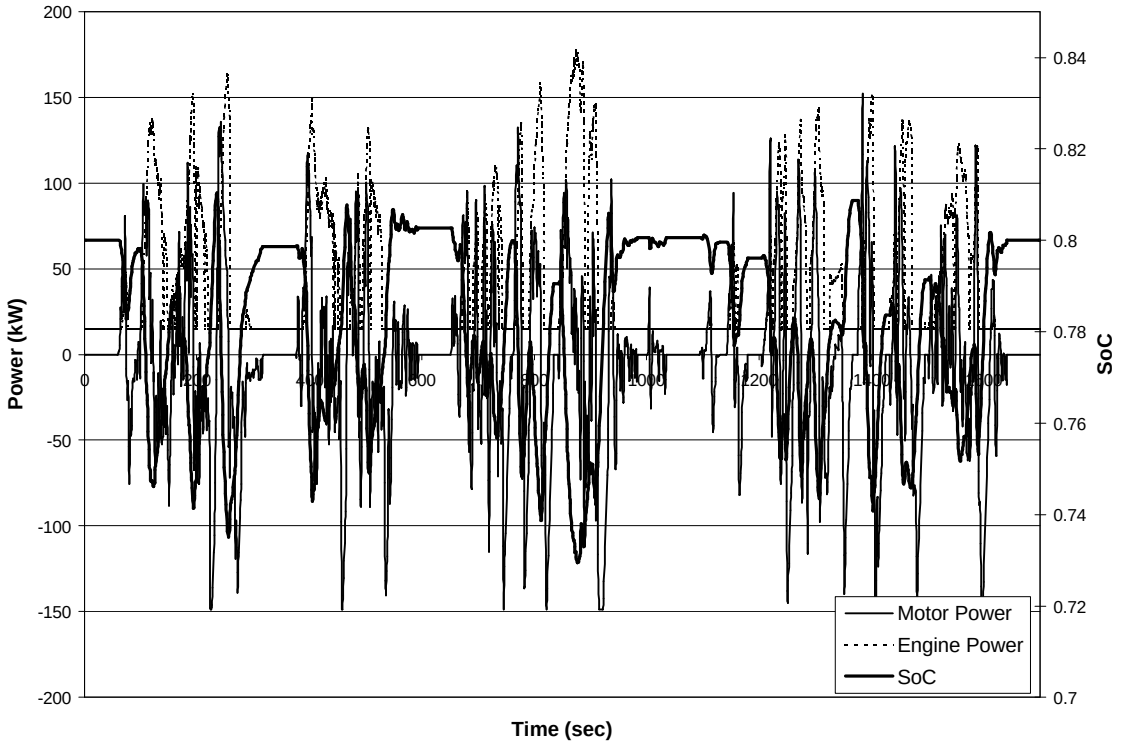

Figure A.24 Class 8 Parallel HEV on CSHVC with auxiliary load.

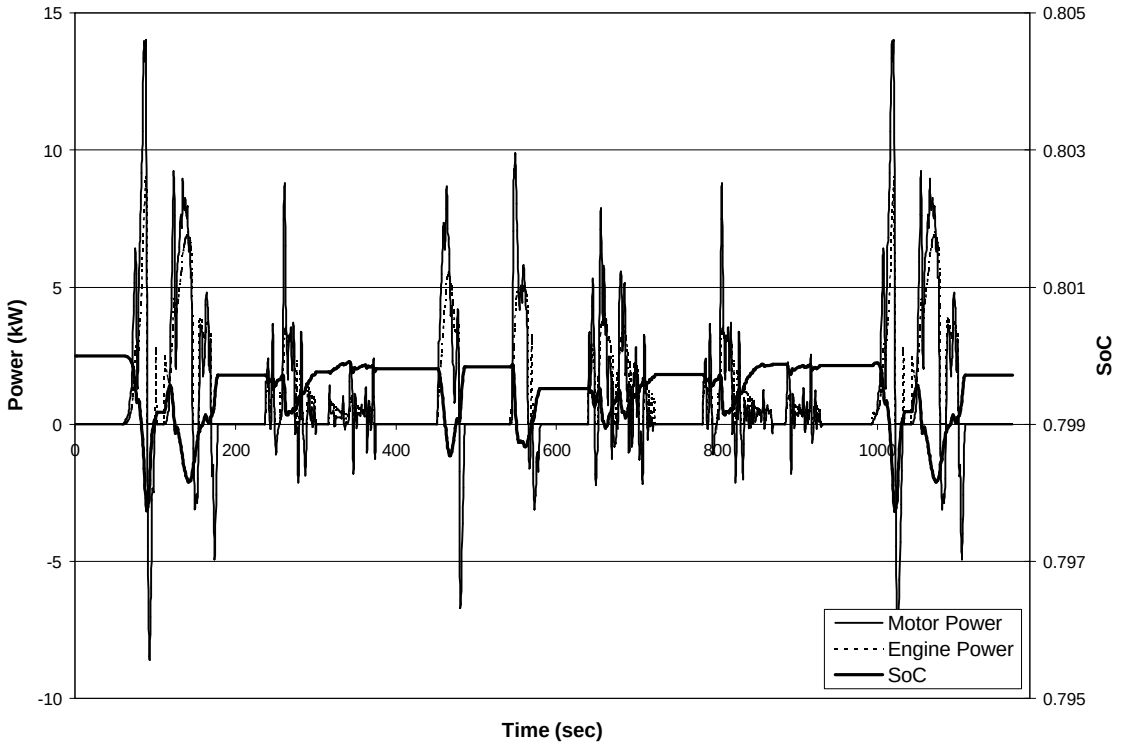

Figure A.25 Class 2B Series HEV on Yard Cycle without auxiliary load.

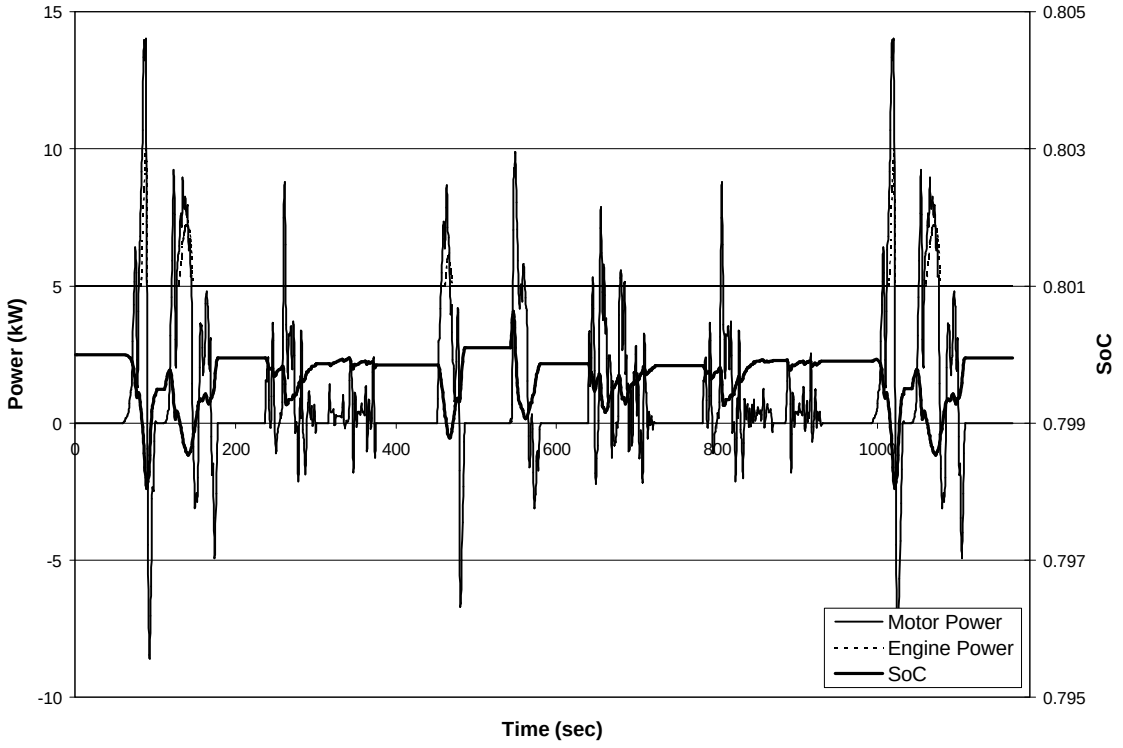

Figure A.26 Class 2B Series HEV on Yard Cycle with auxiliary load.

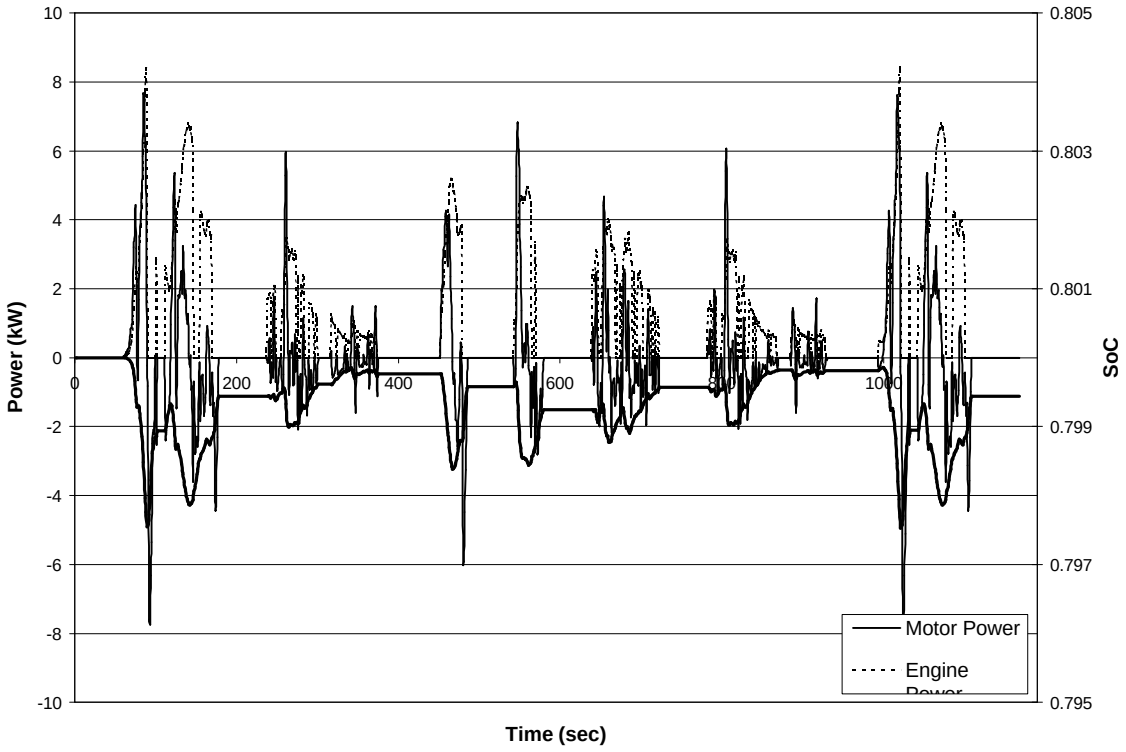

Figure A.27 Class 2B Parallel HEV on Yard Cycle without auxiliary load.

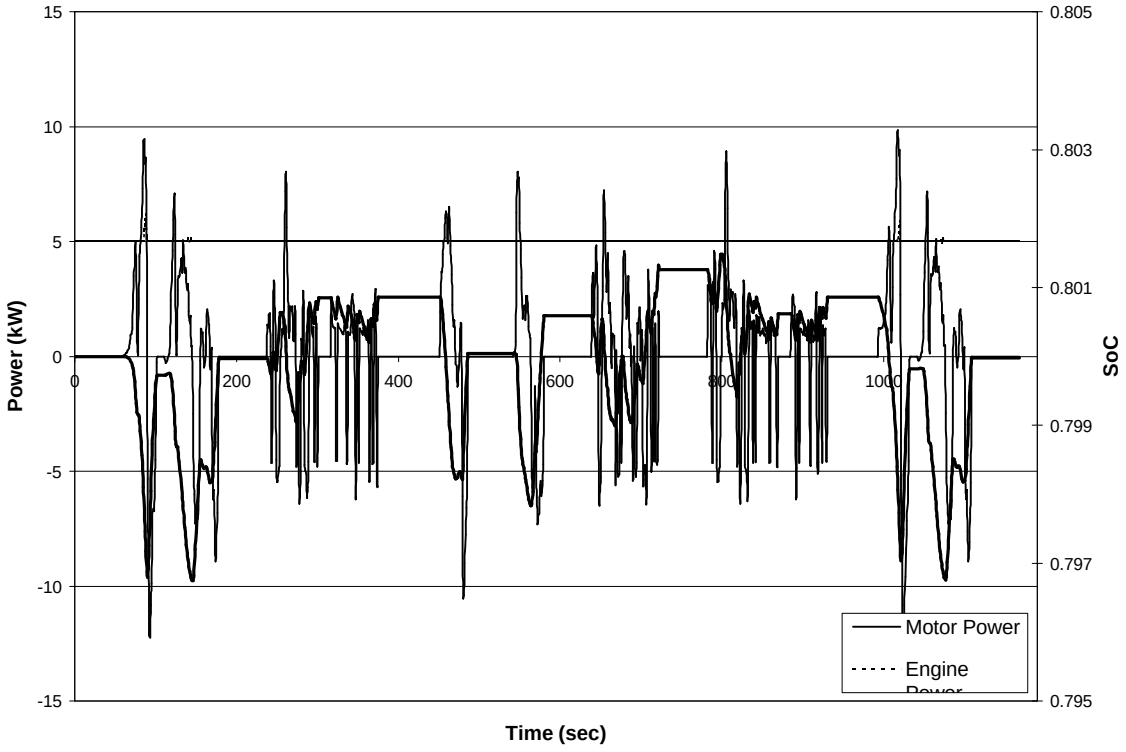

Figure A.28 Class 2B Parallel HEV on Yard Cycle with auxiliary load.

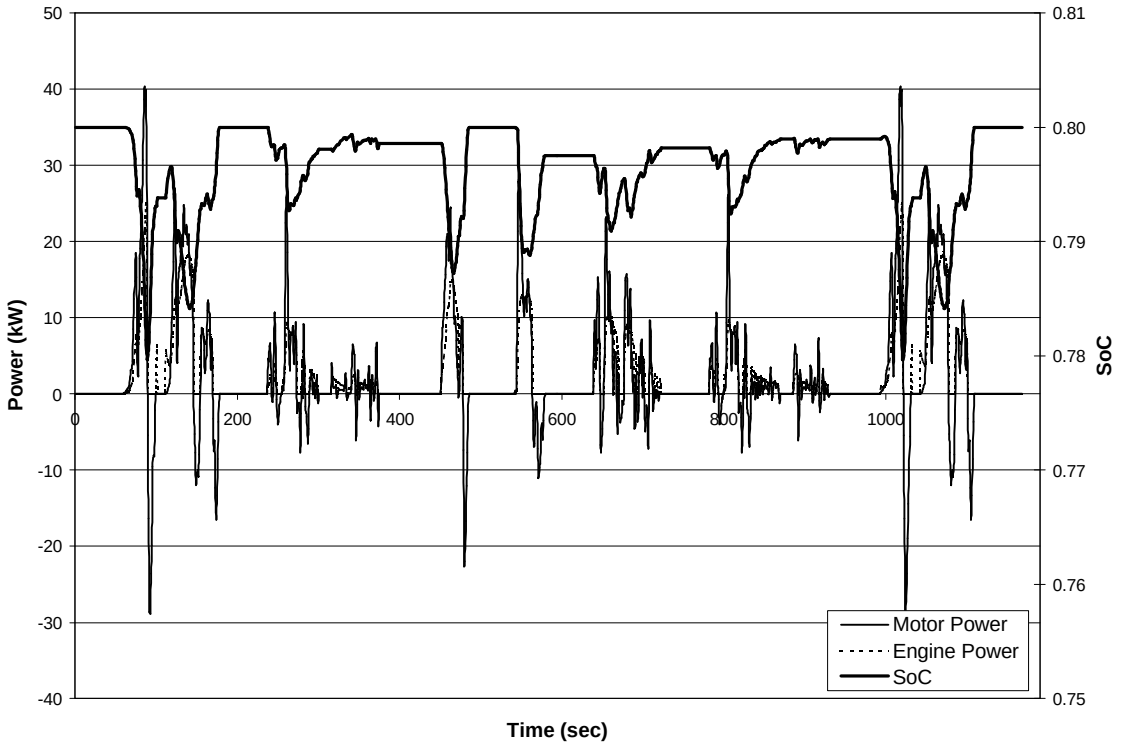

Figure A.29 Class 6 Series HEV on Yard Cycle without auxiliary load.

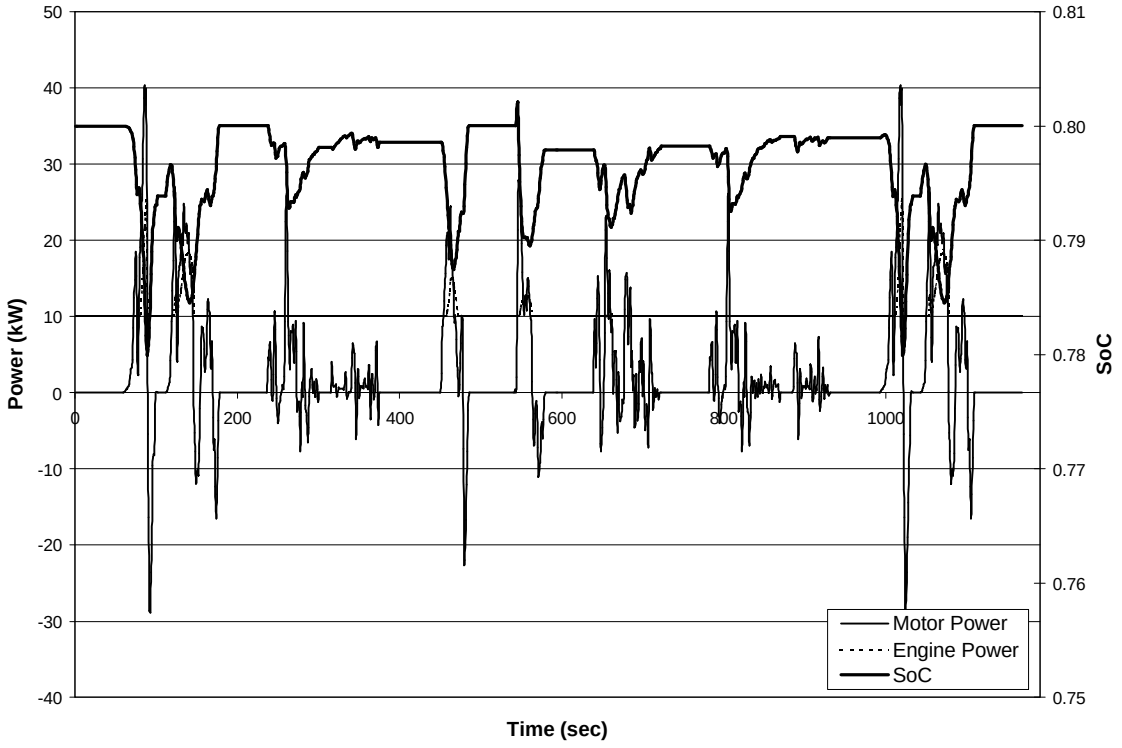

Figure A.30 Class 6 Series HEV on Yard Cycle with auxiliary load.

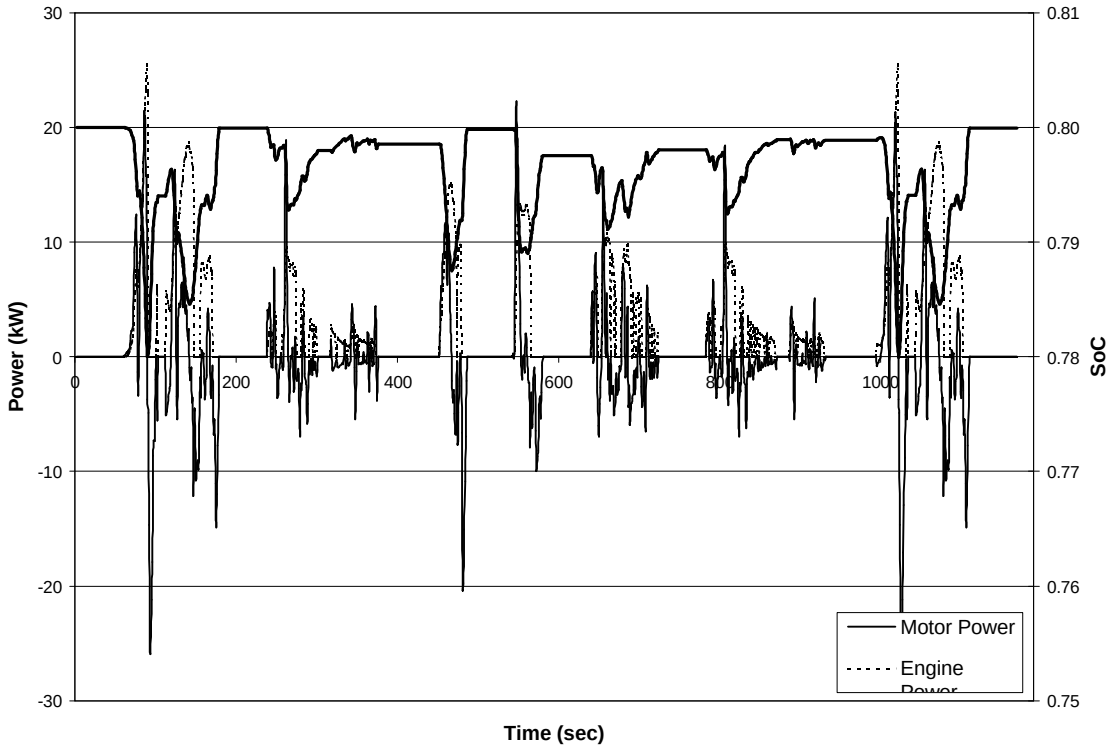

Figure A.31 Class 6 Parallel HEV on Yard Cycle without auxiliary load.

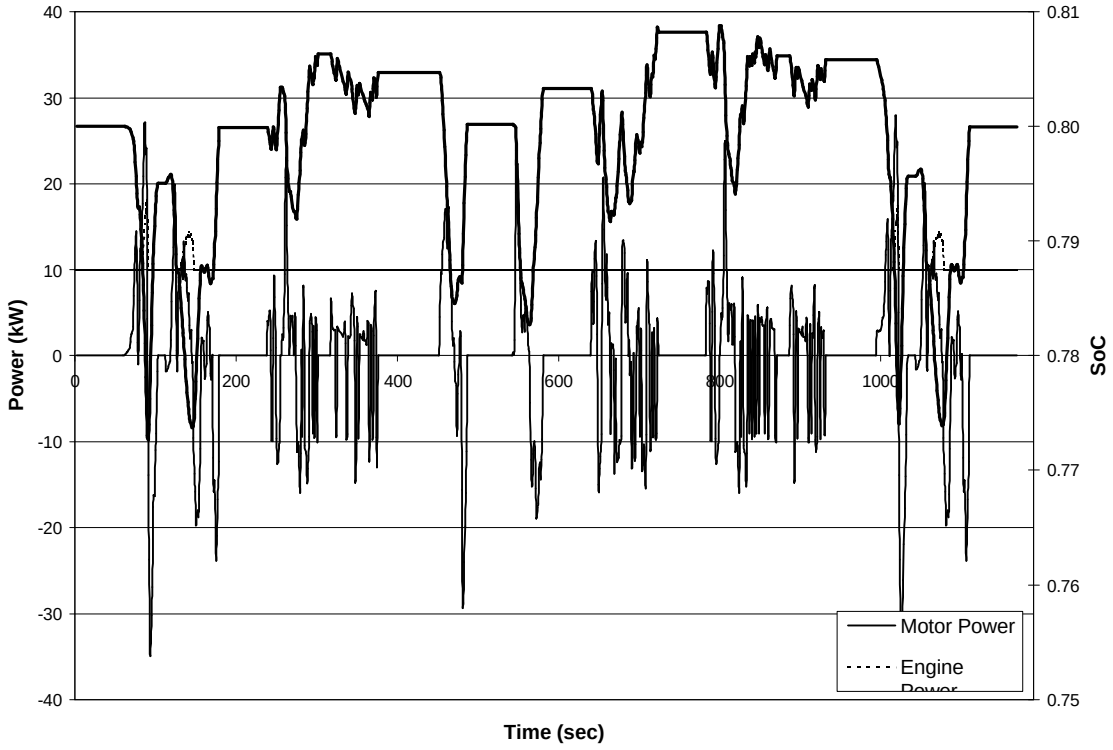

Figure A.32 Class 6 Parallel HEV on Yard Cycle with auxiliary load.

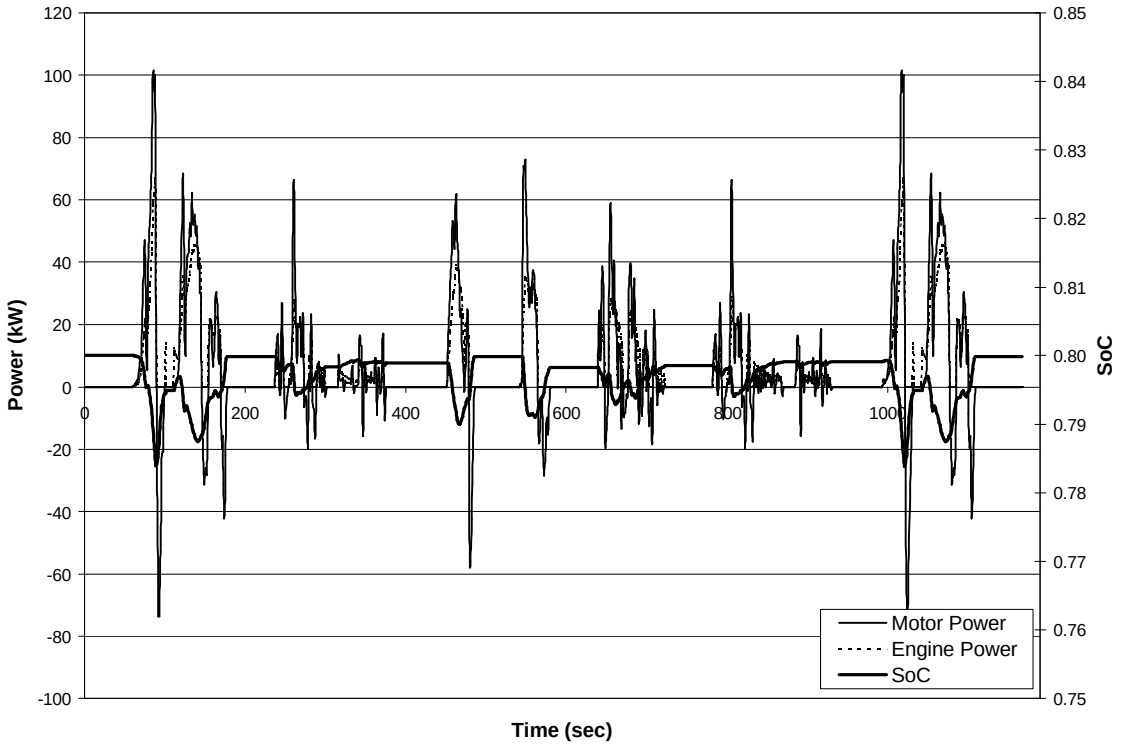

Figure A.33 Class 8 Series HEV on Yard Cycle without auxiliary load.

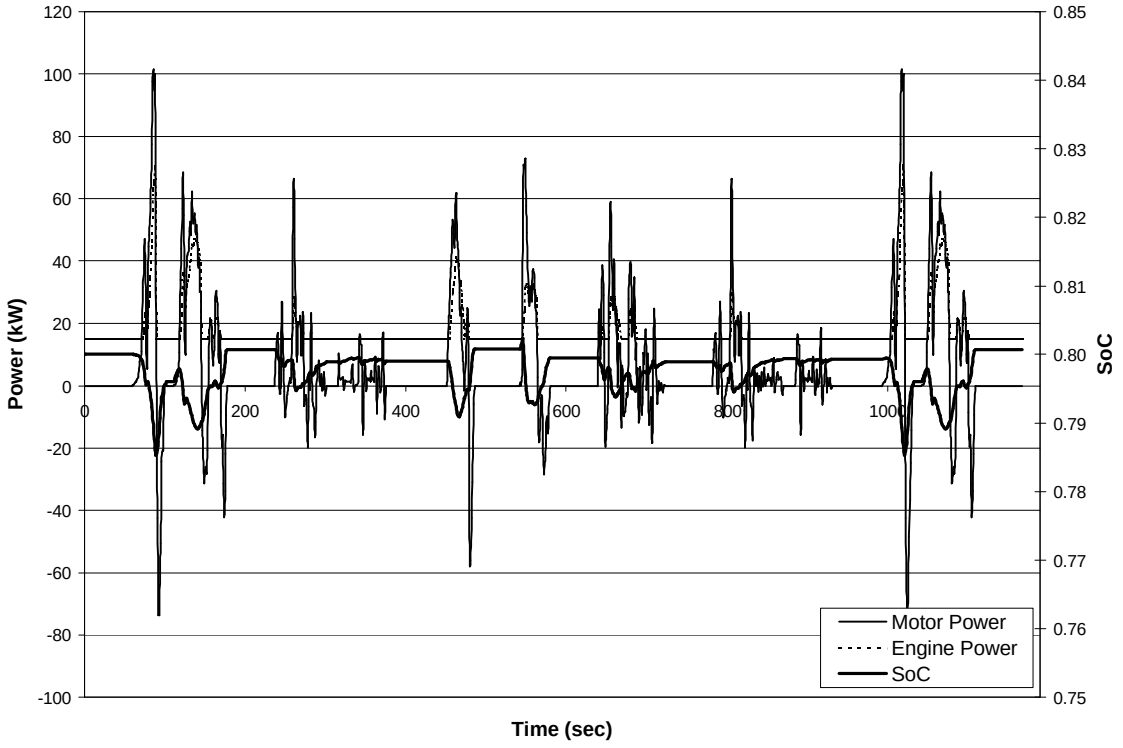

Figure A.34 Class 8 Series HEV on Yard Cycle with auxiliary load.

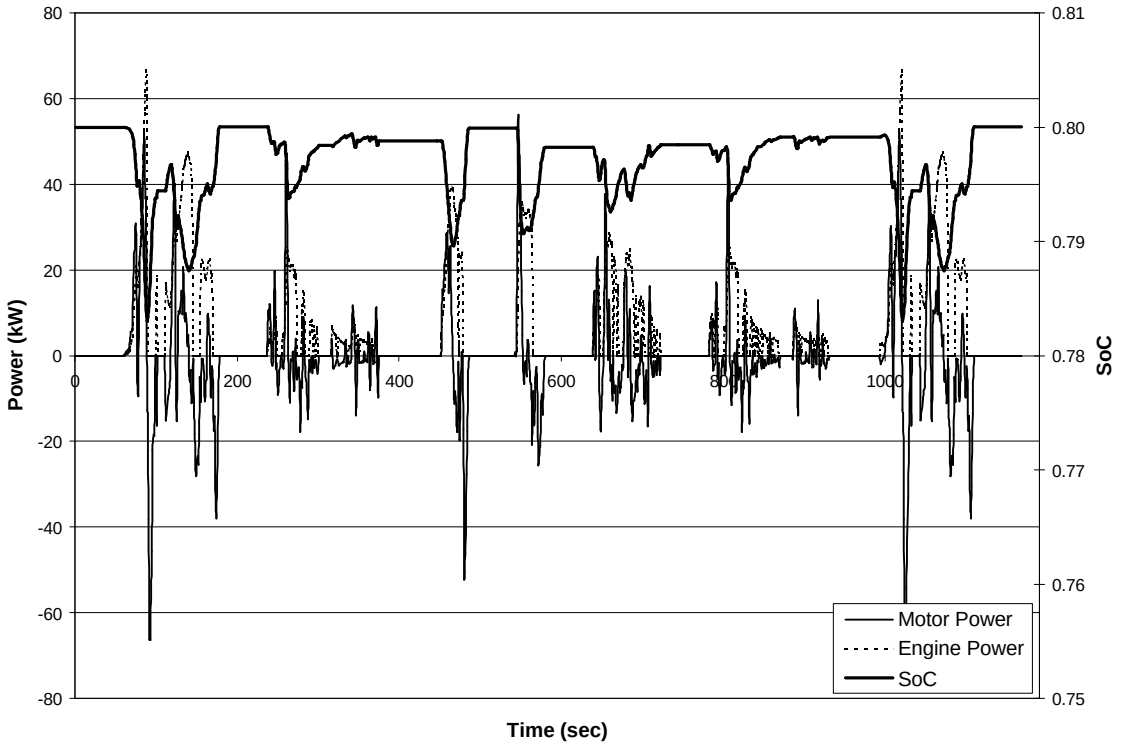

Figure A.35 Class 8 Parallel HEV on Yard Cycle without auxiliary load.

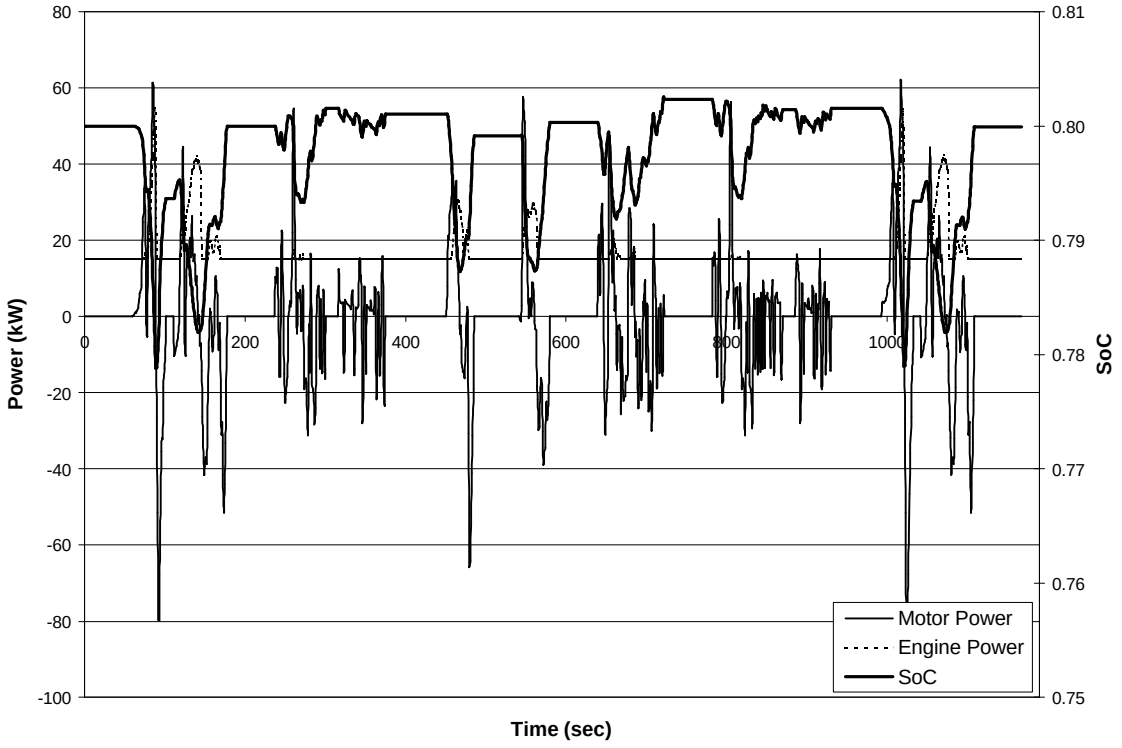

Figure A.36 Class 8 Parallel HEV on Yard Cycle with auxiliary load.

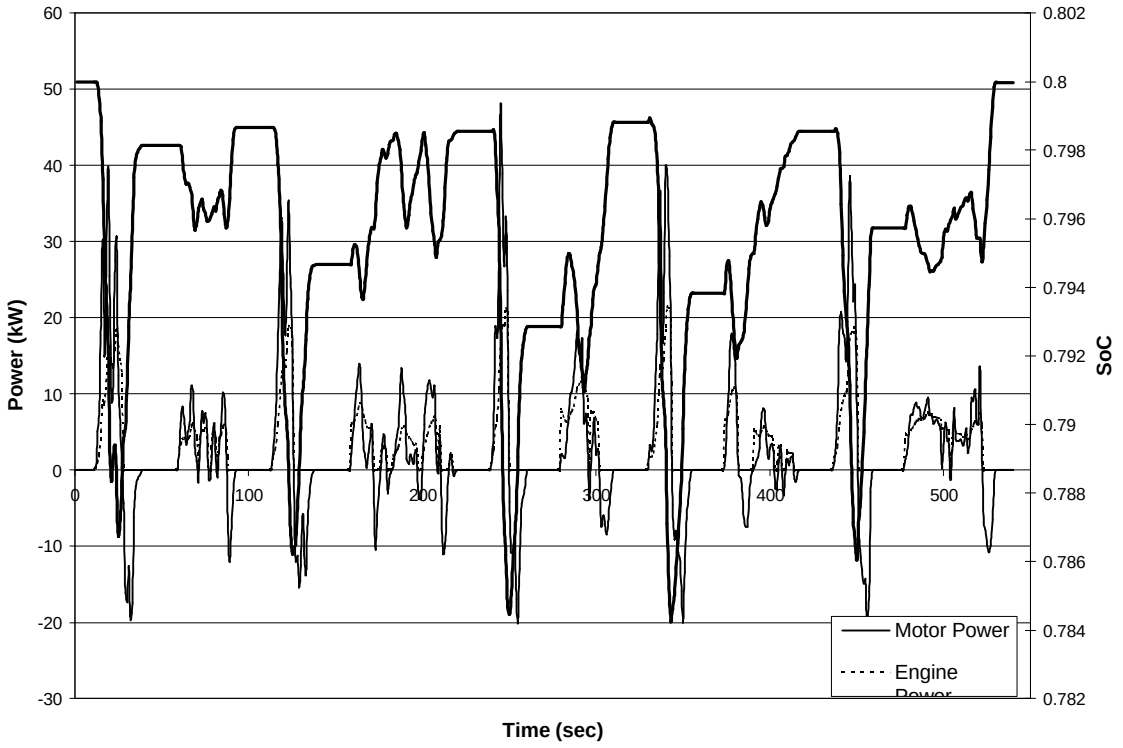

Figure A.37 Class 2B Series HEV on Manhattan Cycle without auxiliary load.

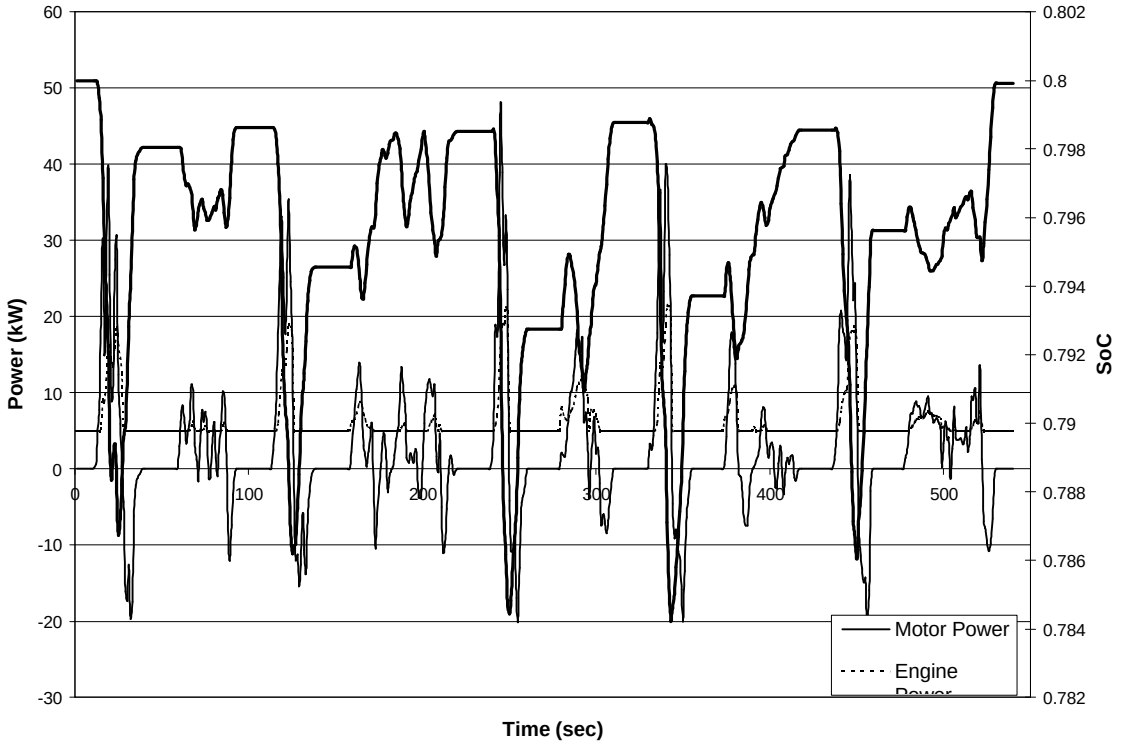

Figure A.38 Class 2B Series HEV on Manhattan Cycle with auxiliary load.

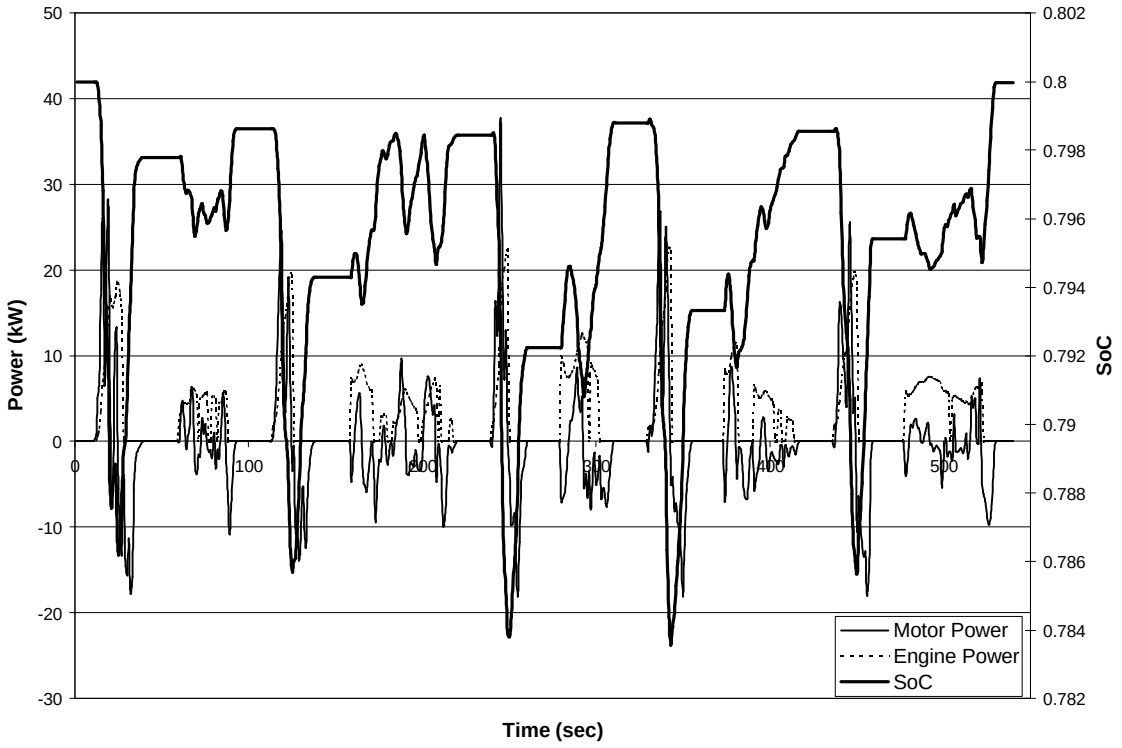

Figure A.39 Class 2B Parallel HEV on Manhattan Cycle without auxiliary load.

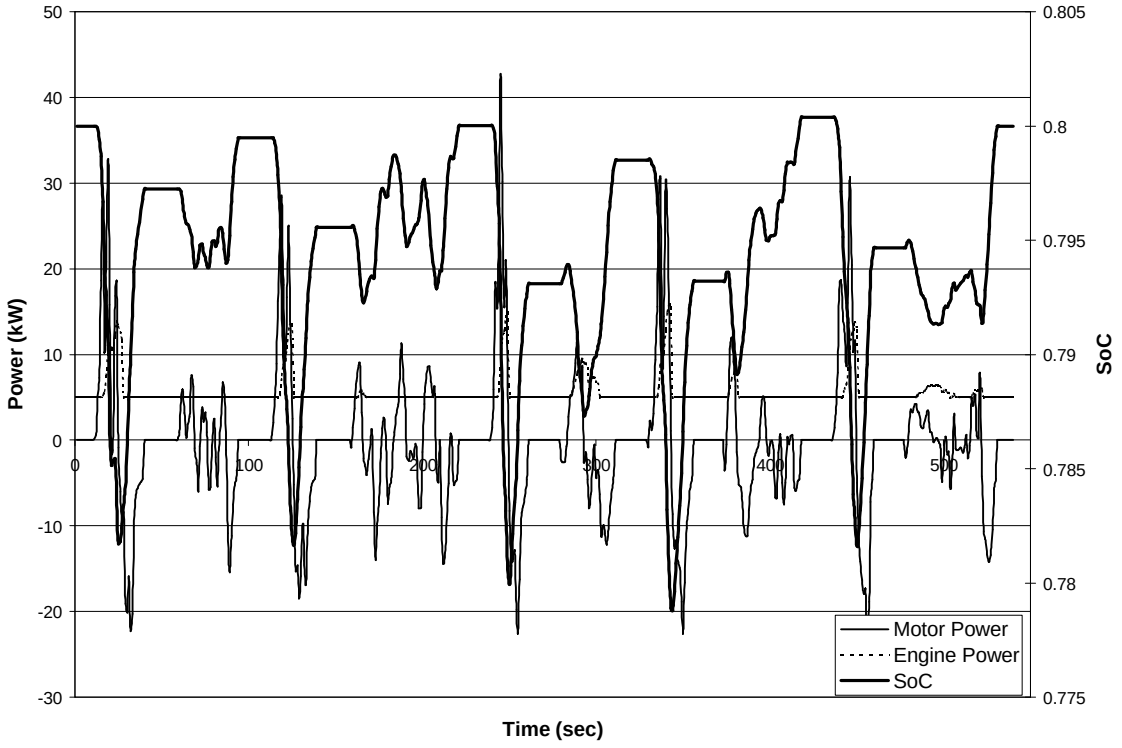

Figure A.40 Class 2B Parallel HEV on Manhattan Cycle with auxiliary load.

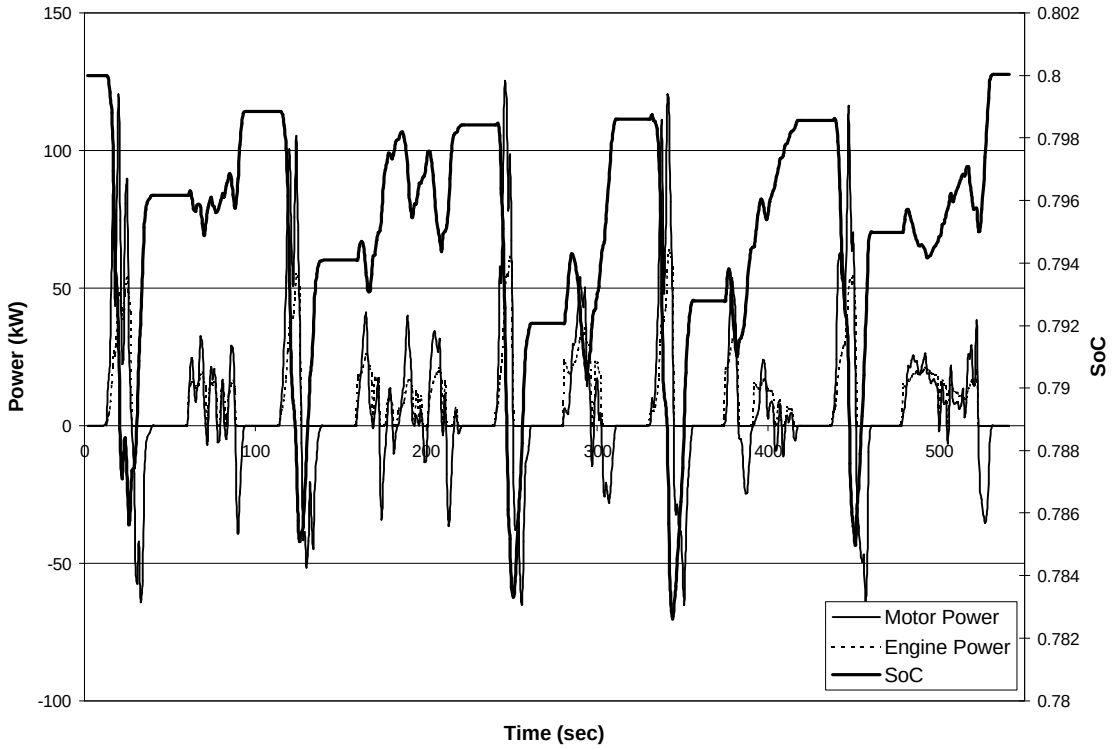

Figure A.41 Class 6 Series HEV on Manhattan Cycle without auxiliary load.

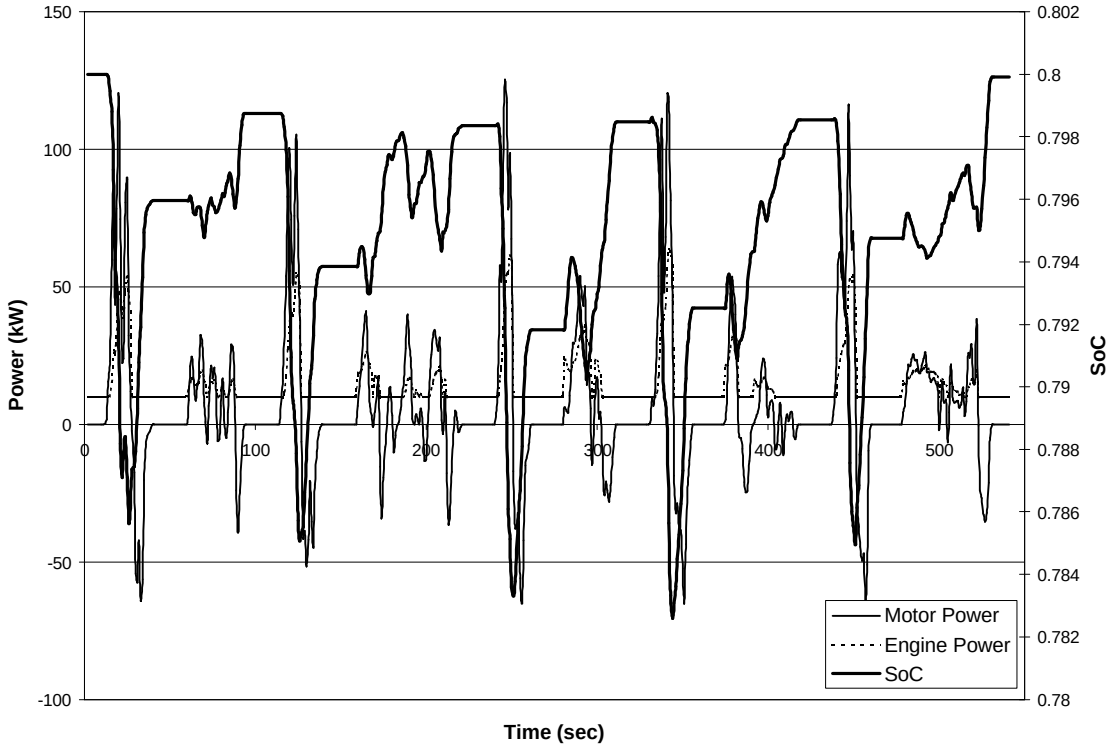

Figure A.42 Class 6 Series HEV on Manhattan Cycle with auxiliary load.

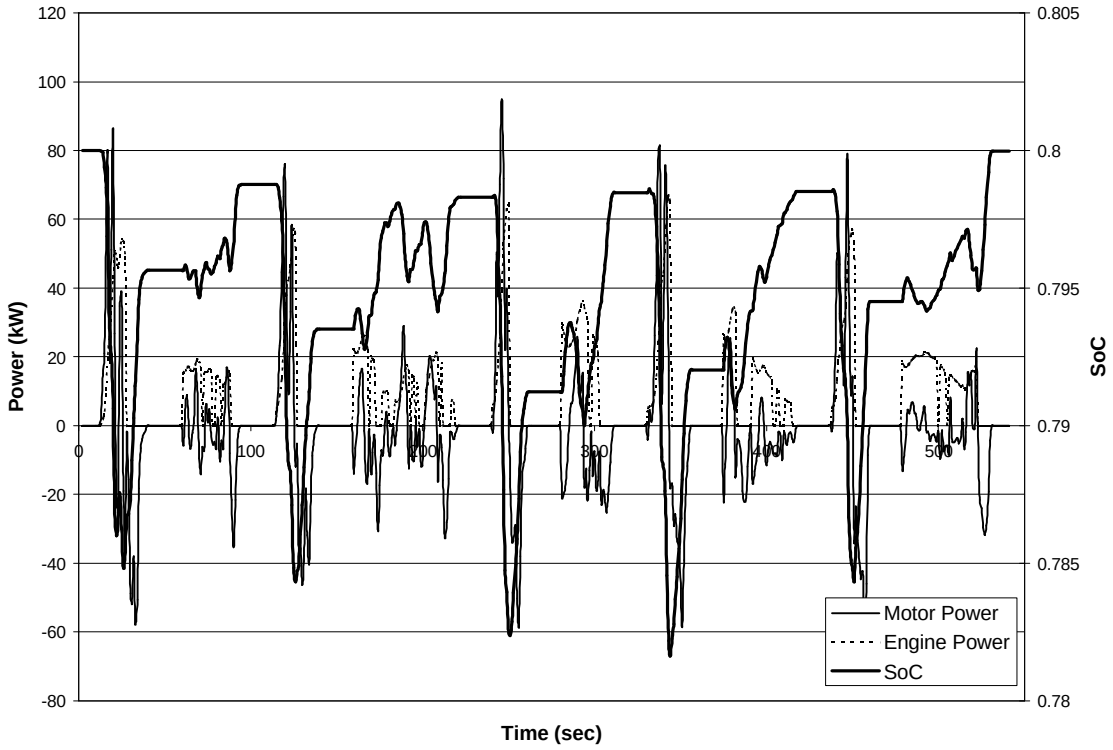

Figure A.43 Class 6 Parallel HEV on Manhattan Cycle without auxiliary load.

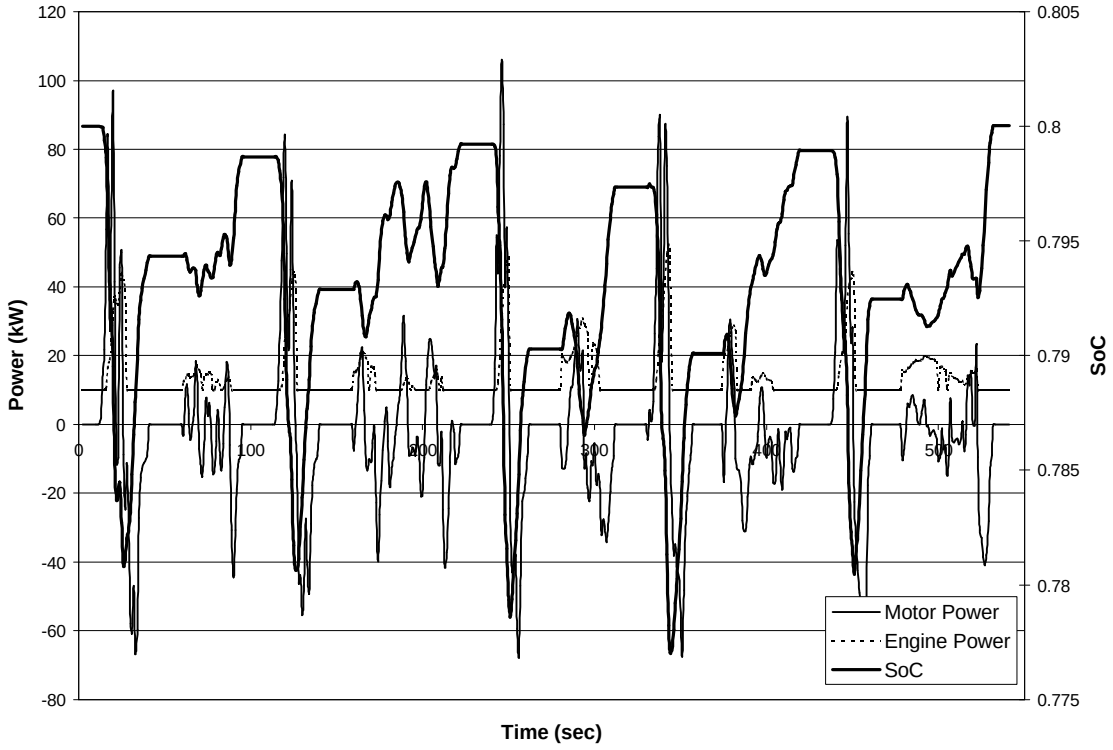

Figure A.44 Class 6 Parallel HEV on Manhattan Cycle with auxiliary load.

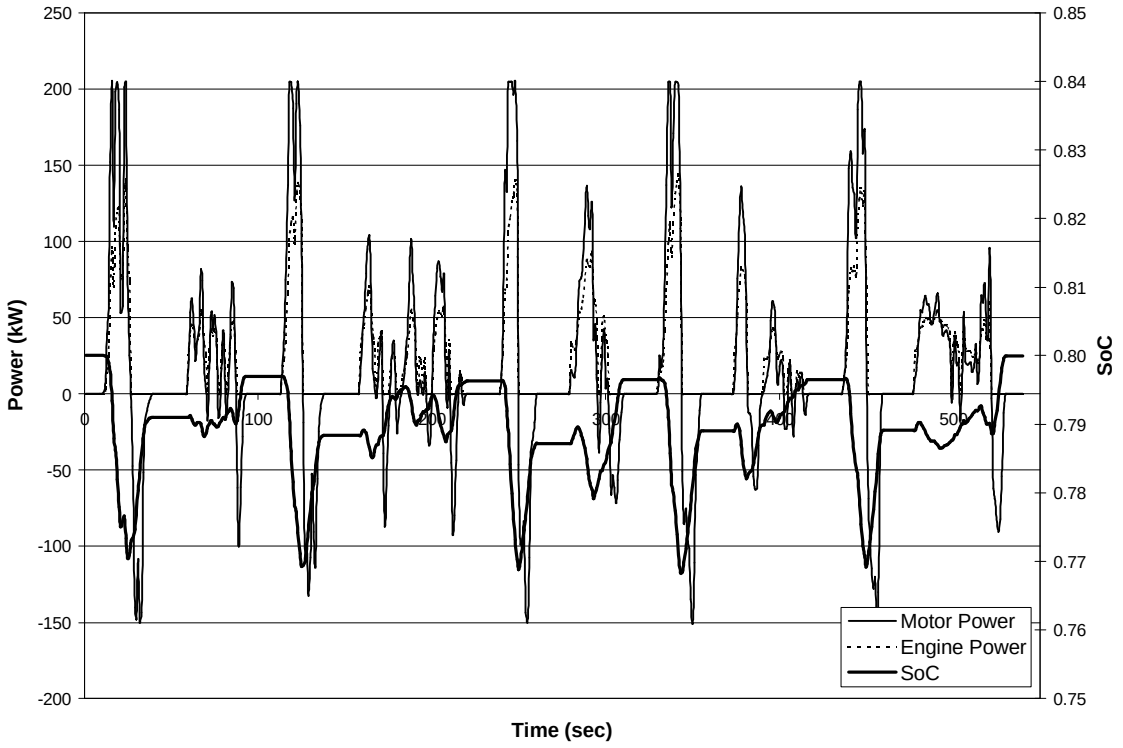

Figure A.45 Class 8 Series HEV on Manhattan Cycle without auxiliary load.

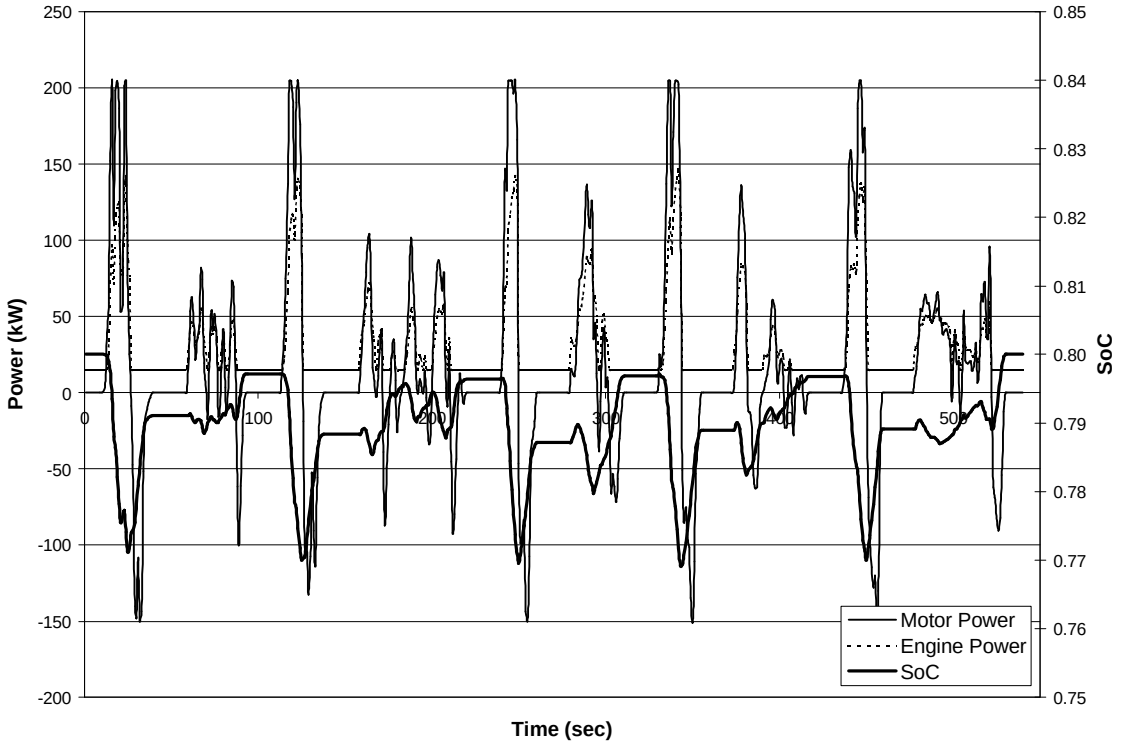

Figure A.46 Class 8 Series HEV on Manhattan Cycle with auxiliary load.

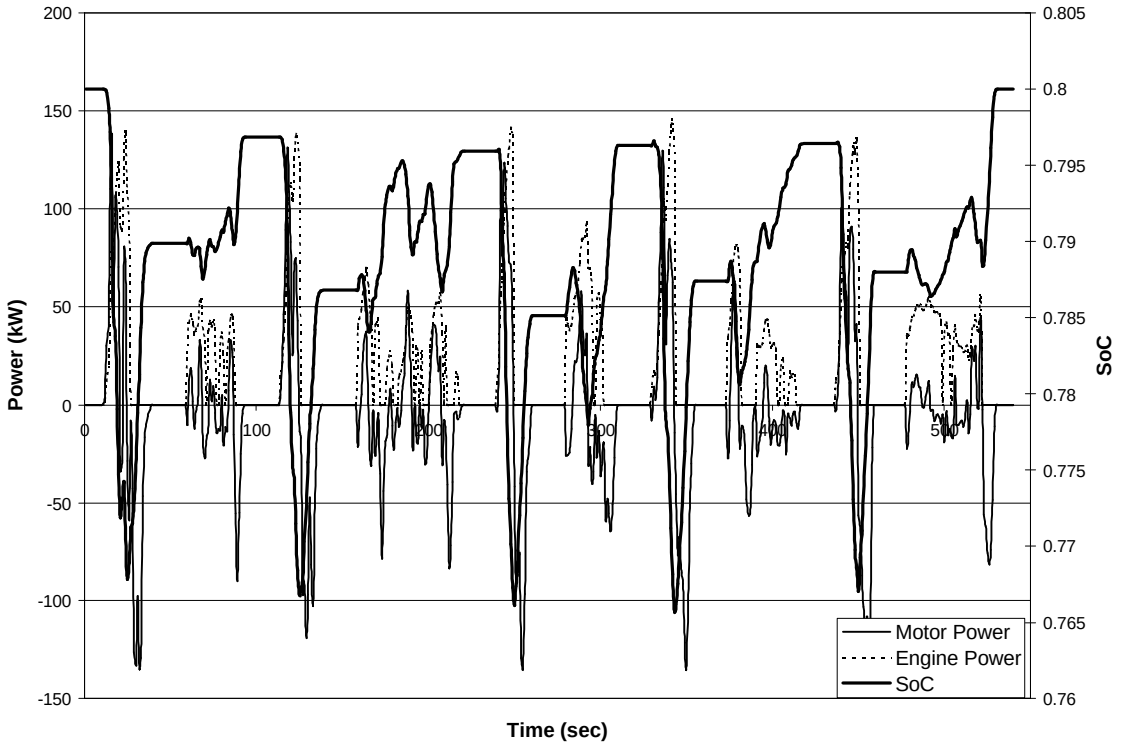

Figure A.47 Class 8 Parallel HEV on Manhattan Cycle without auxiliary load.

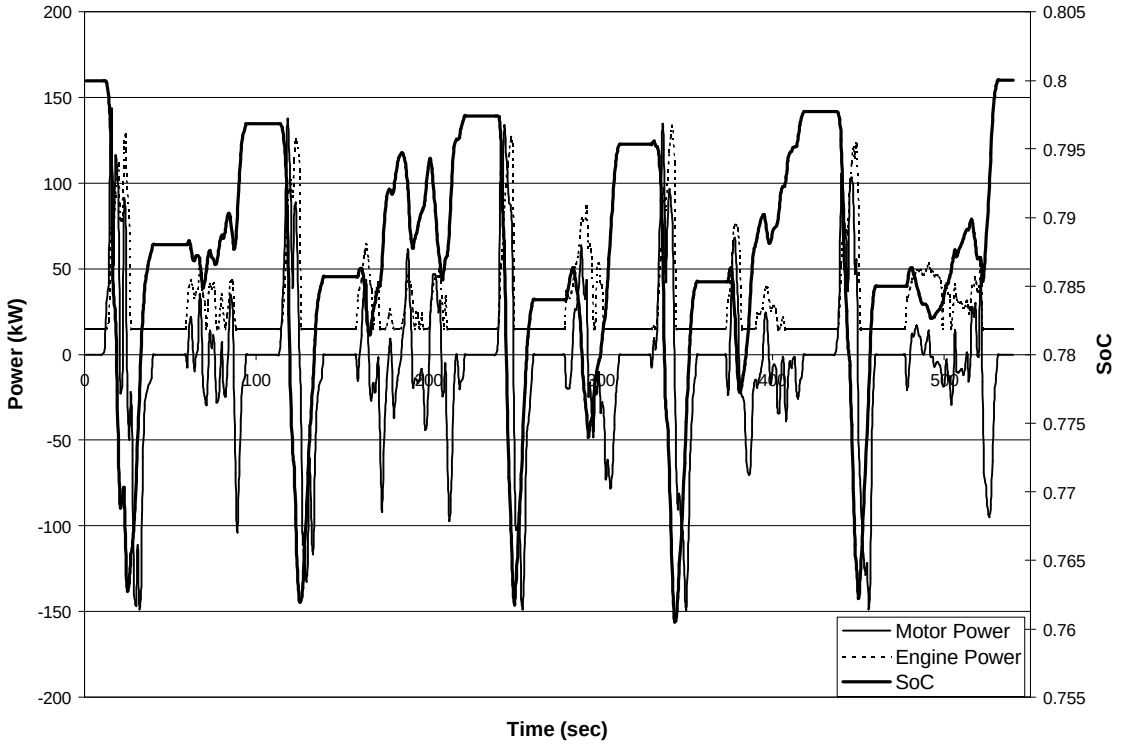

Figure A.48 Class 8 Parallel HEV on Manhattan Cycle with auxiliary load.

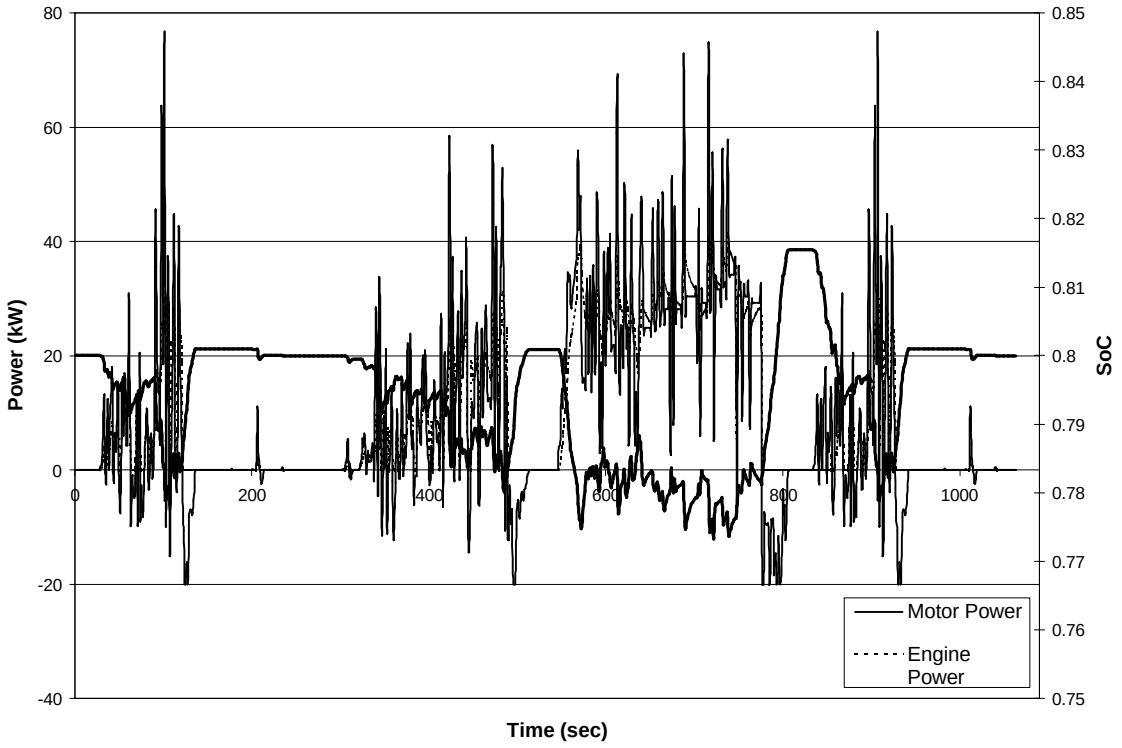

Figure A.49 Class 2B Series HEV on Test D Cycle without auxiliary load.

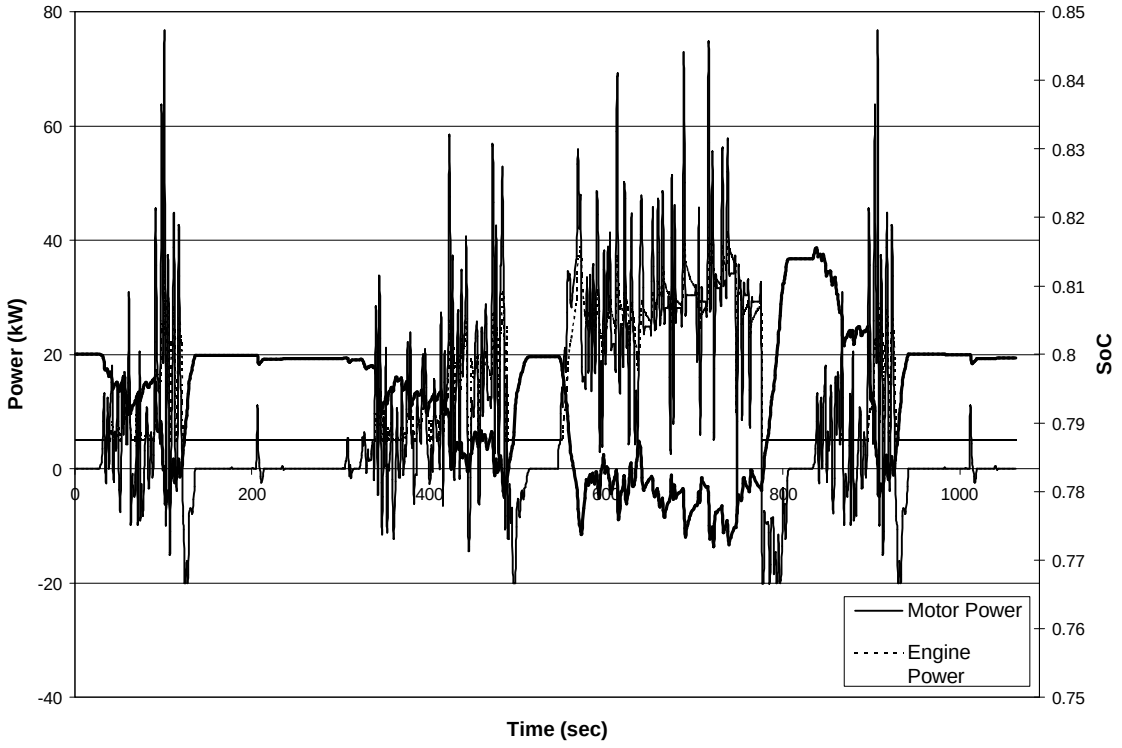

Figure A.50 Class 2B Series HEV on Test D Cycle with auxiliary load.

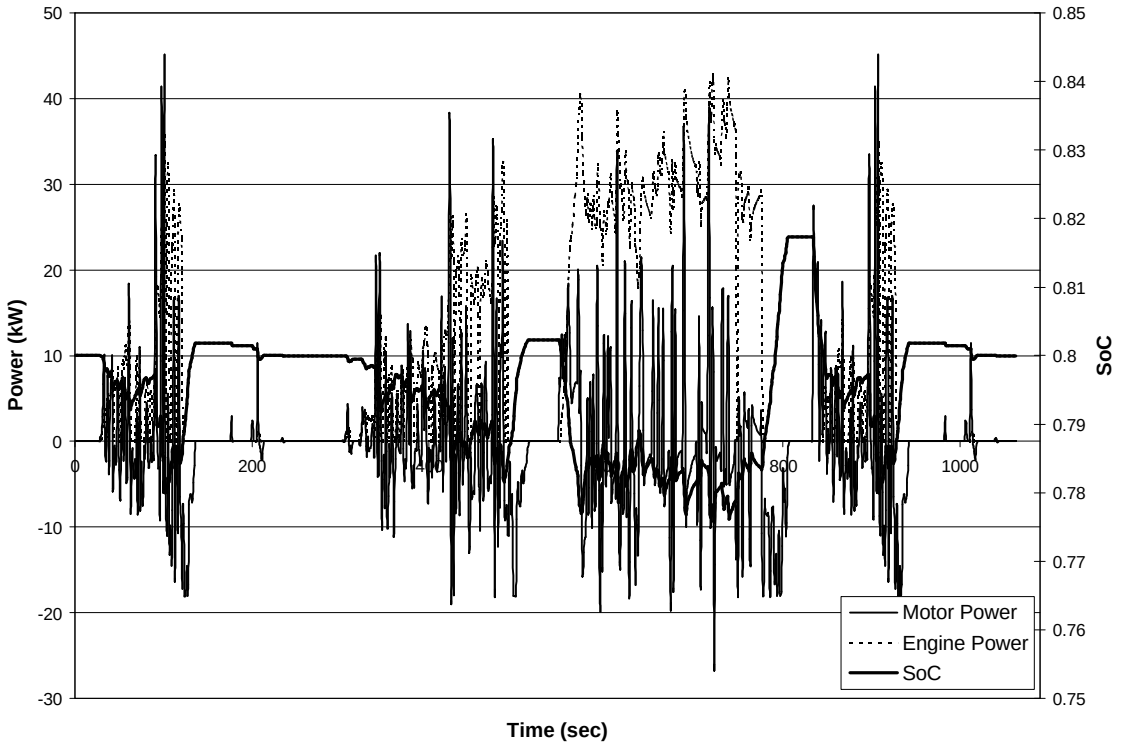

Figure A.51 Class 2B Parallel HEV on Test D Cycle without auxiliary load.

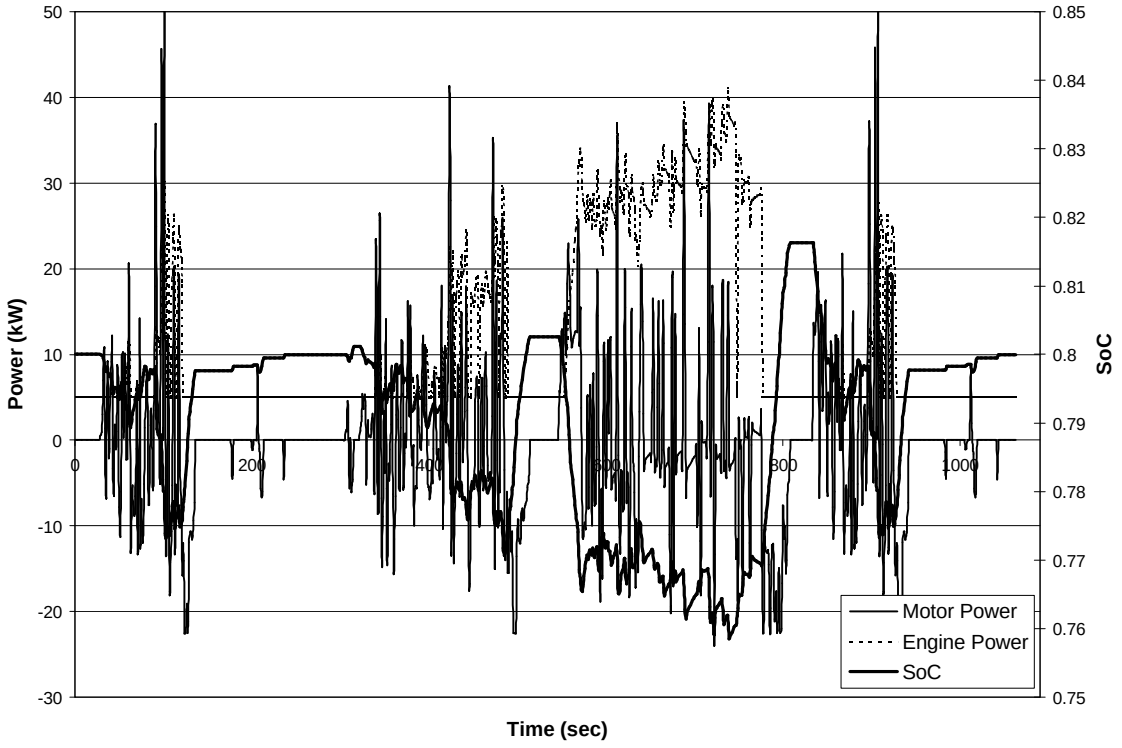

Figure A.52 Class 2B Parallel HEV on Test D Cycle with auxiliary load.

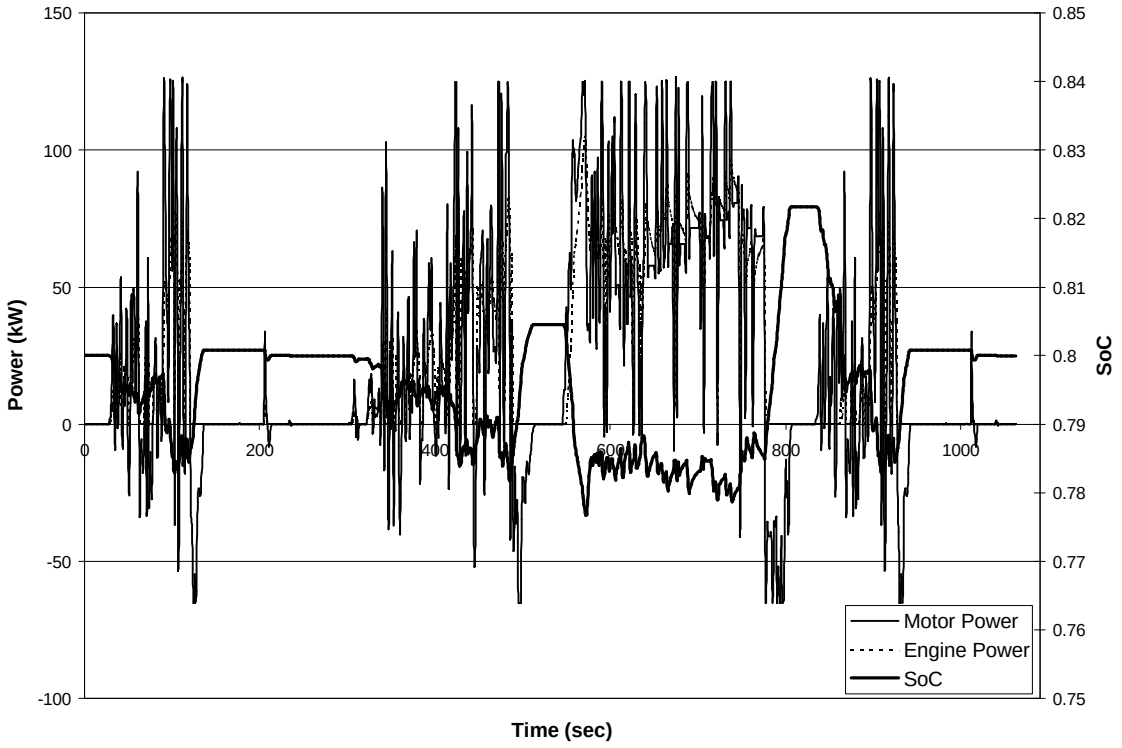

Figure A.53 Class 6 Series HEV on Test D Cycle without auxiliary load.

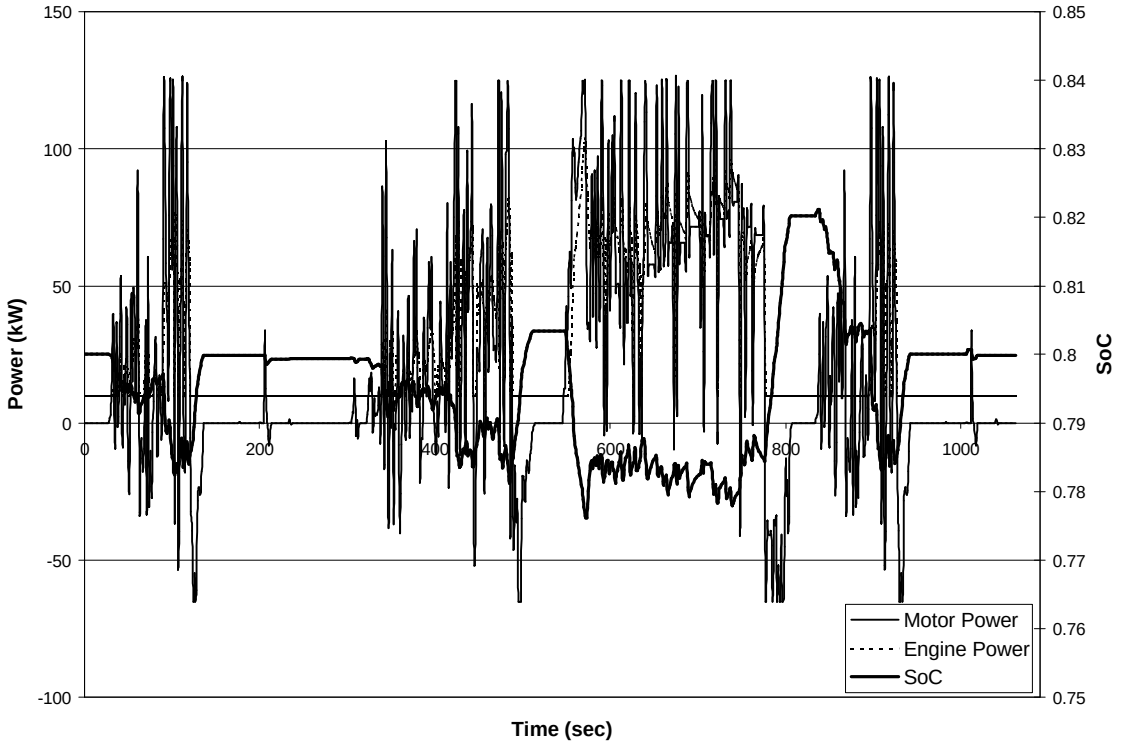

Figure A.54 Class 6 Series HEV on Test D Cycle with auxiliary load.

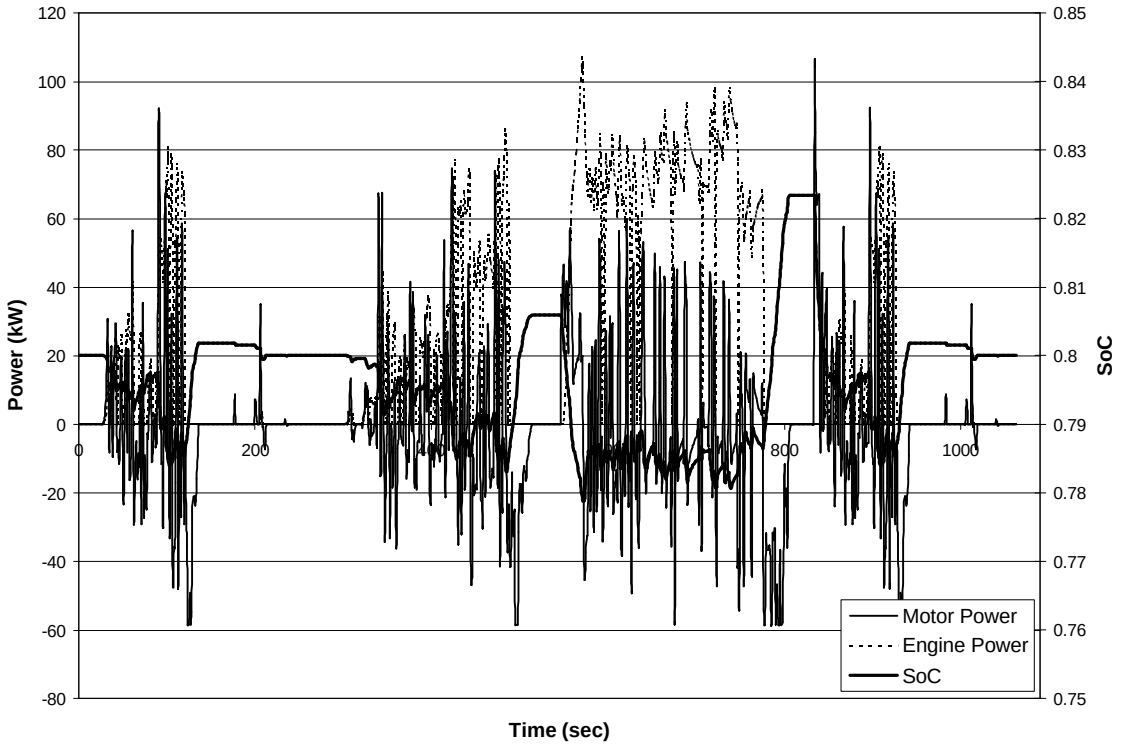

Figure A.55 Class 6 Parallel HEV on Test D Cycle without auxiliary load.

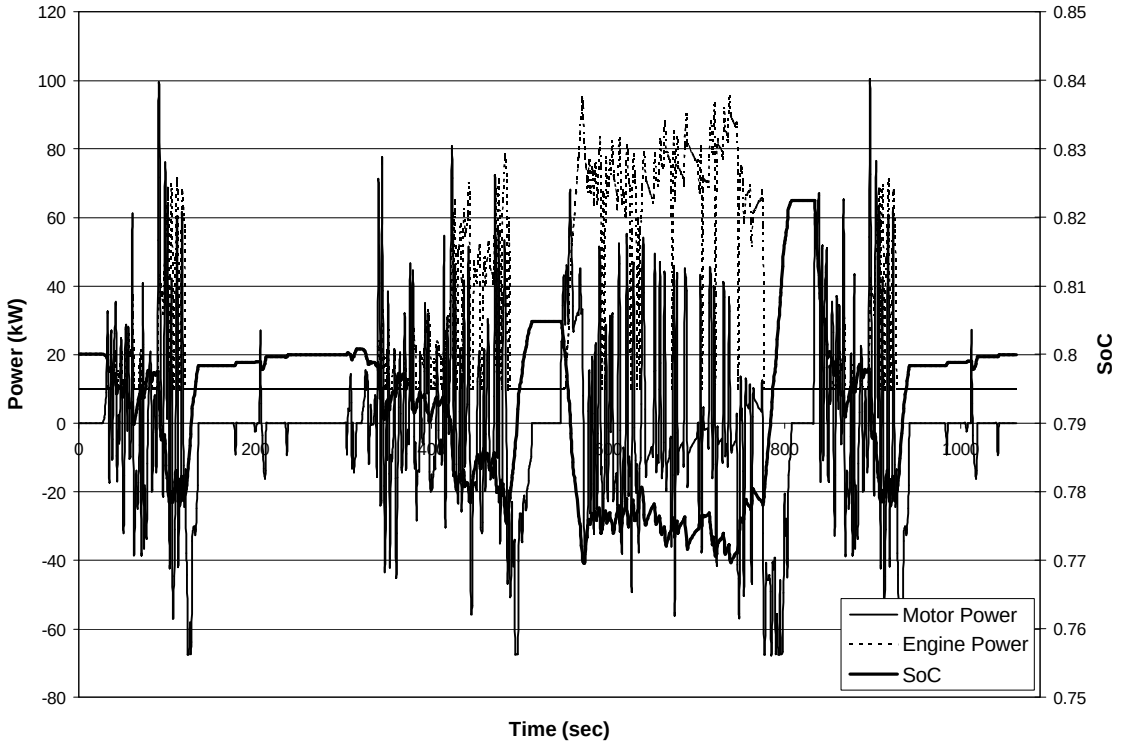

Figure A.56 Class 6 Parallel HEV on Test D Cycle with auxiliary load.

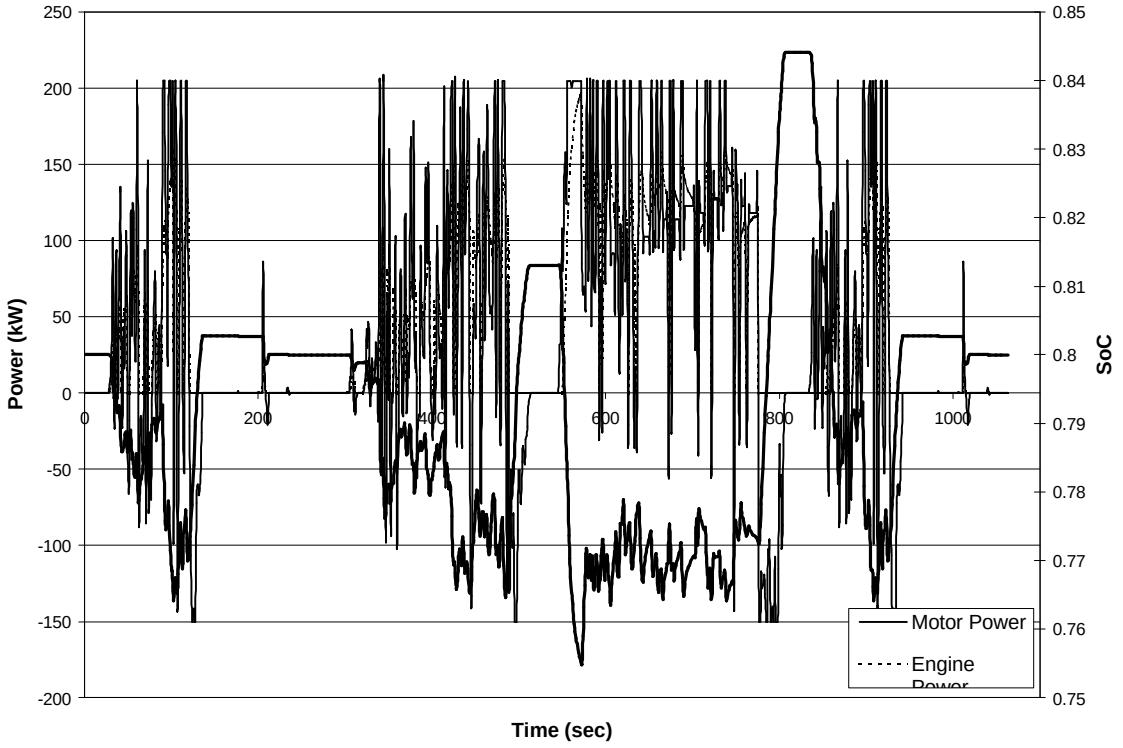

Figure A.57 Class 8 Series HEV on Test D Cycle without auxiliary load.

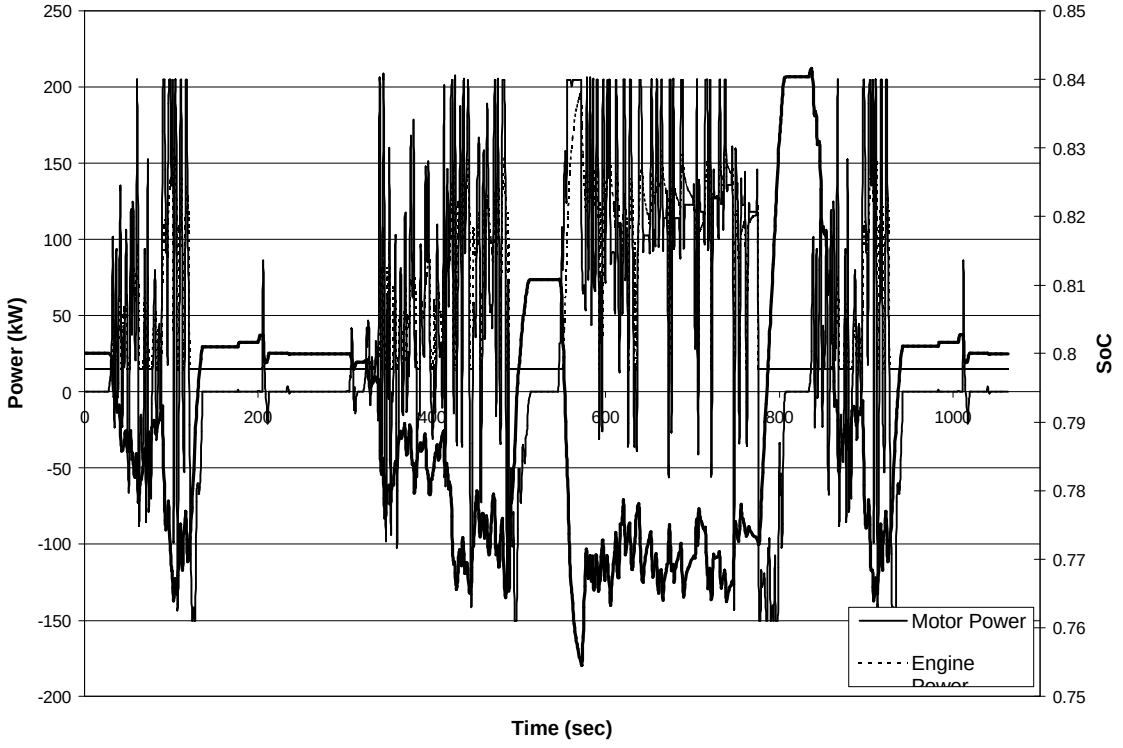

Figure A.58 Class 8 Series HEV on Test D Cycle with auxiliary load.

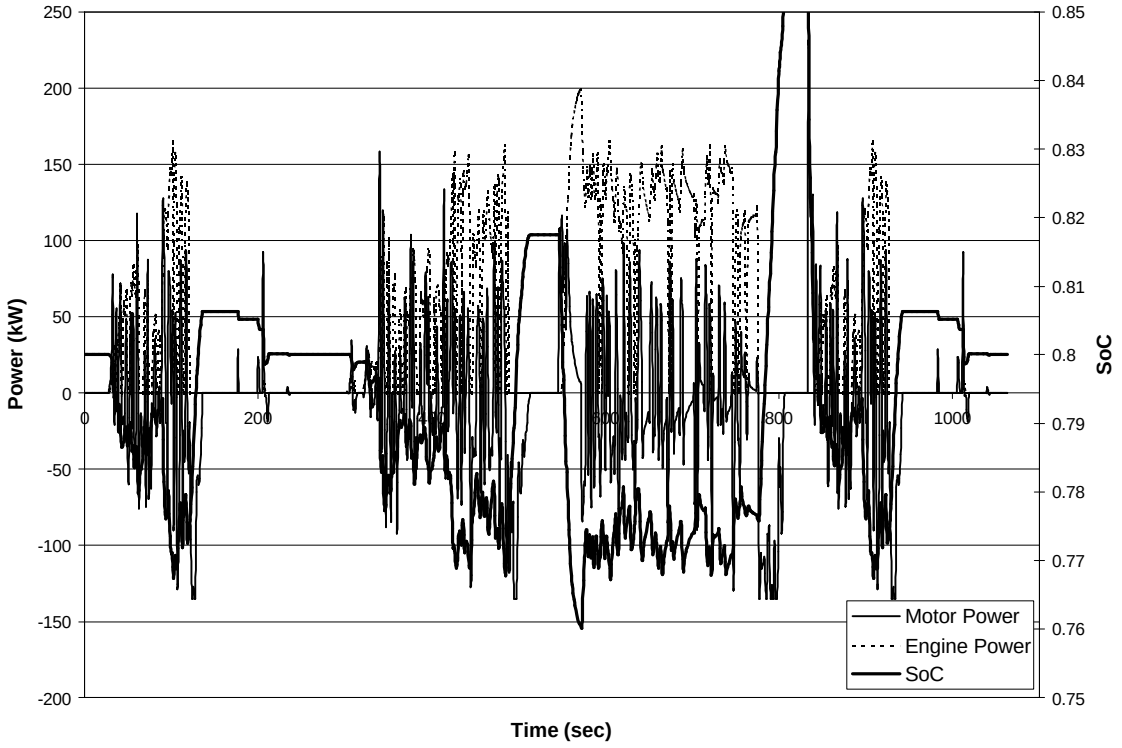

Figure A.59 Class 8 Parallel HEV on Test D Cycle without auxiliary load.

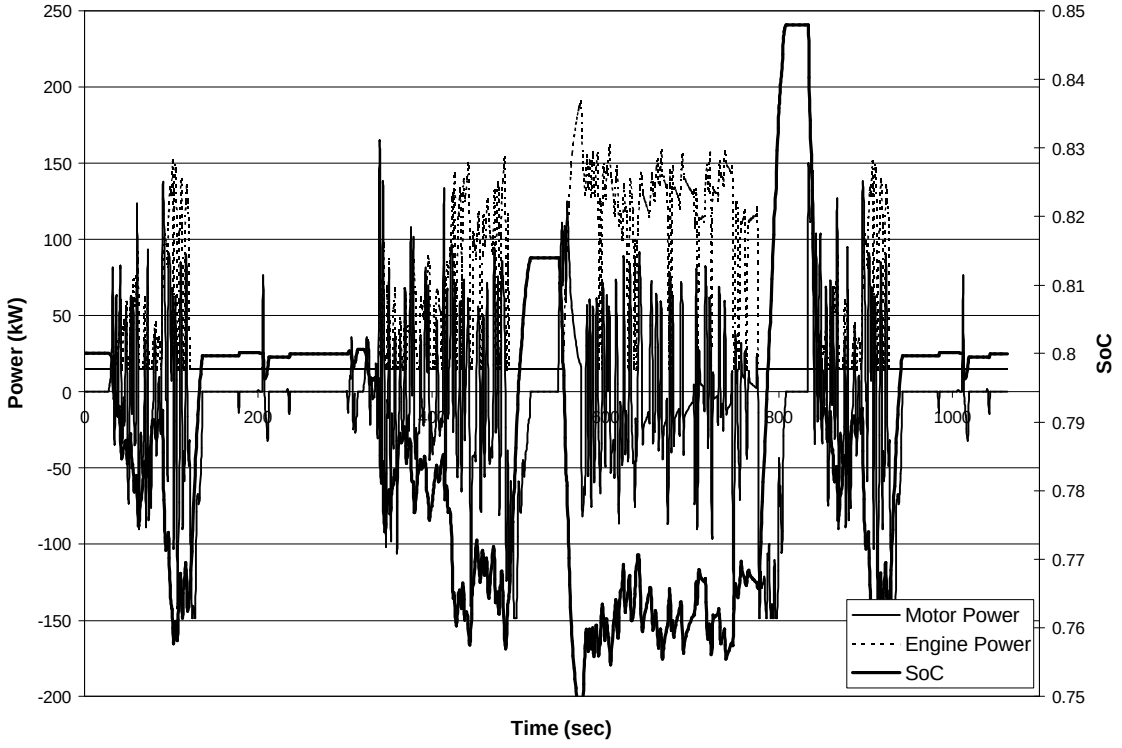

Figure A.60 Class 8 Parallel HEV on Test D Cycle with auxiliary load.

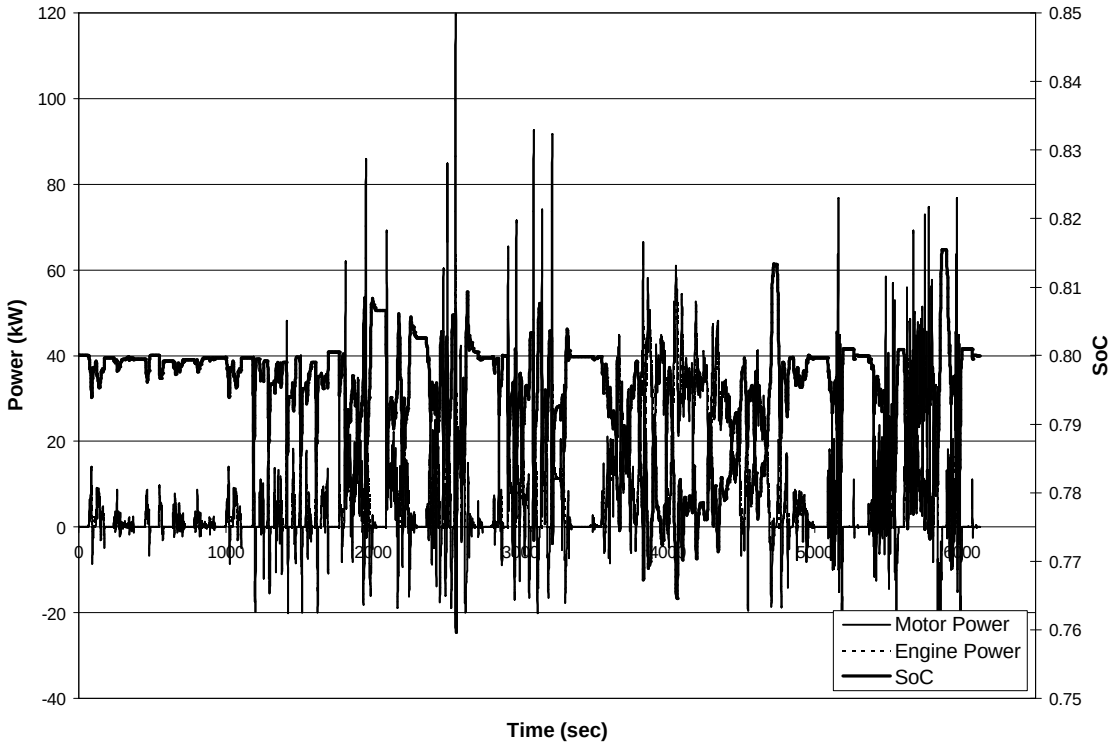

Figure A.61 Class 2B Series HEV on Combined Cycle without auxiliary load.

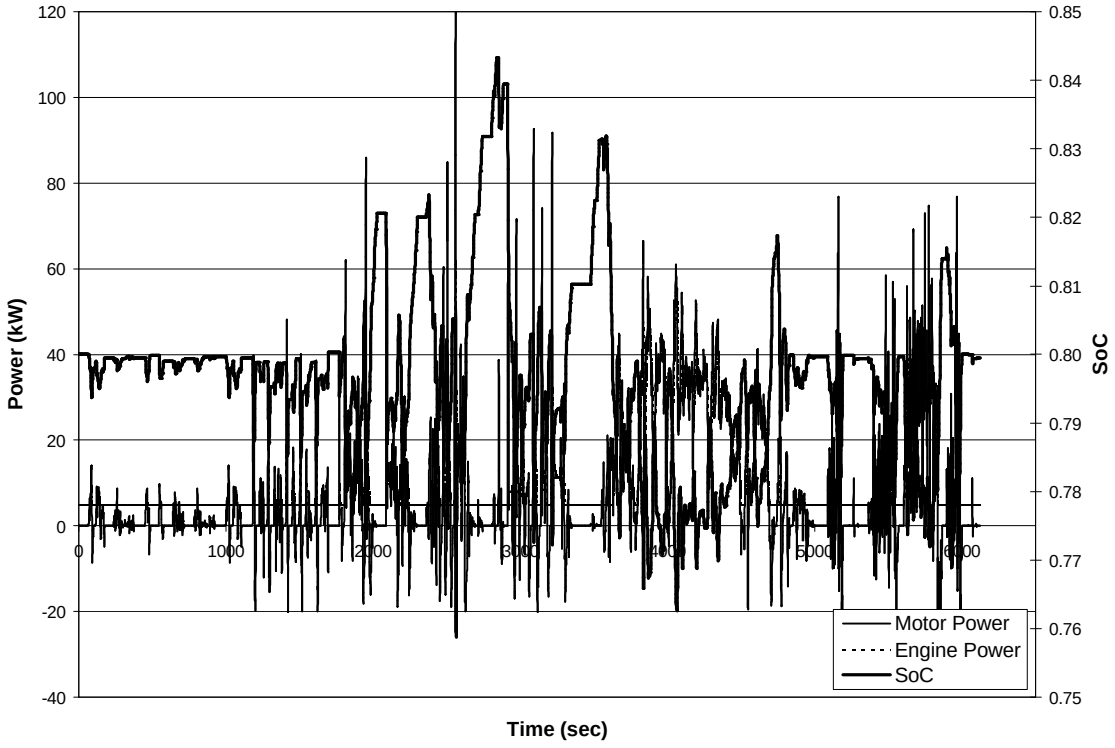

Figure A.62 Class 2B Series HEV on Combined Cycle with auxiliary load.

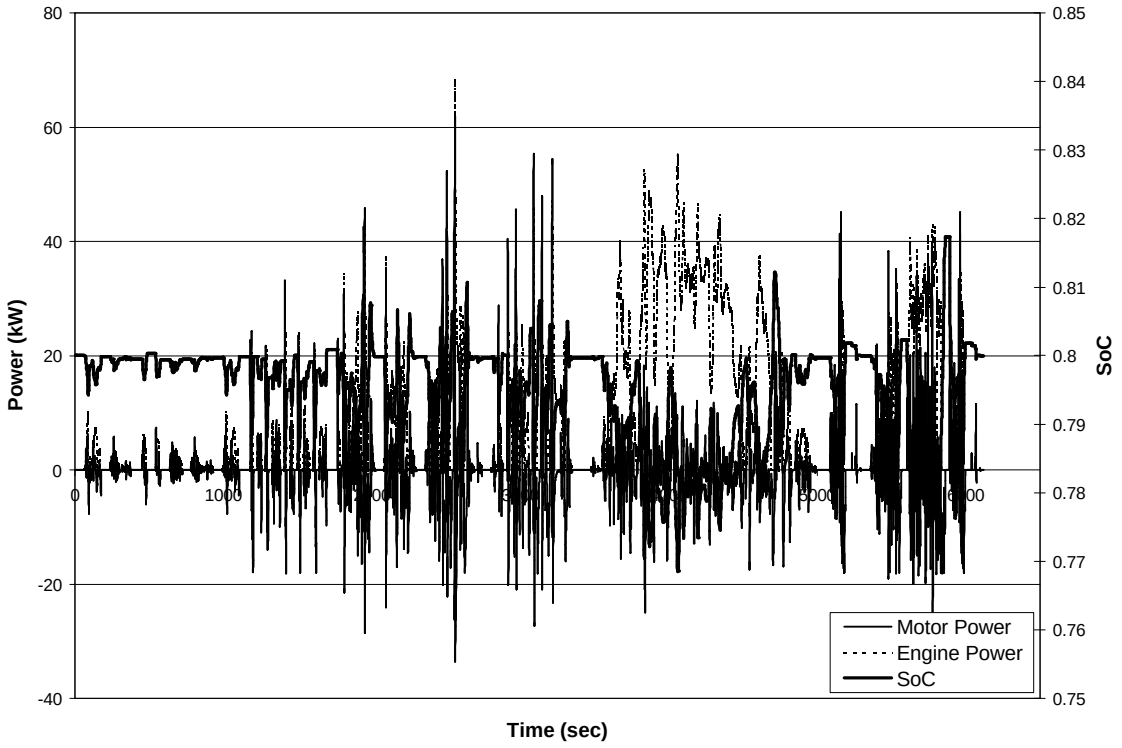

Figure A.63 Class 2B Parallel HEV on Combined Cycle without auxiliary load.

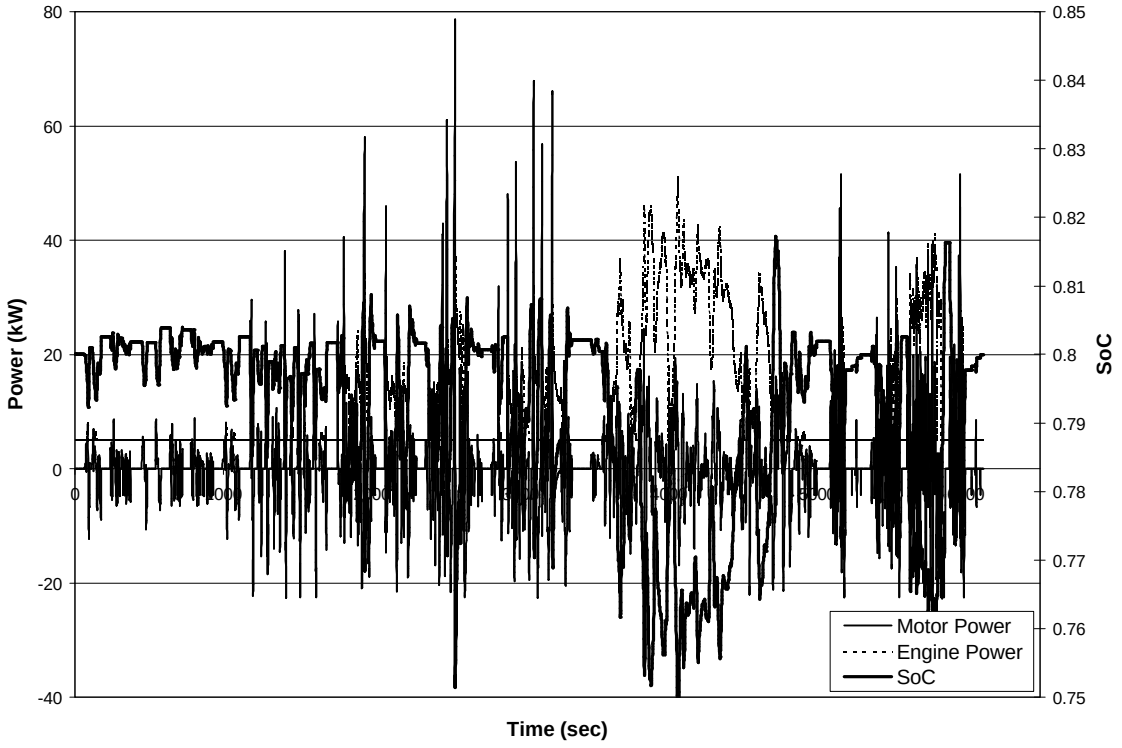

Figure A.64 Class 2B Parallel HEV on Combined cycle with auxiliary load.

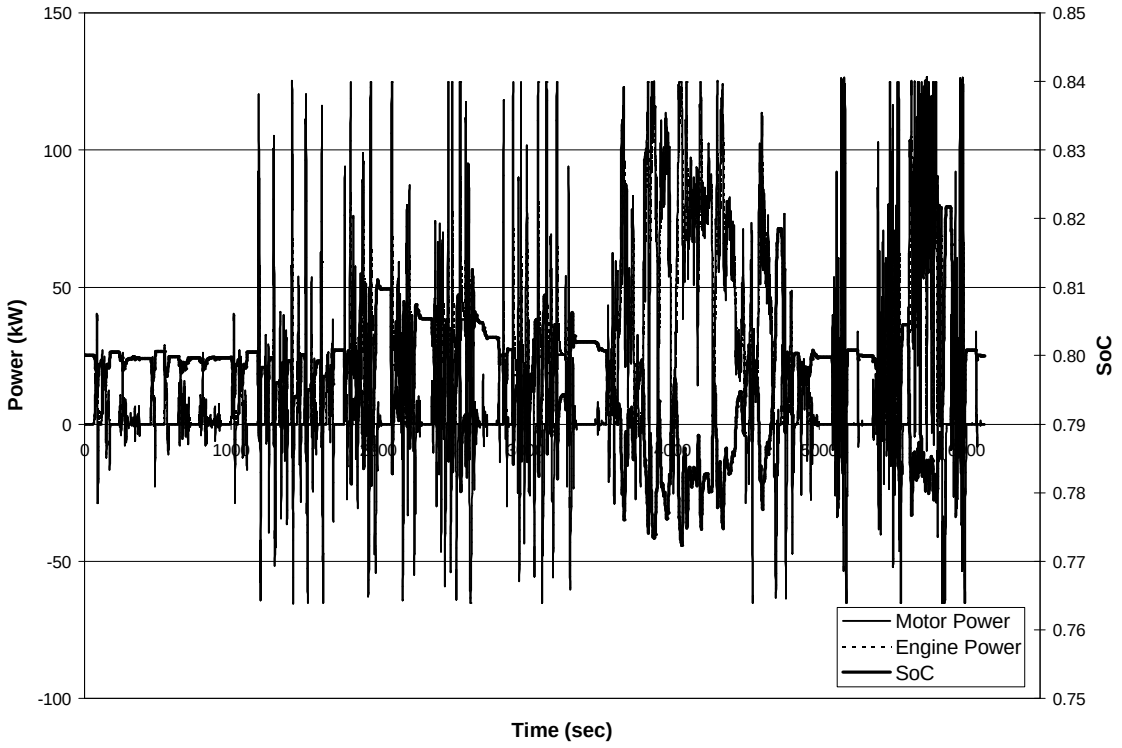

Figure A.65 Class 6 Series HEV on Combined Cycle without auxiliary load.

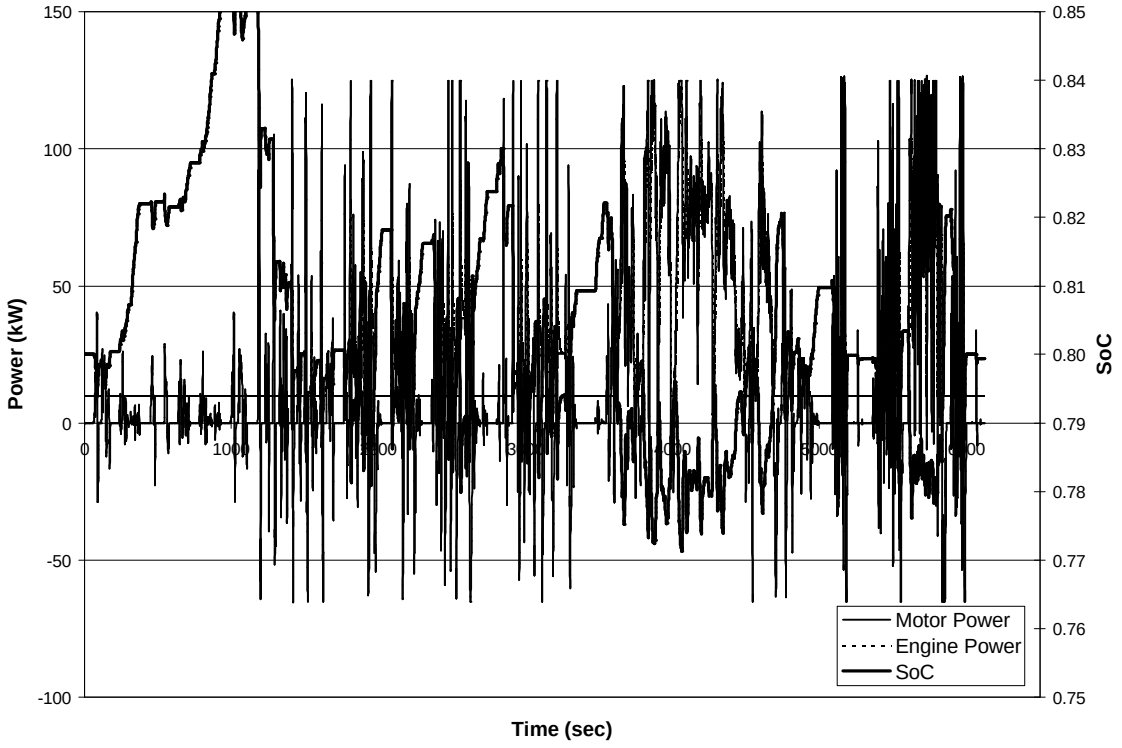

Figure A.66 Class 6 Series HEV on Combined Cycle with auxiliary load.

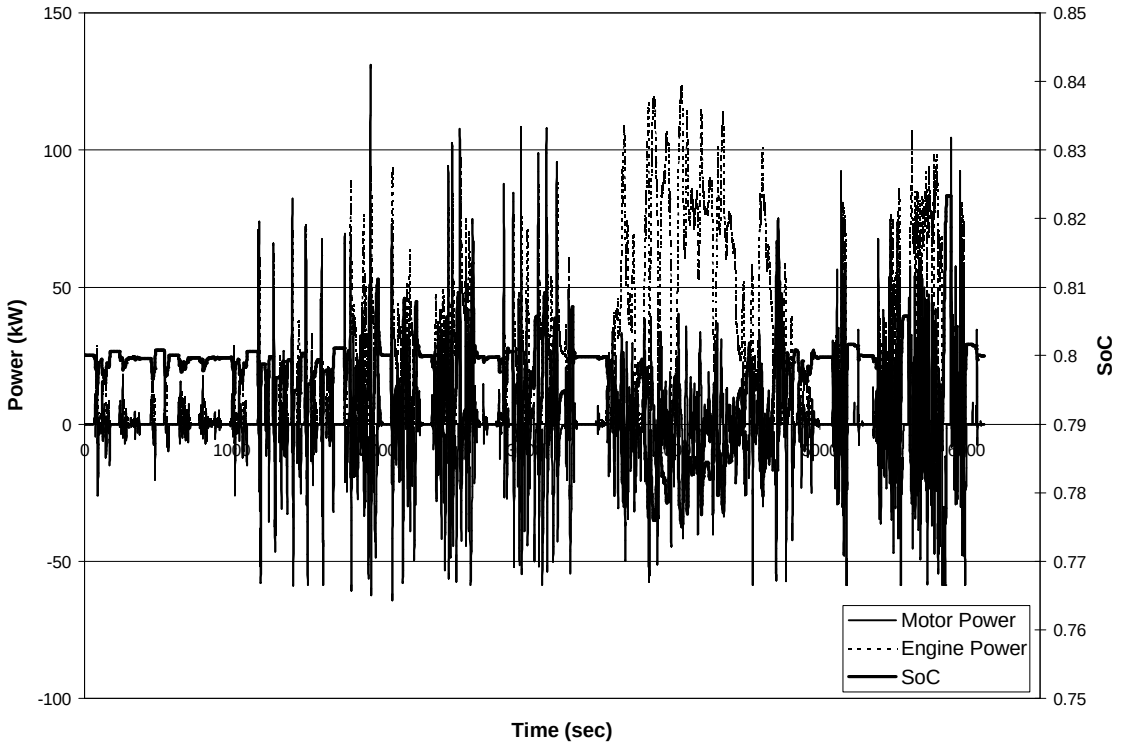

Figure A.67 Class 6 Parallel HEV on Combined Cycle without auxiliary load.

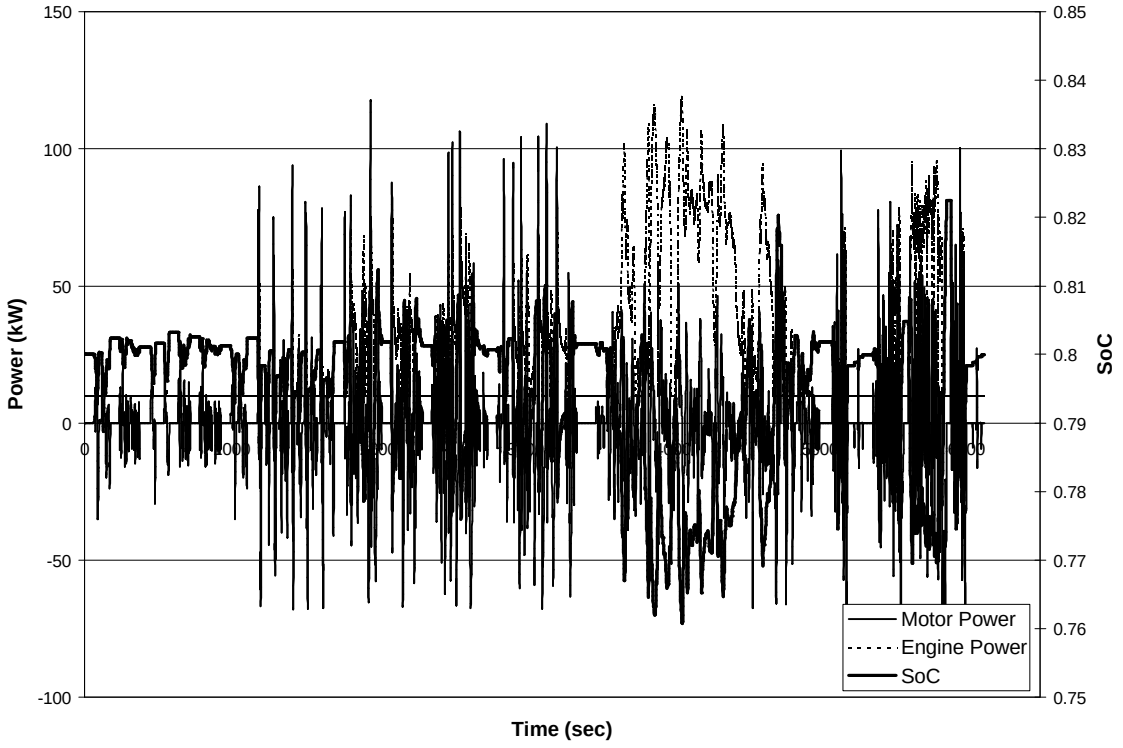

Figure A.68 Class 6 Parallel HEV on Combined Cycle with auxiliary load.

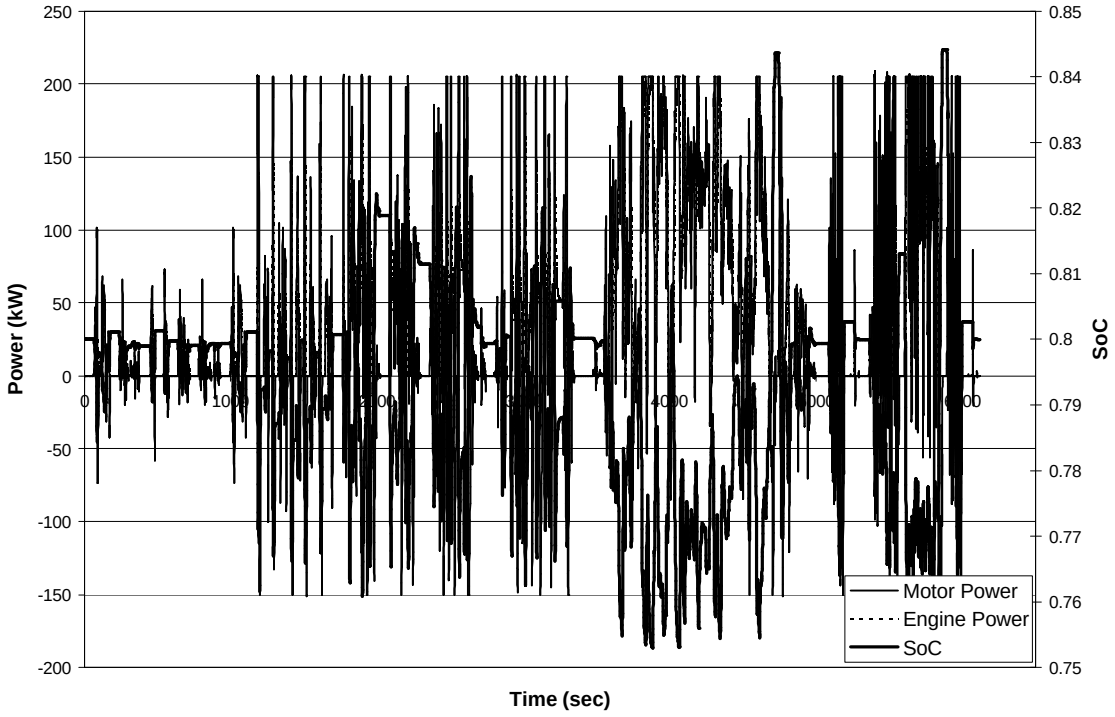

Figure A.69 Class 8 Series HEV on Combined Cycle without auxiliary load.

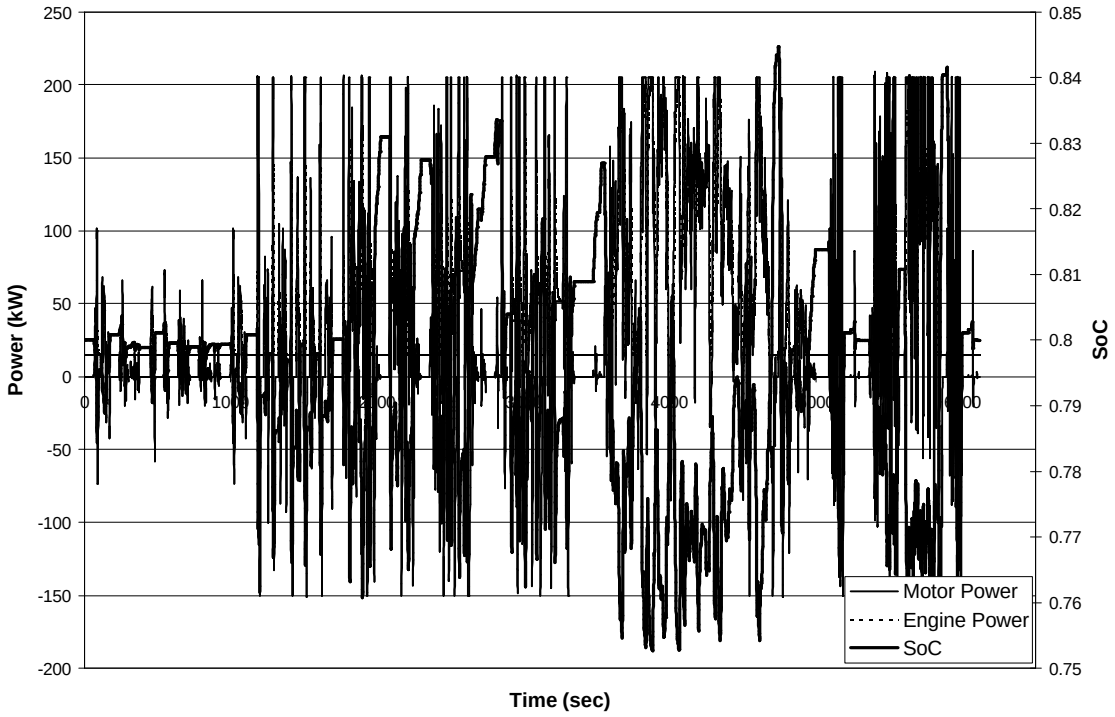

Figure A.70 Class 8 Series HEV on Combined Cycle with auxiliary load.

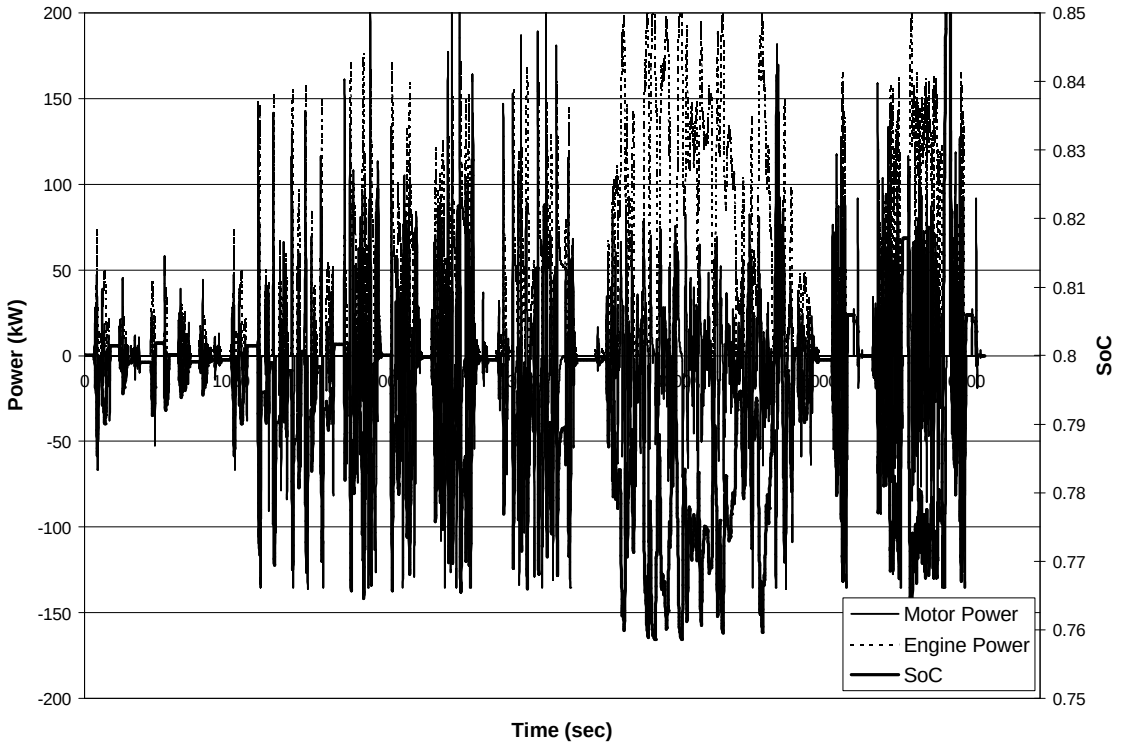

Figure A.71 Class 8 Parallel HEV on Combined Cycle without auxiliary load.

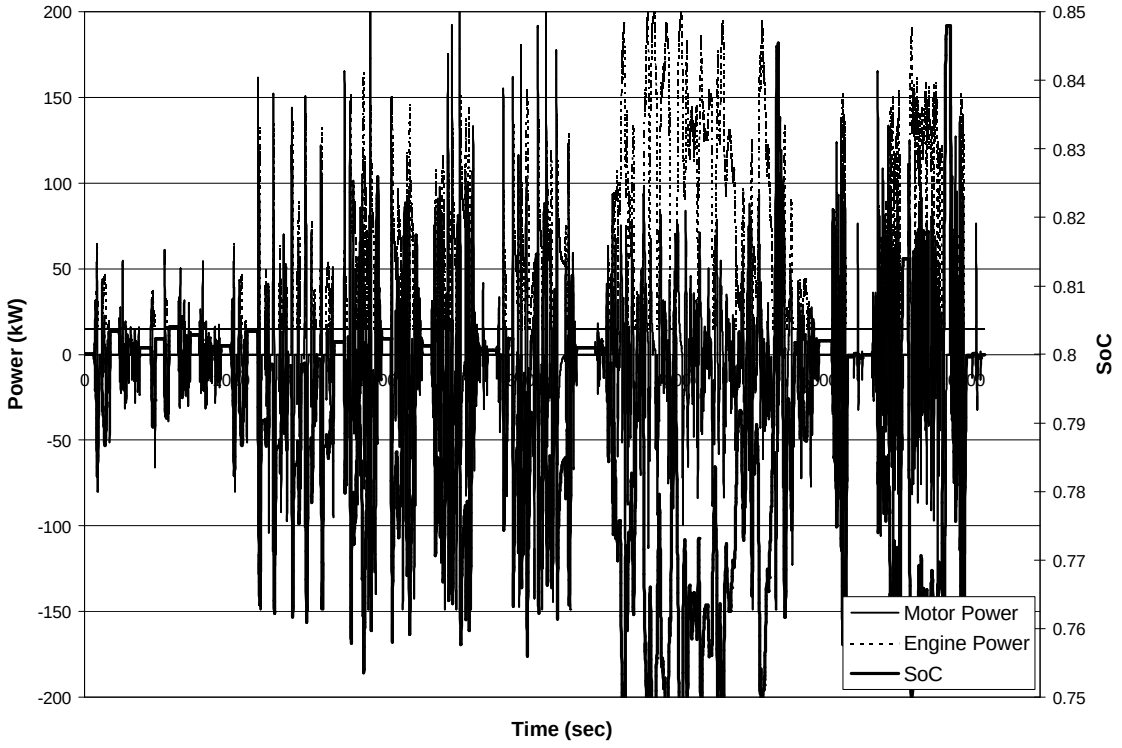

Figure A.72 Class 8 Parallel HEV on Combined Cycle with auxiliary load.